BMP AND NONCANONICAL WNT SIGNALING CO-REGULATE THE TAIL DEVELOPMENT IN ZEBRAFISH

by

YI YANG

B.S., Sichuan University, 2003
M.S., Sichuan University, 2006

AN ABSTRACT OF A DISSERTATION

submitted in partial fulfillment of the requirements for the degree

DOCTOR OF PHILOSOPHY

Division of Biology
College of Arts and Sciences

KANSAS STATE UNIVERSITY
Manhattan, Kansas

2010

Abstract

Multiple signaling pathways regulate development of the posterior zebrafish body, which is derived from a population of progenitor cells called the tailbud, a structure formed at the end of gastrulation. Fate specification and differentiation are closely linked with cell migration to ensure that, as some cells exit the tailbud and differentiate, other cells are retained in the tailbud as undifferentiated precursors to support later growth. The role of BMP signaling in specifying cell fate in the tailbud has been well-characterized. Among the lost ventral tissues like ventral tailfin and cloaca, embryos with compromised BMP signaling produce a curious phenotype-a ventrally located secondary tail containing both somitic muscle and notochord. This phenotype is proposed to be a fate-patterning defect when the BMP gradient lowered to a precise level. However, this morphogen mode is insufficient to explain secondary tail formation without considering BMP also regulates morphogenetic movements during gastrulation, promoting the convergence of lateral mesodermal cells towards the dorsal axis. In this study, we provide evidence that BMP signaling continues to mediate cell movements during tail development. Our data indicate that BMP signaling is activated in the ventroposterior tailbud to promote cell migration during tailbud protrusion, and that it is the defective migration of these cells which ultimately leads to bifurcation of the CNH domain, a presumptive stem cell pool in the tailbud, and formation of a secondary tail in BMP mutants. In parallel, the morphogenesis of tailbud cells is known to be under the control of noncanonical Wnt signaling, although the exact nature of the defect remains unclear. We find that inhibition of noncanonical Wnt signaling also leads to secondary tail formation. Additionally, we show that noncanonical Wnt signaling interacts with BMP signaling to maintain CNH integrity by affecting cadherin localization in CNH cells, possibly disrupting cell cohesion. We propose a model that BMP and a noncanonical Wnt pathway regulate tail morphogenesis by controlling cell migration and cell adhesion within the tailbud.

BMP AND NONCANONICAL WNT SIGNALING CO-REGULATE THE TAIL DEVELOPMENT IN ZEBRAFISH

by

YI YANG

B.S., Sichuan University, 2003
M.S., Sichuan University, 2006

A DISSERTATION

submitted in partial fulfillment of the requirements for the degree

DOCTOR OF PHILOSOPHY

Division of Biology
College of Arts and Sciences

KANSAS STATE UNIVERSITY
Manhattan, Kansas

2010

Approved by:

Major Professor
Alexander Beeser

Copyright

Abstract

Multiple signaling pathways regulate development of the posterior zebrafish body, which is derived from a population of progenitor cells called the tailbud, a structure formed at the end of gastrulation. Fate specification and differentiation are closely linked with cell migration to ensure that, as some cells exit the tailbud and differentiate, other cells are retained in the tailbud as undifferentiated precursors to support later growth. The role of BMP signaling in specifying cell fate in the tailbud has been well-characterized. Among the lost ventral tissues like ventral tailfin and cloaca, embryos with compromised BMP signaling produce a curious phenotype-a ventrally located secondary tail containing both somitic muscle and notochord. This phenotype is proposed to be a fate-patterning defect when the BMP gradient lowered to a precise level. However, this morphogen mode is insufficient to explain secondary tail formation without considering BMP also regulates morphogenetic movements during gastrulation, promoting the convergence of lateral mesodermal cells towards the dorsal axis. In this study, we provide evidence that BMP signaling continues to mediate cell movements during tail development. Our data indicate that BMP signaling is activated in the ventroposterior tailbud to promote cell migration during tailbud protrusion, and that it is the defective migration of these cells which ultimately leads to bifurcation of the CNH domain, a presumptive stem cell pool in the tailbud, and formation of a secondary tail in BMP mutants. In parallel, the morphogenesis of tailbud cells is known to be under the control of noncanonical Wnt signaling, although the exact nature of the defect remains unclear. We find that inhibition of noncanonical Wnt signaling also leads to secondary tail formation. Additionally, we show that noncanonical Wnt signaling interacts with BMP signaling to maintain CNH integrity by affecting cadherin localization in CNH cells, possibly disrupting cell cohesion. We propose a model that BMP and a noncanonical Wnt pathway regulate tail morphogenesis by controlling cell migration and cell adhesion within the tailbud.

Table of Contents

List of Figures

List of Tables

Acknowledgements

I give my most sincere thanks and gratefulness to Dr. Chris Thorpe for leading me into the wonderland of zebrafish research. His hand-to-hand training and word-by-word education prepared me for the future academic career. My achievements cannot be fulfilled without other professors' efforts. My committee members: Dr. Michael Herman, Dr. Alexander Beeser and Dr. Anna Zolkiewska kept giving me advices and providing very insightful suggestions on my research projects. Also I feel very honored to have Dr. Susan Brown and Dr. Richard Todd in my defense panel.

As an international student, I would like to give my hugs to people I worked with, especially Susan Hettenbach and Katelyn O'Neill, who taught me a lot in languages and cultures and gave me the happiest moments at work.

Thanks to Division of Biology for taking good care of my study life and MCDB program for creating harmonious academic atmosphere.

Last but not least, I thank my parents and friends who are very supportive all these years.

Dedication

I dedicate this work to my wife Yang, Chun-hui. She is one of the major reasons that make me want to pursue a Ph.D. and her blesses from across the Pacific Ocean helped me through all those hard times.

CHAPTER 1 - Introduction

Developmental biology is the study of the process by which organisms grow and develop, and it is originated from classical experimental embryology. Since the beginning of the 20th century, through extensive microsurgical experiments on embryos of frogs and sea urchins, people started to believe that chemical signals induce embryonic development, but it was not until the mid-1890s the first signals (fibroblast growth factors and activins) were actually identified (Slack, 2001). With the advent of molecular biology and genetics, it is now possible for scientists to identify these previously mysterious inducing factors and the genes regulated by them.

Inducing factors are mainly proteins secreted by signaling cells that exert effects on target cells via binding to specific receptors and activating signal transduction pathways within the cell, which eventually cause a series of cellular responses such as proliferation, migration and differentiation. By comparing development of diverse species, scientists have identified many important inducing factors that are widely used by most animals during embryogenesis.

The conserved inducing factors include Bone Morphogenic Protein (BMP), Fibroblast Growth Factor (FGF), Hedgehog (a polypeptide ligand), Nodal (a subset of proteins in the transforming growth factor beta superfamily) and Wnt (a glycoprotein named by combining of Wg/wingless in fly and Int-1 in mouse). These signaling-molecule-activated pathways control the formation of body plans as well as cellular organization from the zygote to a complete organism. Cell fate specification and morphological changes (by cell movements) are two concurrent processes in body plan formation. Recently, growing evidence indicates that many signaling pathways, such as BMP, Nodal and FGF instruct cell fate and also regulate cell movements (Heisenberg and Solnica-Krezel, 2008), which supports the idea that cell fate and cell movement are intrinsically connected (Ip and Gridley, 2002; Myers et al., 2002a; Myers et al., 2002b). However, it is still unclear to what extent these two seemingly distinct processes are mechanistically linked. How does a cell behave in the context of multiple signaling inputs, is cell fate pre-determined before its migratory behavior, or is migration required for cell fate acquisition?

Over the last three decades, *Danio rerio*, commonly called the zebrafish, has become an ideal model system for the study of vertebrate development. The zebrafish embryo is fertilized and develops in exutero in optically transparent embryos, which makes the manipulation and visualization of embryos very easy and cost-efficient compared to the efforts to study mouse embryos. The three-month generation time and high fecundity (hundreds of embryos from one pair can be obtained weekly) make zebrafish optimal to perform genetic tests and produce statistically significant results. Large-scale random mutant screening of zebrafish in the 1990s identified sets of mutations responsible for a series of patterning defect phenotypes during embryonic development (Driever et al., 1996; Haffter et al., 1996). With morpholino MO anti-sense oligonucleotide induced gene silencing and the completed genome sequence, reverse genetics can be performed in zebrafish by analyzing the loss-of-function phenotypes and biological functions of any genes involved in early development (Nasevicius and Ekker, 2000). GFP (green fluorescent protein) transgenic reporter is a very useful modern molecular tool widely used in zebrafish. Briefly, the GFP gene is fused downstream of a tissue-specific promoter and this construct is then inserted into the genome of zebrafish to generate a transgenic line (Long et al., 1997). The in vivo tissue-specific expression of GFP in optically transparent zebrafish embryos can highlight the cells within a particular region, which allows for the real time imaging of cells undergoing morphogenetic movement.

Tail development in zebrafish

In vertebrates, posterior body (posterior trunk and tail) growth is a central event of body plan formation, which requires properly coordinated cell fate specification and movements to ensure normal development. Generally, tail development involves the addition of segmented muscle tissue (somites) and growth of the spinal cord that extends between somites along the midline of the body axis. In chordates, the post-anal tail is one of the definitive features, which is different from the tail-like appendages in invertebrates. The internal composition of a tail--with neural tube, notochord and muscle--is the same as that of the main body axis, so tail formation is expected to share similar molecular mechanisms underlying pattern formation, morphogenesis, cell determination and differentiation with that of the vertebrate body plan as a whole. Humans also have a tail during embryogenesis but it is a vestigial structure that transiently exists during the first two months of development (Fuhrmann, 1965).

Formation of the tailbud

After fertilization, the zebrafish zygote multiplys by mitotic cell division during the first 3 hours, which results in a cell mass in the animal pole region (developmental stages are thoroughly described in Kimmel et al., 1995). Then, this clump of cells becomes motile and thins in a sheet of cells called the blastoderm that moves towards the vegetal pole to envelope the yolk in a process is called epiboly. Stages of zebrafish development are identified as percentage of epiboly, depending on how much of the yolk has been covered. At 50% epiboly (5.5 hpf), cells at the leading edge of the migrating blastoderm, also called the margin, begin to involute. This process, called gastrulation, generates three distinct germ layers, endoderm, mesoderm and ectoderm (Fig. 1.1A). Beginning during early stages of gastrulation, a series of morphogenic movements known as 'convergence and extension' (CE) start to elongate the body axis from the original oval shape and consequently push the tail away from the head (Keller, 2002). Laterally positioned cells migrate toward the dorsal midline (dorsal convergence). When they reach the dorsal midline at late gastrulation, cells insert into the presumptive notochord region and get rearranged by changing their neighbors (mediolateral intercalation), which consequently narrows the body axis and contributes to anteriorposterior extension (Wallingford et al., 2002). (Fig. 1.1A). Epiboly finishes as blastoderm marginal cells come together at the vegetal pole to form a bud-like structure at 11-12 hpf (Fig. 1.1B).

Fate mapping evidence demonstrates this bud-like cell aggregate is capable of giving rise to the entire posterior body including tail, so it is called the tailbud (Kanki and Ho, 1997; Agathon et al., 2003) (Fig. 1.1C). Formation of the tailbud is generally considered the end of gastrulation and the starting point of tail development. This group of cells gradually differentiates into the complete posterior body (posterior trunk and tail) over the next 12 hours (Kanki and Ho, 1997) (Fig. 1.1A-C). Transplantation experiments in zebrafish embryos show that the tailbud is not homogenous. The anterior tailbud, derived from dorsal mesoderm, is primarily patterned into axial structures like the notochord, while the posterior tailbud, derived from ventral mesoderm, gets patterned into paraxial tissues like tail somites (Agathon et al., 2003).

Tail development

During post-gastrula stages, tail development is divided into several steps: extension (12-16 hpf, when the tailbud extends along the surface of yolk), protrusion (16-18 hpf, when the tailbud begins to leave yolk) and eversion (>18 hpf, when the tailbud protrudes out away from the yolk and the tail starts to emerge) (Kanki and Ho, 1997). During these steps, the gastrula-like convergence and extension movements continue to shape the tail. As the tailbud extends, paraxial tissues converge towards the midline to facilitate the posteriorward extension of the body (Fig. 1.1D). Meanwhile, there are unique tailbud movements: the posterior tailbud cells diverge away from the midline by moving laterally and anteriorly and subduct underneath the posteriorly migrating anterior tailbud cells (Fig. 1.1D).

As in many teleosts, a transiently ciliated organ called Kupffer's vesicle is found in the zebrafish tailbud (Essner et al., 2005). It originates from the dorsal forerunner cells during gastrulation and is involved in the establishment of left and right symmetry (Essner et al., 2005). The Kupffer's vesicle is located between the yolk and tailbud during the extension stage, and gradually incorporates into the tailbud and eventually disappears during tail eversion. Since physical ablation of Kupffer's vesicle or perturbation of its formation by morpholinos result in a normal tail (Essner et al., 2005), whether Kupffer's vesicle plays a role in tail development is still unknown, but it is normally treated as a morphological landmark that marks the interface between the anterior and posterior tailbud (Fig. 1.1B, inset).

Within the developing tailbud, not all cells are determined. A minority of dorsal derived cells lying posterior to the notochord, termed the chordoneural hinge (CNH), are suggested to be a pluripotent stem cell-like population (Cambray and Wilson, 2002; Cambray and Wilson, 2007). In *Xenopus*, CNH cells contribute to notochord, neurons and somites and are capable of producing ectopic tails when grafted to host embryos (Charrier et al., 1999). In mice, in addition to giving rise to equivalent tissue types as in *Xenopus*, CNH cells contribute to the tailbud mesoderm and retain the self-renewable ability(Cambray and Wilson, 2002). In zebrafish, CNH can differentiate into notochord, hypochord and ventral neural tube (Agathon et al., 2003).

The BMP signaling pathway in zebrafish

The BMP signaling pathway in vertebrates has been demonstrated to have a crucial role in trunk and tail formation (reviewed in von Bubnoff and Cho, 2001) (see Fig. 1.2E for

schematic BMP pathway). BMP proteins are members of the TGFβ superfamily, and dimerized BMP ligands (BMP2/4/7) bind to type I and type II transmembrane receptors of activin receptor-like kinase (Alk) family, which result in the phosphorylation of type I receptors (von Bubnoff and Cho, 2001). Activated type I receptors phosphorylate downstream effectors r-Smads (Smad1/5/8) to enable their association with co-Smad (Smad4). The complex of r-Smads and Smad4 shuttles into the nucleus to initiate transcripition of targets. BMP signaling activity is regulated by a myriad of inhibitory proteins such as extracellular antagonists: Chordin, Noggin and Follistatin as well as intracellular inhibitory Smads (I-Smads): Smad6 and Smad7. Excessive Chordin is degraded by metalloproteinase, Tolloid (Little and Mullins, 2006).

BMP signaling in fate specification

In zebrafish, during the early blastula stage, *bmp2b* and *bmp7* expression is initially ubiquitous (Kishimoto et al., 1997; Dick et al., 2000) (Fig. 1.2A), but then becomes extinguished from the dorsal side (Fig. 1.2B). During this stage, BMP starts to define the presumptive ventral side by inducing the ventrolateral expression of transcription factor genes *vox*, *vent* and *ved* (Imai et al., 2001; Shimizu et al., 2002). BMP is suppressed dorsally by *bozozok*, a transcriptional repressor that directly inhibits expression of *bmps* (Fekany et al., 1999) (Fig. 1.2B). The initial ventral and dorsal domains are defined through the establishment of BMP-positive and BMP-negative regions during the blastula stage

During gastrulation, BMP act as a morphogen to pattern DV fates (reviewed in Little and Mullins, 2006). According to this model, a gradient of BMP activity is established along the DV axis due to interaction of BMP agonists and antagonists. Ventral and ventrolateral mesoderm that receives high and intermediate BMP signaling adopts the fates of blood, vasculature, pronephoros and tail somites, while low BMP activity specifies dorsal fates such as notochord and trunk somites (Fig. 1.2D). Loss of BMP signaling causes dorsalized phenotypes with expansion of dorsal fates at the expense of ventral fates (Fig. 1.2F).

BMP signaling also patterns ectoderm in a gradient. A high level of BMPs is required for the specification of epidermis; an intermediate level of BMPs is required for the specification of neural crest and BMPs need to be inhibited to promote the fates of neurectoderm (Fig. 1.2D). Inhibiting BMPs by inducing overexpression of *hsp70:chd* (*chordin/chd* under control of heatshock inducible promoter *hsp70*) at 30 minutes progression from early to late gastrulation (4

hpf-6.5 hpf) reveals BMP signaling progressively patterns ventrolateral ectodermal tissues along the anterior-posterior axis with more anterior cells being patterned prior to posterior ones (Tucker et al., 2008).

This BMP morphogen model in the gastrula is supported by a series of mutants that are defective in BMP signaling. *swirl*/*bmp2b* mutants represent the most severe loss of BMP signaling, in which derived trunk somites (specified on the dorsal side of embryo during gastrulation) are expanded, ventrally derived blood, vasculature and pronephros are reduced and the tail is literally absent (Kishimoto et al., 1997) (Fig. 1.2F C5). Other mutants that are defective in components of the BMP pathway, including *snailhouse*/*bmp7* (Dick et al., 2000) (Fig. 1.2F C4), *piggytail*/*smad5* (Kramer et al., 2002) (Fig. 1.2F C3), *lost-a-fin*/*alk8* (Mintzer et al., 2001) (Fig. 1.2F C2) and *minifin*/*tolloid* (Connors et al., 1999) (Fig. 1.2F C1), exhibit progressively less severe phenotypes than *swirl*. In *minifin* embryos, which are defective in the BMP agonist Tolloid, which promotes BMP signaling by degrading Chordin (an inhibitor that directly binds to BMP ligands), tail structures are largely complete, except for reduced ventral tail fin and vascular structures (Connors et al., 1999). In contrast, *chordino/chordin* mutants with excess BMP activity, show reduced notochord with fused tail somites and extra blood, kidney, vasculature and tail fins (Schulte-Merker et al., 1997) (Fig. 1.2F V1).

In zebrafish, the tail organizer is a group of cell from the ventral margin that, when transplanted to a different region of the embryo, can direct the formation of an extensive tail, lacking only notochord (Agathon et al., 2003). Ectopic expression of BMP, together with Wnt and Nodal, in blastula cells is capable of specifying a new tail organizer (Agathon et al., 2003). Transplantation experiments suggest ventral marginal cells from the blastula and early gastrula have the more potential to induce tail structure than donor cells from later stages (Agathon et al., 2003). These results suggest BMP signaling starts to exert its effect in tail development from the blastula stage, almost ten hours before the emergence of the tailbud itself.

Inhibition of BMP signaling by using the BMP-specific small-molecule inhibitor Dorsomorphin (Yu et al., 2008) or transgenic zebrafish lines carrying a heat-shock inducible dominant-negative truncated BMP receptor (dnBMPR) (Pyati et al., 2005) or Chordin (*hsp70:chd*) (Tucker et al., 2008), reveals the temporal roles of BMP signaling in specifying ventral mesoderm tissues. Inhibiting BMP signaling in embryos at an early gastrula stage phenocopies *swirl* and *snailhouse* mutants, confirming an early role for BMP signaling in

specifying primary tail tissue. From late gastrula to early somitogenesis stage, inhibiting BMP phenocopies those weakly dorsalized mutants such as *piggytail*, *lost-a-fin*, *minifin* and recently characterized *bmp4* mutants (Stickney et al., 2007) that commonly have reduced tail fin and cloaca (opening of gut and kidney). Taken together, the role of BMP signaling during early development is to pattern ventral derivatives and specify a primary tail, while the late phase BMP signaling patterns ventroposterior fates like the ventral tail fin and cloaca.

Secondary tail formation in BMP-deficient embryos

Interestingly, inhibiting BMP signaling at post-gastrula stages in dnBMPR (transgenic zebrafish lines carrying a heat-shock inducible dominant-negative truncated BMP receptor) embryos sometimes results in the formation of a short secondary tail, a phenotype also observed in some *minifin* zygotes (Pyati et al., 2005). The secondary tail always emerges from the ventral side of the primary tail and is smaller in size, which makes the end of the tail looks bifurcated (Fig. 1.2F arrow). It has been shown that secondary tails can have many of the same tissues as primary tails, including tailbud cells, somatic tissue, notochord, hypochord, epidermis and pigment (Pyati et al., 2005). So far, there are two distinct models that have been proposed to explain these phenotypes. One model proposes that BMP signaling functions to prevent secondary tail formation independently from its fate-patterning role in the tailbud (Pyati et al., 2005). The other model proposes that BMP continues to act as morphogen after gastrulation and that a secondary tail is formed as a result of expanded mesoderm fates (Stickney et al., 2007). More specifically, the morphogen model predicts that a high level of BMP signaling is required for the ventral tail fin and cloaca fates and that an intermediate level of BMP signaling is required for the tail mesoderm and blood fates. When BMP signaling is slightly reduced, ventral tail fin and cloaca-fated cells fall into the intermediate level range of BMP signaling and acquire the fates of tail mesoderm and blood cells. This expansion of tail mesoderm accounts for the emergence of a secondary tail. When BMP signaling is reduced below the intermediate level, tail mesoderm and blood fates are reduced, which results in a shortening of the primary tail, thus there are no mesodermal cells that could be patterned to form a secondary tail. However, the later model is not fully supported by the experimental results. Several experiments suggest that the extreme ventral mesoderm is mis-fated into blood and vascular progenitors from ventral tail fin and cloaca only when BMP signaling is inhibited within a short time frame at mid-gastrula stage.

This does not explain the secondary tail formed when BMP is inhibited at later stages. The model is weakened by the observation that *bmp4* mutants that show the expected expansion of somites and blood do not develop secondary tails (Stickney et al., 2007). So far, why and how BMP-deficient embryos produce secondary tails is still unclear.

BMP signaling in cell movements

In other systems, BMP has been suggested to be involved in cell movement regulation. For example, in the mouse embryo, *bmp4* negatively regulates ectoderm migration during lung bud morphogenesis (Weaver et al., 2000). In zebrafish, BMP signaling has also been demonstrated to play a role in the regulation of cell movements. A BMP gradient appears to regulate cell movements during gastrulation. Cell-tracking experiments indicate that gastrula cells along the DV axis can be divided into three domains based on their convergence (mediolateral narrowing) and extension (anterioposterior elongation) (CE) movements (Myers et al., 2002a). On the ventral side, high levels of BMP signaling create a no-convergence-no-extension domain where cells move directly to the vegetal pole to participate in tailbud formation. Lower BMP activity promotes the CE movements of lateral gastrula cells by polarizing them along the mediolateral axis, where they actively translocate to the dorsal side with increasing speed. In the dorsal domain, where BMP activity is lowest, cells exhibit strong extension but only modest convergence movements as a result of intercalation of dorsolateral cells. BMP has been suggested to affect cell movements in parallel to cell fate specification by suppressing the expression of *wnt11* and *wnt5a*, two genes involved in a noncanonical Wnt pathway that specifically regulates CE movements without impacting cell fate (see below for more detailed description of the noncanonical Wnt pathway) (Myers et al., 2002a). However, a recent study has shown that the migratory behavior of gastrula cells is able to respond to BMP independently of *wnt5a* or *wnt11* (von der Hardt et al., 2007). Moreover, during gastrulation, BMP negatively regulates Cadherin-mediated cell-cell adhesion (for a more detailed description, see 'Cadherin' section, below) (von der Hardt et al., 2007). Along the DV axis of gastrula-stage embryos, cell adhesion is lowest on the ventral side and highest on the dorsal side, which opposes the BMP gradient. This adhesion between cells is important for lamellipodia-driven directional migration of mesodermal progenitors (Bakkers et al., 2004). As lateral cells converge to the dorsal midline with increasing speed, they require higher adhesion with neighboring cells

in order to exchange places and move. The ventral cells do not converge, as there is little adhesion between these cells. This BMP-mediated adhesion gradient provides an explanation to the three CE domains described earlier. More importantly, this mechanism does not alter cell fates, which indicates that BMP signaling has separable roles in cell fate specification and morphogenesis regulation (von der Hardt et al., 2007). However, the current studies only address the role of BMP signaling during gastrulation. Whether BMP signaling continues to regulate cell movements after gastrulation is largely unknown.

The noncanonical Wnt signaling pathway

Over the past two decades, an abundance of evidence from multiple experimental systems has demonstrated a conserved role for the noncanonical Wnt signaling pathway (also known as β-catenin independent Wnt signaling) in the regulation of cell polarity and cell movements (reviewed in Veeman et al., 2003a). Unlike so-called canonical Wnts, noncanonical Wnt ligands such as Wnt5 and Wnt11 transduce signals without stabilization of β-catenin (Moon et al., 1993; Du et al., 1995). In vertebrates, a major function of noncanonical Wnt signaling is to regulate CE movements without affecting cell fates. The noncanonical Wnt pathway is also referred to as the Wnt/PCP pathway, because it governs CE movements in vertebrates in a mechanism similar to planar cell polarity (PCP) pathway in the fruit fly, *Drosophila melanogaster* (Veeman et al., 2003a). In vertebrates, the mesenchymal cells undergoing CE movements need to be polarized to move collectively, just as the epithelial cells in the wing and eye of *Drosophila* need polarity to be arrayed consistently (Keller, 2002). Many of the components involved in the PCP pathway in *Drosophila* have been shown to function in noncanonical Wnt pathways in vertebrates.

The PCP pathway in Drosophila

In *Drosophila*, the PCP pathway has a clear requirement in the polarity of wing hair and ommatidia (reviewed in Adler, 2002). Upon disruption of PCP signaling, distally-pointing wing hairs become mis-oriented and ommatidia become disorganized. The establishment of cellular polarity is thought to require the asymmetric subcellular localization of the core PCP factors, including the transmembrane proteins Frizzled (Fz) and Strabismus (Stbm), the cytoplasmic protein Dishevelled (abbreviated as Dsh in *Drosophila* and *Xenopus*; Dvl in mouse and

zebrafish) and Prickle (Pk). Pk and Dsh are recruited to the cell membrane in response to active PCP signaling. As modeled in the wing epithelia cell (Fig. 1.3A), upon activation of the PCP pathway, Fz-Dsh complexes become anchored at the distal surface, while Stbm-Pk complexes become localized at the opposite side of the cell, at the proximal surface. It has been suggested that this asymmetry leads to polarity establishment via the rearrangement of cytoskeletal components (Harris and Peifer, 2007; Kim et al., 2010). Genetic studies so far find these opposing components of the PCP pathway genetically antagonize each other. For instance, in the *Drosophila* wing, the overexpression phenotype of *stbm* resembles the loss-of-function phenotype of *fz* , and the converse is also true (Adler et al., 1997; Bastock et al., 2003). In addition, a loss of *stbm* is able to suppress the *fz* mutant phenotype (Wu and Mlodzik, 2008). A generally accepted model suggests that Fz promotes the Dsh-dependent activation of a downstream cascade, while the Stbm-Pk complex functions to inhibit Dsh activation (Tree et al., 2002; Jenny et al., 2005).

The noncanonical Wnt pathway in zebrafish

In zebrafish, CE movements involve complex polarized behaviors including directional migration (i.e., dorsal convergence), orientation of cell division, cell-shape changes and cell rearrangement (intercalation of cells at the midline, for example) (reviewed in Wallingford et al., 2002). Zebrafish *silberblick/*(*slb*)*/wnt11* (Ulrich et al., 2005) and *pipetail*(*ppt*)*/wnt5* (Kilian et al., 2003) are two mutants that affect noncanonical Wnt genes and show morphogenic defects in CE movements . Phenotypically, these mutant embryos have a shortened body axis, thinner and wider somites and occasional cyclopia. This is quite different from the phenotype of canonical Wnt mutants, *wnt3* and *wnt8*, which affect cell fate specification, particularly in the posterior (Thorpe et al., 2005).

The first evidence that correlates noncanonical Wnt signaling to PCP signaling came from the studies of the Dsh protein (reviewed in Wallingford and Habas, 2005). In *Drosophila*, Dsh is a central protein involved both in canonical Wnt and PCP signaling (Axelrod et al., 1998; Boutros et al., 1998). Deletion constructs of Dsh show that three separate functional domains (DIX, PDZ and DEP domains) are involved in different signaling pathways: for canonical Wnt signaling the DIX and PDZ domains are used and for PCP signaling the PDZ and DEP domains are used (Axelrod et al., 1998; Boutros et al., 1998; Moriguchi et al., 1999). Overexpressing Dsh

variant (Dsh-DEP+: DEP domain only) that blocks the PCP pathway in the fly could also disrupt CE movements in frog and zebrafish (Heisenberg et al., 2000; Tada and Smith, 2000). Correspondingly, overexpressing a variant Dsh (DshΔDIX: DIX domain truncated) that blocks the canonical Wnt pathway in the fly could rescue *wnt11* mutants in frog and zebrafish (Heisenberg et al., 2000; Tada and Smith, 2000). With the identification of more vertebrate homologs of PCP pathway components, the conserved Wnt/PCP pathway becomes recognized, including the core components of the PCP pathway such as Pk, Fz, Stbm and Dsh/Dvl. It is worth noting that the noncanonical Wnt pathway in vertebrates involves PCP-exclusive Wnt ligands that have yet to be identified in the *Drosophila* PCP pathway. In zebrafish, the *trilobite*(*tri*)*/stbm* (Park and Moon, 2002), *knypek*(*kny*)*/glypican4* (a gene encoding a putative co-receptor for noncanonical Wnt proteins) mutants (Topczewski et al., 2001), together with *pk* (Carreira-Barbosa et al., 2003; Veeman et al., 2003b) *and dvl2*/3 morphants (Angers et al., 2006) all exhibit CE defects without obviously affected cell fates. Morpholino-induced loss-of-function studies in zebrafish embryos suggest that *dvl2* and *dvl3* are exclusively involved in the noncanonical Wnt pathway (Angers et al., 2006). In the epithelial wing cells of the fly, the asymmetric distribution of core PCP factors is well characterized, but whether this is consistent in the highly motile vertebrate cells is just beginning to be investigated.

Several experiments provide evidence suggesting that the mechanism underlying the Wnt/PCP pathway might be conserved between fly and fish. In zebrafish embryo, GFP-tagged Pk and Dsh do become asymmetrically localized in migrating cells (Yin et al., 2008). Pk-GFP is preferentially localized anteriorly on the membrane of axial and presomitic mesoderm cells that are undergoing a cell rearrangement called mediolateral intercalation (Yin et al., 2008). Further, this localization is dependent on the functions of *kny, stbm and dvl* (Yin et al., 2008). In *kny;tri* double mutants, and in embryos overexpressing dominant-negative *Xenopus* Dsh, the anterior localization of Pk is abolished and become more cytoplasmic, accompanied by defective cell intercalation (Yin et al., 2008). Moreover, in axial mesoderm, Dsh-GFP is enriched along the posterior membrane, which is mediated by *kny* and *tri* (Yin et al., 2008). In *kny* and *tri* mutants, Dsh becomes more cytoplasmic and in the *kny;tri* double mutant the posterior localized Dsh is nearly absent (Yin et al., 2008). This suggests Dsh and Pk have opposite localization in migrating gastrula cells of the zebrafish embryo. The results are consistent with the protein interaction model in the fly wing that suggests that Dsh and Pk become localized to opposite

sides of the cell. The results also suggest *kny* functions mutually with *stbm* to regulate CE movements. In zebrafish, serial double-mutant, double-morpholino, and morpholino/mutant experiments with following genes: *slb;ppt* (Kilian et al., 2003), *pk1* and *stbm* (Carreira-Barbosa et al., 2003; Veeman et al., 2003b), *pk1* and *slb* (Carreira-Barbosa et al., 2003) and *pk1* and *ppt* (Carreira-Barbosa et al., 2003) all show a more severe CE phenotype.

In searching for the mechanism underlying noncanonical Wnt signaling, three downstream cascades have been proposed. One pathway downstream of Dsh leads to the activation of small GTPases of the Rho family, including Rho, Rac and Cdc42 (Habas et al., 2001; Choi and Han, 2002; Habas et al., 2003; Penzo-Mendez et al., 2003). Overexpression of these GTPases in *Xenopus* causes a CE phenotype. In zebrafish, Rho-bridging protein Daam1 (Kida et al., 2007) and Rho kinase (ROK2) (Marlow et al., 2002) have been show to affect CE movements in downstream of noncanonical Wnt signaling. Another potential target of noncanonical Wnt signaling is the c-Jun N-terminal kinases, JNK pathway. In the fly, blocking the JNK pathway suppresses the Dsh overexpression phenotype (Boutros et al., 1998). In vertebrate cells, Dvl is also shown to activate JNK signaling (Boutros et al., 1998; Li et al., 1999; Moriguchi et al., 1999). The third noncanonical Wnt pathway involves calcium signaling. As shown in zebrafish embryos, overexpression of Wnt5a or Pk1 at the blastula stage stimulates calcium flux (rapid, aperiodic transient increase of intracellular free Ca^{2+}) (Slusarski et al., 1997). In *Xenopus*, overexpression of Wnt5 or Wnt11 activates two calcium-dependent kinases, PKC and CamKII (Sheldahl et al., 1999; Kuhl et al., 2000). These are potential targets downstream of noncanonical Wnt signaling that could affect CE movements. However, these branches of noncanonical Wnt signaling still require further characterization and validation.

Most of the current studies mainly concern the roles of noncanonical Wnt signaling in the regulation of CE movements during gastrulation. Less is understood about the role of noncanonical Wnt signaling after gastrulation. From the study of *ppt* and *kny*, noncanonical Wnt signaling appears to regulate tail morphogenesis. The *ppt* and *kny* single mutants have shortened tails without loss of tail tissues (Marlow et al., 2004). A T-box transcription factor gene, *ntl* cooperates with *ppt* and *kny* to regulate CE-like movements within the tailbud, and to promote the tailbud-specific subduction movements (Marlow et al., 2004). Double mutants *kny;ntl* and *ppt;ntl* exhibit a synergistic tail shortening phenotype (Marlow et al., 2004). By cell labeling experiments, it was found that posterior tailbud cells in *ppt* and *kny* have a reduced rate of

extension and lateral divergent movements (Marlow et al., 2004). In *kny;ntl* and *ppt;ntl*, the labeled cells are retained in the posterior tailbud, suggesting a total loss of movements (Marlow et al., 2004). It was further demonstrated that the shortened tail is due to cell movement defects but not fate mis-specification, reduced proliferation or increased apoptosis (Marlow et al., 2004). The function of other components of noncanonical Wnt signaling after gastrulation is still unclear. How this signaling is used in distinct contexts and developmental stages is one of the key questions that needs to be addressed in the future.

Cadherin in zebrafish development

Tissue morphogenesis during development requires cadherin-mediated cell-cell adhesion. Migrating cells rapidly de-adhere and re-adhere to neighboring cells during translocation, and this is achieved through dynamic disassembly and reassembly of adhesion complexes (Ulrich et al., 2005). The cadherin family is composed of classical cadherins, protocadherins and atypical cadherins (reviewed in Halbleib and Nelson, 2006). Generally, classical cadherins are characterized by an extracellular domain that forms Ca^{2+}-dependent homophilic interactions, a transmembrane domain and an intracellular domain that directly binds to β-catenin and p120. Protocadherins and atypical cadherins are distinguished from classical cadherins by their additional extracellular motifs and different cytoplasmic tails that interact with selective binding partners (Halbleib and Nelson, 2006).

In zebrafish, *flamingo*, a gene encoding an atypical cadherin, functions with *stbm* and *wnt11* to regulate CE movements during gastrulation (Formstone and Mason, 2005). Inhibiting *flamingo* suppresses the extension of the anterior-posterior body axis (Formstone and Mason, 2005; Carreira-Barbosa et al., 2009). A hanging drop aggregation assay (measuring adhesive properties of cells) shows that embryonic cells with compromised *flamingo* have different cohesive properities from wide type cells (Carreira-Barbosa et al., 2009). Zebrafish *paraxial protocadherin* (*papc*) encodes a protocadherin that is expressed in trunk mesoderm during gastrulation (Yamamoto et al., 1998). Blocking *papc* activity by expressing a dominant-negative secreted construct blocks proper dorsal convergence movements during gastrulation, indicating that *papc* is required for early morphogenentic movements in the embryo (Yamamoto et al., 1998).

Classical cadherins, including E-cadherin (epithelial) and N-cadherin (neuronal) are also required for mesodermal morphogenesis (Halbleib and Nelson, 2006). Zebrafish embryos carrying different mutated alleles of *e-cadherin* exhibit a series of movement defects during gastrulation, including arrested epiboly, defective intercalation and impaired overall CE movements (Kane et al., 2005). N-cadherin in zebrafish has a broad expression pattern during early development and N-cadherin deficient mutants have abnormal brain and tail morphogenesis (Lele et al., 2002). Moreover, a semi-dominant *N-cadherin* allele genetically interacts with *stbm* to mediate elongation of the posterior body (Warga and Kane, 2007).

Growing evidence has shown that distinct signaling pathways regulate cell movements by impinging on cadherin through a variety of mechanisms. During gastrulation, Wnt11 has been proposed to regulate the endocytosis of E-cadherin in migrating prechordal plate cells via the GTPase Rab5 (Ulrich et al., 2005). Wnt11-deficient cells were also shown to adhere more weakly to an E-cadherin coated substrate, suggesting that noncanonical Wnt signaling may regulate morphogenesis by promoting intercellular adhesion (Ulrich et al., 2005). As mentioned previously, BMP signaling guides gastrula cell movements by negatively regulating cadherin-dependent cell adhesion. Thus, a gradient of intercellular adhesion is established across the DV axis in response to graded BMP activity. Adhesion strength is highest dorsally, where BMP activity is lowest, and declines in more lateral and ventral regions, where BMP activity is higher. When mesodermal cells converge to the dorsal midline, they project lamellipodia in all directions. Lamellipodia that contact more dorsally positioned neighboring cells are more likely to form a stable contact with that cell (due to the higher adhesive properties) and pull the cell extending the lamellipodia in a dorsal direction. It will be interesting to see whether and how cadherin interacts with these signaling pathways to regulate tail morphogenesis after gastrulation.

Summary

Morphogenesis refers to the cell movements that shape the organism in three dimensions. This controls the organized spatial distribution of cells during embryonic development. How the cells move in response to the signals induced by multiple morphogenetic cues is not well understood. This dissertation focuses on the roles of intercellular signaling pathways underlying tail development and dorsoventral patterning in the zebrafish embryo. Chapter 2 describes our investigations into how BMP and noncanonical Wnt signaling function together to regulate tail

morphogenesis. The studies described in this chapter form the basis of a manuscript currently under consideration by the journal *Development*. The formation of secondary tails in BMP-compromised embryos has been observed for a long time, going back to the isolation of the first BMP pathway mutants, but no convincing explanation for their development has been put forward. We discovered that this phenotype in BMP-deficient embryos is primarily due to the mis-migration of a group of posterior mesoderm cells, not due to the production of excess tail mesoderm, as had been previously proposed (Stickney et al,. 2007). BMP signaling has to be activated at the right time and right place to ensure normal tail morphogenesis. Additionally, we found that noncanonical Wnt signaling functions redundantly but independently with BMP signaling to prevent secondary tail formation. As in BMP-compromised embryos, the secondary tails are primarily composed of mesoderm tissues. Defective cell migration early in tail development results in a bifurcation of a population of pluriopotent cells in the tailbud called the chordoneural hinge (CNH). Ectopic CNH cells subsequently give rise to secondary tails.

We also assessed the potential role of cadherin in tail morphogenesis. We find that noncanonical Wnt signaling regulates the localization of cadherin within the CNH, likely affecting the cohesion of this group of cells. We propose a model that during tail morphogenesis BMP signaling is activated in the posterior mesoderm of tailbud to ensure their proper migration and noncanonical Wnt signaling is required in the CNH region of tailbud to promote cadherin-dependent cell cohesiveness. This study demonstrates that BMP and noncanonical Wnt pathways are also required after gastrulation to control morphogenetic movements in the embryo.

In Chapter 3, we describe the characterization of two homologs of *smad6* (*smad6.1* and *smad6.2*), and *smad6.2* was identified in a yeast two hybrid screen for candidate proteins that bind to Spork (the ortholog of human ARHGAP21 in zebrafish). The rationale of this screening is that knocking down *spork* leads to secondary tail formation and we are looking for other Spork-associated proteins and study their roles in tail development. However, loss-of-function studies of the two *smad6* homologs do not show any obvious tail phenotype. From initial studies, we found that *smad6* functions as BMP signaling inhibitor to impact dorsoventral patterning during gastrulation, and that *smad6* expression is responsive to down- and up-regulated BMP activity. These results suggest that in zebrafish *smad6* functions as a feedback inhibitor of BMP signaling in order to fine tune BMP activity.

Lastly, we describe further genetic studies concerning secondary tail formation in the Appendix. We found that *pk1* and *stbm* genetically antagonize *dvl* and *kny* in secondary tail formation, similar to the inhibitory interactions between homologs of these genes observed in studies of *Drosophila* PCP signaling. Unexpectedly, we observed that inhibition of *pk1* suppressed secondary tail formation in *mfn*, while inhibition of *stbm* promoted secondary tail development in *mfn.* The mechanisms behind these genetic interactions await further investigation. In addition to their well described roles in development, BMP and noncanonical Wnt signaling play a critical role in cancer progression and metastasis (reviewed in Jessen, 2009; Ye et al., 2009). As many tumors initiate with aberrant cell movements, secondary tail formation may also serve us a tumorigenesis model, so understanding the genetic regulation and identifying enhancers and suppressors involved in this process could give us insight into areas potentially impacting human health.

Figures and Tables

Figure 1.1 Tail development in zebrafish.

(A) Position and movement of ventral (red) and dorsal (blue) marginal cells at the shield stage. Green arrows indicate the involution at the margin. Yellow arrow indicates the convergence of lateral margin. Purple arrow indicates the epibolic movement.

(B) At the end of gastrulation, ventral (red) and dorsal (blue) marginal cells form tailbud. Tailbud is formed as shown in the inset. kv, Kupffer's vesicle.

(**C**) At 24 h after fertilization, the dorsal margin contributes to axial structures (blue); ventral margin contributes to non-axial tissues (red).

(D) Dorsal view of schematic cell movements in tail development.

(A-C) is adapted from (Agathon et al., 2003). (D) is adapted from (Kanki and Ho, 1997).

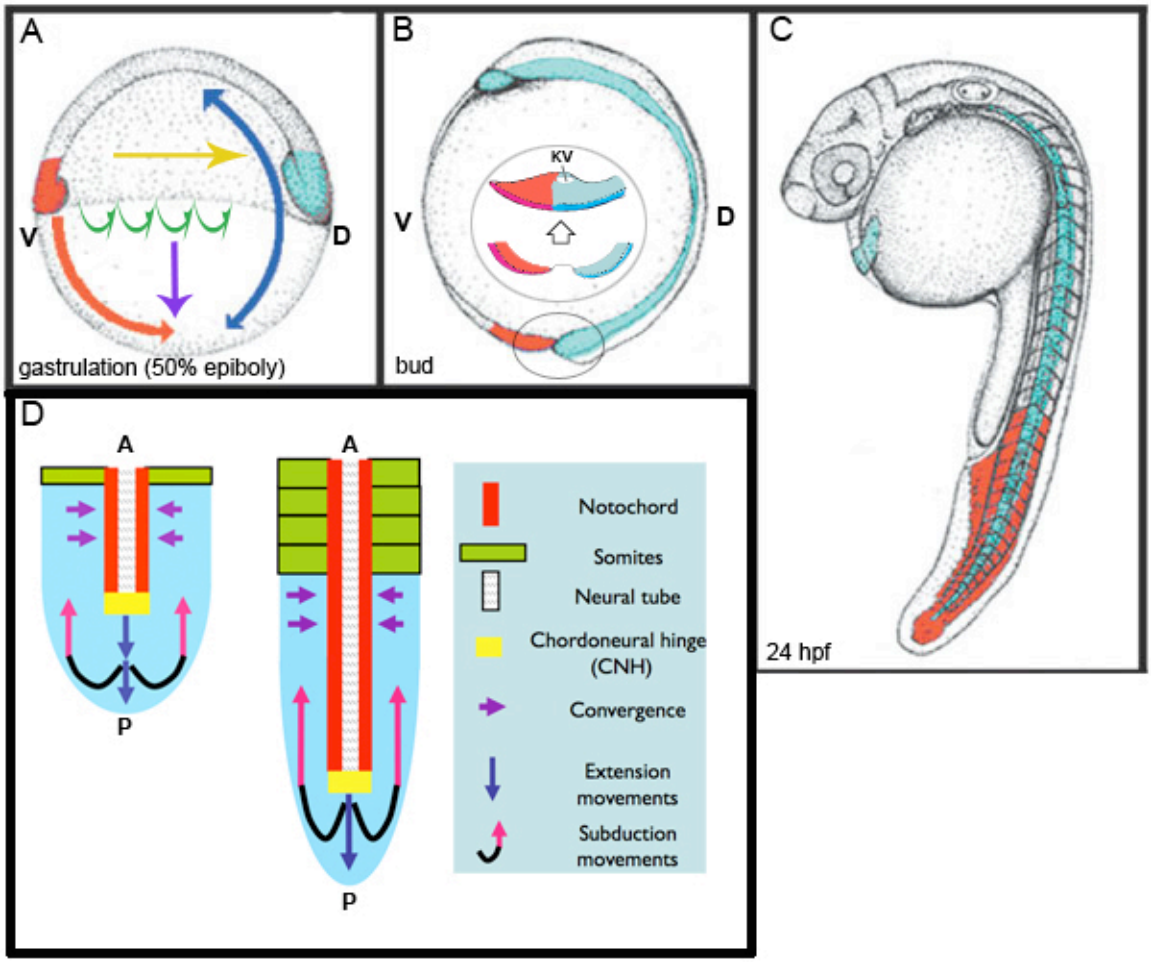

Figure 1.2 BMP signaling in zebrafish.

(A-C) Schematic of BMP signaling in the zebrafish embryo. (A) At early blastula, genes encoding BMP ligands are expressed throughout the blastoderm. (B) BMP expression is subsequently eliminated in the dorsal domain by *bozozok*. (C) By the onset of gastrulation, an established BMP signaling gradient establishes three CE domains. A high level of BMP on the ventral side creates a no-convergence-no-extension domain where cells move directly to the vegetal pole. Lower BMP activity promotes the CE movements of lateral gastrula cells, which eventually converge on the dorsal side. In the dorsal domain, where BMP activity is lowest, cells exhibit strong extension.

(D) Low resolution fate map of the zebrafish embryo at the start of gastrulation.

(E) Model of the BMP signal transduction pathway. Extracellular BMP dimers bind to the type I and type II BMP receptor complexes at the cell membrane. The BMP type II receptor phosphorylates the type I receptor, which transduces the signal by phosphorylating an R-Smad protein. The phosphorylated R-Smad binds with a Co-Smad, and the complex is translocated into the nucleus, where it activates transcription of target genes. Regulators of BMP pathway include Tolloid, Chordin and I-Smads. P, phosphorylations.

(F) Morphologies of normal (N), dorsalized (C1–C5) and ventralized (V1) embryos. V1 and C1embryos are weakly ventralized or dorsalized, respectively. arrowhead indicates the secondary tail formed in part of the C1 embryos.

(A-D) is adapted from (Little and Mullins, 2006). (E-F) is adapted from (Kondo, 2007).

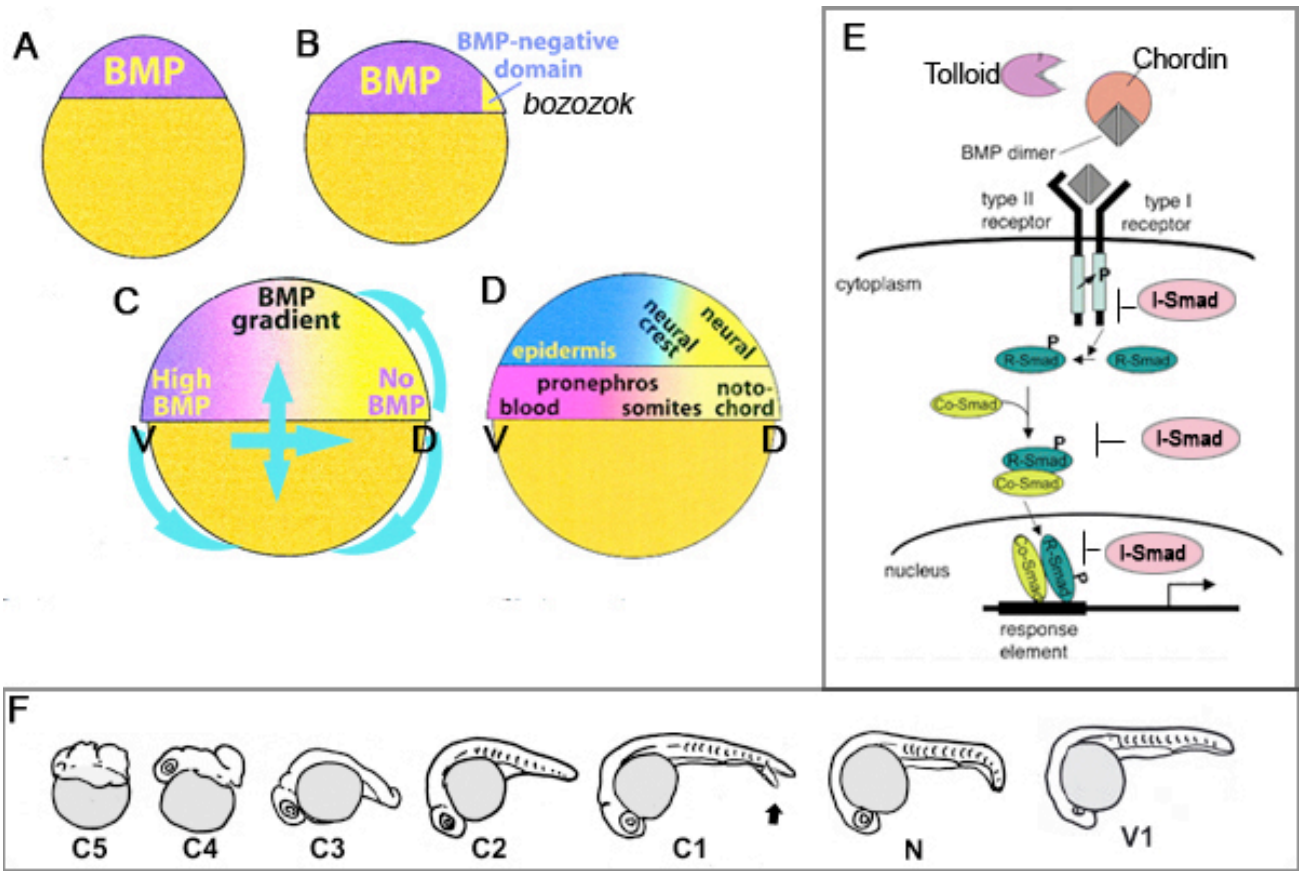
A
BMP
B
BMP
BMP-negative domain
bozozok
C
BMP gradient
High BMP
No BMP
V
D
D
neural crest
neural
epidermis
pronephros
somites
notochord
blood
V
D
E
Tolloid
Chordin
BMP dimer
type II receptor
type I receptor
cytoplasm
P
I-Smad
R-Smad
Co-Smad
nucleus
response element
F
C5
C4
C3
C2
C1
N
V1

Figure 1.3 Models of Planar Cell Porlarity (PCP) and noncanonical Wnt signaling pathways

(Adapted from Veeman et al., 2003a).

(A) The *Drosophila* PCP pathway includes Frizzled, Dishevelled, Rho, Rho Kinase, Flamingo, Strabismus, and Prickle. It is not a simple, linear pathway and is best appreciated in a spatial context. Frizzled, Dishevelled, and Rho, become localized specifically to the distal side, whereas Prickle and Strabismus become localized to the proximal side. The function of all of these proteins is required to ensure both their correct segregation into proximal and distal domains and the subsequent development of correct planar polarity.

(B) Vertebrate noncanonical Wnt signaling requires Frizzled receptors and the proteoglycan coreceptor Knypek. This pathway involves the cytoplasmic signal transduction protein Dishevelled. A main branch downstream of Dishevelled involves the small GTPases of the Rho family. Dishevelled activation of Rho requires the bridging molecule Daam1. The precise roles of Rho, Rac and Cdc42 remain unclear, as is the potential role of the JNK pathway. Dsh can also stimulate calcium flux and the activation of the calcium-sensitive kinases PKC and CamKII, suggesting a Wnt/calcium pathway. As in the *Drosophila* PCP pathway, Prickle and Strabismus appear to have some role in this process, but not in a linear or well-understood way.

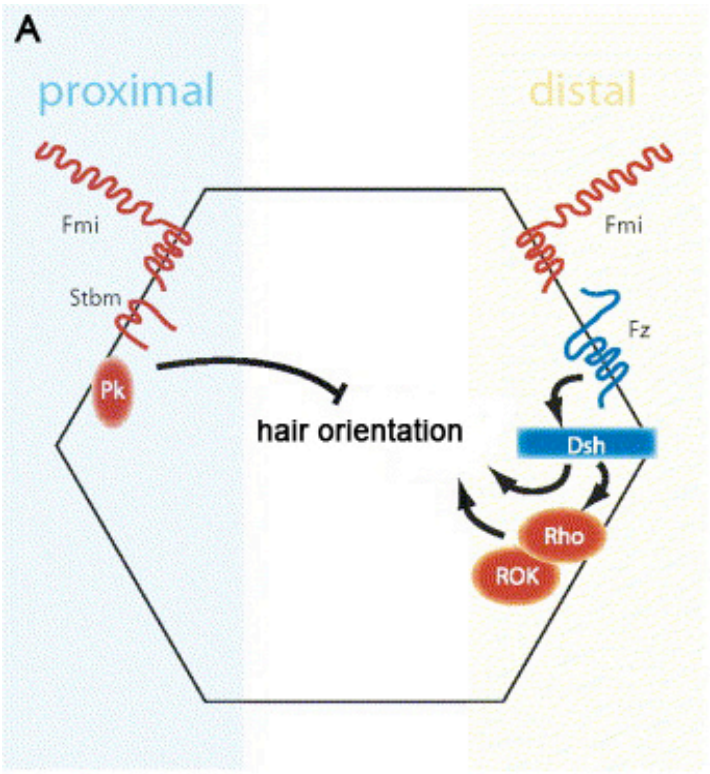
A
proximal
distal
Fmi
Stbm
Pk
hair orientation
Fmi
Fz
Dsh
Rho
ROK

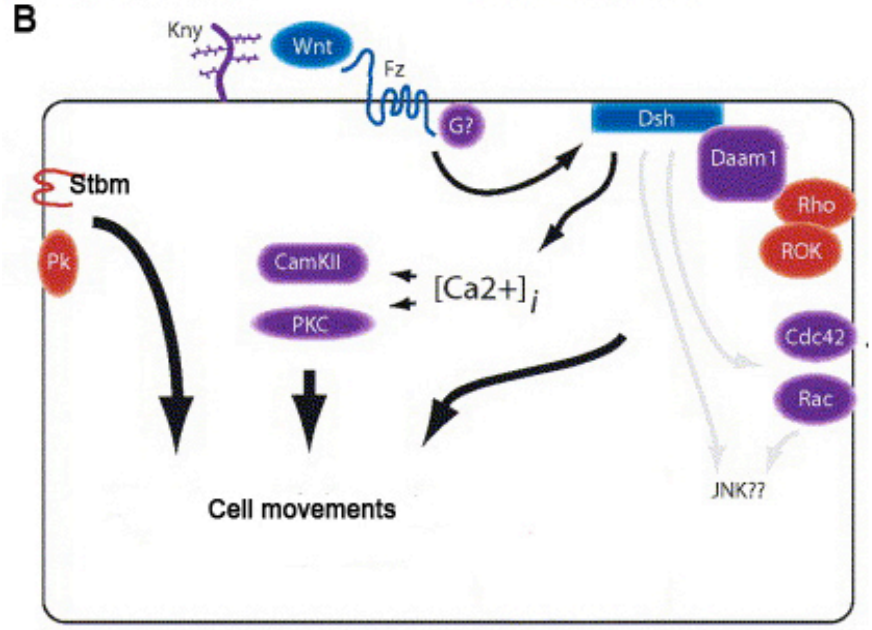
B
Kny
Wnt
Fz
G?
Dsh
Daam1
Rho
ROK
Stbm
Pk
CamKII
PKC
[Ca2+]i
Cdc42
Rac
JNK??
Cell movements

Copyrights

Permissions of reusing figures of published journals in this dissertation were granted.

Figure 1 A-C was adapted from **Agathon, A., Thisse, C. and Thisse, B.** (2003). The molecular nature of the zebrafish tail organizer. *Nature* **424**, 448-452. Permission from Nature Publishing Group was provided by Copyright Clearance Center.

Figure 1 D was reproduced / adapted with permission. **Kanki, J. P. and Ho, R. K.** (1997). The development of the posterior body in zebrafish. *Development* **124**, 881-893.

Figure 2 A-D was adapted from **Little, S. C. and Mullins, M. C.** (2006). Extracellular modulation of BMP activity in patterning the dorsoventral axis. *Birth Defects Res C Embryo Today* **78**, 224-242. This material was reproduced with permission of John Wiley & Sons, Inc.

Figure 2 E,F was adapted from **Kondo, M.** (2007). Bone morphogenetic proteins in the early development of zebrafish. *FEBS J* **274**, 2960-2967. Permission from John Wiley and Sons was provided by Copyright Clearance Center.

Figure 3 was adapted from **Veeman, M. T., Axelrod, J. D. and Moon, R. T.** (2003a). A second canon. Functions and mechanisms of beta-catenin-independent Wnt signaling. *Dev Cell* **5**, 367-377. Permission from Elsevier was provided by Copyright Clearance Center.

References

Adler, P. N. (2002). Planar signaling and morphogenesis in Drosophila. *Dev Cell* **2**, 525-535.

Adler, P. N., Krasnow, R. E. and Liu, J. (1997). Tissue polarity points from cells that have higher Frizzled levels towards cells that have lower Frizzled levels. *Curr Biol* **7**, 940-949.

Agathon, A., Thisse, C. and Thisse, B. (2003). The molecular nature of the zebrafish tail organizer. *Nature* **424**, 448-452.

Angers, S., Thorpe, C. J., Biechele, T. L., Goldenberg, S. J., Zheng, N., MacCoss, M. J. and Moon, R. T. (2006). The KLHL12-Cullin-3 ubiquitin ligase negatively regulates the Wnt-beta-catenin pathway by targeting Dishevelled for degradation. *Nat Cell Biol* **8**, 348-357.

Axelrod, J. D., Miller, J. R., Shulman, J. M., Moon, R. T. and Perrimon, N. (1998). Differential recruitment of Dishevelled provides signaling specificity in the planar cell polarity and Wingless signaling pathways. *Genes Dev* **12**, 2610-2622.

Bakkers, J., Kramer, C., Pothof, J., Quaedvlieg, N. E., Spaink, H. P. and Hammerschmidt, M. (2004). Has2 is required upstream of Rac1 to govern dorsal migration of lateral cells during zebrafish gastrulation. *Development* **131**, 525-537.

Bastock, R., Strutt, H. and Strutt, D. (2003). Strabismus is asymmetrically localised and binds to Prickle and Dishevelled during Drosophila planar polarity patterning. *Development* **130**, 3007-3014.

Boutros, M., Paricio, N., Strutt, D. I. and Mlodzik, M. (1998). Dishevelled activates JNK and discriminates between JNK pathways in planar polarity and wingless signaling. *Cell* **94**, 109-118.

Cambray, N. and Wilson, V. (2002). Axial progenitors with extensive potency are localised to the mouse chordoneural hinge. *Development* **129**, 4855-4866.

Cambray, N. and Wilson, V. (2007). Two distinct sources for a population of maturing axial progenitors. *Development* **134**, 2829-2840.

Carreira-Barbosa, F., Concha, M. L., Takeuchi, M., Ueno, N., Wilson, S. W. and Tada, M. (2003). Prickle 1 regulates cell movements during gastrulation and neuronal migration in zebrafish. *Development* **130**, 4037-4046.

Carreira-Barbosa, F., Kajita, M., Morel, V., Wada, H., Okamoto, H., Martinez Arias, A., Fujita, Y., Wilson, S. W. and Tada, M. (2009). Flamingo regulates epiboly and convergence/extension movements through cell cohesive and signalling functions during zebrafish gastrulation. *Development* **136**, 383-392.

Charrier, J. B., Teillet, M. A., Lapointe, F. and Le Douarin, N. M. (1999). Defining subregions of Hensen's node essential for caudalward movement, midline development and cell survival. *Development* **126**, 4771-4783.

Choi, S. C. and Han, J. K. (2002). Xenopus Cdc42 regulates convergent extension movements during gastrulation through Wnt/Ca2+ signaling pathway. *Dev Biol* **244**, 342-357.

Connors, S. A., Trout, J., Ekker, M. and Mullins, M. C. (1999). The role of tolloid/mini fin in dorsoventral pattern formation of the zebrafish embryo. *Development* **126**, 3119-3130.

Dick, A., Hild, M., Bauer, H., Imai, Y., Maifeld, H., Schier, A. F., Talbot, W. S., Bouwmeester, T. and Hammerschmidt, M. (2000). Essential role of Bmp7 (snailhouse) and its prodomain in dorsoventral patterning of the zebrafish embryo. *Development* **127**, 343-354.

Driever, W., Solnica-Krezel, L., Schier, A. F., Neuhauss, S. C., Malicki, J., Stemple, D. L., Stainier, D. Y., Zwartkruis, F., Abdelilah, S., Rangini, Z. et al. (1996). A genetic screen for mutations affecting embryogenesis in zebrafish. *Development* **123**, 37-46.

Du, S. J., Purcell, S. M., Christian, J. L., McGrew, L. L. and Moon, R. T. (1995). Identification of distinct classes and functional domains of Wnts through expression of wild-type and chimeric proteins in Xenopus embryos. *Mol Cell Biol* **15**, 2625-2634.

Essner, J. J., Amack, J. D., Nyholm, M. K., Harris, E. B. and Yost, H. J. (2005). Kupffer's vesicle is a ciliated organ of asymmetry in the zebrafish embryo that initiates left-right development of the brain, heart and gut. *Development* **132**, 1247-1260.

Fekany, K., Yamanaka, Y., Leung, T., Sirotkin, H. I., Topczewski, J., Gates, M. A., Hibi, M., Renucci, A., Stemple, D., Radbill, A. et al. (1999). The zebrafish bozozok locus encodes Dharma, a homeodomain protein essential for induction of gastrula organizer and dorsoanterior embryonic structures. *Development* **126**, 1427-1438.

Formstone, C. J. and Mason, I. (2005). Combinatorial activity of Flamingo proteins directs convergence and extension within the early zebrafish embryo via the planar cell polarity pathway. *Dev Biol* **282**, 320-335.

Fuhrmann, W. (1965). Genetics of Growth and Development of the Fetus. *Pediatr Clin North Am* **12**, 457-475.

Habas, R., Kato, Y. and He, X. (2001). Wnt/Frizzled activation of Rho regulates vertebrate gastrulation and requires a novel Formin homology protein Daam1. *Cell* **107**, 843-854.

Habas, R., Dawid, I. B. and He, X. (2003). Coactivation of Rac and Rho by Wnt/Frizzled signaling is required for vertebrate gastrulation. *Genes Dev* **17**, 295-309.

Haffter, P., Granato, M., Brand, M., Mullins, M. C., Hammerschmidt, M., Kane, D. A., Odenthal, J., van Eeden, F. J., Jiang, Y. J., Heisenberg, C. P. et al. (1996). The identification of genes with unique and essential functions in the development of the zebrafish, Danio rerio. *Development* **123**, 1-36.

Halbleib, J. M. and Nelson, W. J. (2006). Cadherins in development: cell adhesion, sorting, and tissue morphogenesis. *Genes Dev* **20**, 3199-3214.

Harris, T. J. and Peifer, M. (2007). aPKC controls microtubule organization to balance adherens junction symmetry and planar polarity during development. *Dev Cell* **12**, 727-738.

Heisenberg, C. P. and Solnica-Krezel, L. (2008). Back and forth between cell fate specification and movement during vertebrate gastrulation. *Curr Opin Genet Dev* **18**, 311-316.

Heisenberg, C. P., Tada, M., Rauch, G. J., Saude, L., Concha, M. L., Geisler, R., Stemple, D. L., Smith, J. C. and Wilson, S. W. (2000). Silberblick/Wnt11 mediates convergent extension movements during zebrafish gastrulation. *Nature* **405**, 76-81.

Holley, S. A. (2007). The genetics and embryology of zebrafish metamerism. *Dev Dyn* **236**, 1422-1449.

Imai, Y., Gates, M. A., Melby, A. E., Kimelman, D., Schier, A. F. and Talbot, W. S. (2001). The homeobox genes vox and vent are redundant repressors of dorsal fates in zebrafish. *Development* **128**, 2407-2420.

Ip, Y. T. and Gridley, T. (2002). Cell movements during gastrulation: snail dependent and independent pathways. *Curr Opin Genet Dev* **12**, 423-429.

Jenny, A., Reynolds-Kenneally, J., Das, G., Burnett, M. and Mlodzik, M. (2005). Diego and Prickle regulate Frizzled planar cell polarity signalling by competing for Dishevelled binding. *Nat Cell Biol* **7**, 691-697.

Jessen, J. R. (2009). Noncanonical Wnt signaling in tumor progression and metastasis. *Zebrafish* **6**, 21-28.

Kane, D. A., McFarland, K. N. and Warga, R. M. (2005). Mutations in half baked/E-cadherin block cell behaviors that are necessary for teleost epiboly. *Development* **132**, 1105-1116.

Kanki, J. P. and Ho, R. K. (1997). The development of the posterior body in zebrafish. *Development* **124**, 881-893.

Keller, R. (2002). Shaping the vertebrate body plan by polarized embryonic cell movements. *Science* **298**, 1950-1954.

Kida, Y. S., Sato, T., Miyasaka, K. Y., Suto, A. and Ogura, T. (2007). Daam1 regulates the endocytosis of EphB during the convergent extension of the zebrafish notochord. *Proc Natl Acad Sci U S A* **104**, 6708-6713.

Kilian, B., Mansukoski, H., Barbosa, F. C., Ulrich, F., Tada, M. and Heisenberg, C. P. (2003). The role of Ppt/Wnt5 in regulating cell shape and movement during zebrafish gastrulation. *Mech Dev* **120**, 467-476.

Kim, S. K., Shindo, A., Park, T. J., Oh, E. C., Ghosh, S., Gray, R. S., Lewis, R. A., Johnson, C. A., Attie-Bittach, T., Katsanis, N. et al. (2010). Planar cell polarity acts through septins to control collective cell movement and ciliogenesis. *Science* **329**, 1337-1340.

Kimmel, C. B., Ballard, W. W., Kimmel, S. R., Ullmann, B. and Schilling, T. F. (1995). Stages of embryonic development of the zebrafish. *Dev Dyn* **203**, 253-310.

Kishimoto, Y., Lee, K. H., Zon, L., Hammerschmidt, M. and Schulte-Merker, S. (1997). The molecular nature of zebrafish swirl: BMP2 function is essential during early dorsoventral patterning. *Development* **124**, 4457-4466.

Kondo, M. (2007). Bone morphogenetic proteins in the early development of zebrafish. *FEBS J* **274**, 2960-2967.

Kramer, C., Mayr, T., Nowak, M., Schumacher, J., Runke, G., Bauer, H., Wagner, D. S., Schmid, B., Imai, Y., Talbot, W. S. et al. (2002). Maternally supplied Smad5 is required for ventral specification in zebrafish embryos prior to zygotic Bmp signaling. *Dev Biol* **250**, 263-279.

Kuhl, M., Sheldahl, L. C., Malbon, C. C. and Moon, R. T. (2000). Ca(2+)/calmodulin-dependent protein kinase II is stimulated by Wnt and Frizzled homologs and promotes ventral cell fates in Xenopus. *J Biol Chem* **275**, 12701-12711.

Lele, Z., Folchert, A., Concha, M., Rauch, G. J., Geisler, R., Rosa, F., Wilson, S. W., Hammerschmidt, M. and Bally-Cuif, L. (2002). parachute/n-cadherin is required for morphogenesis and maintained integrity of the zebrafish neural tube. *Development* **129**, 3281-3294.

Li, L., Yuan, H., Xie, W., Mao, J., Caruso, A. M., McMahon, A., Sussman, D. J. and Wu, D. (1999). Dishevelled proteins lead to two signaling pathways. Regulation of LEF-1 and c-Jun N-terminal kinase in mammalian cells. *J Biol Chem* **274**, 129-134.

Little, S. C. and Mullins, M. C. (2006). Extracellular modulation of BMP activity in patterning the dorsoventral axis. *Birth Defects Res C Embryo Today* **78**, 224-242.

Long, Q., Meng, A., Wang, H., Jessen, J. R., Farrell, M. J. and Lin, S. (1997). GATA-1 expression pattern can be recapitulated in living transgenic zebrafish using GFP reporter gene. *Development* **124**, 4105-4111.

Marlow, F., Topczewski, J., Sepich, D. and Solnica-Krezel, L. (2002). Zebrafish Rho kinase 2 acts downstream of Wnt11 to mediate cell polarity and effective convergence and extension movements. *Curr Biol* **12**, 876-884.

Marlow, F., Gonzalez, E. M., Yin, C., Rojo, C. and Solnica-Krezel, L. (2004). No tail co-operates with non-canonical Wnt signaling to regulate posterior body morphogenesis in zebrafish. *Development* **131**, 203-216.

Mintzer, K. A., Lee, M. A., Runke, G., Trout, J., Whitman, M. and Mullins, M. C. (2001). Lost-a-fin encodes a type I BMP receptor, Alk8, acting maternally and zygotically in dorsoventral pattern formation. *Development* **128**, 859-869.

Moon, R. T., Campbell, R. M., Christian, J. L., McGrew, L. L., Shih, J. and Fraser, S. (1993). Xwnt-5A: a maternal Wnt that affects morphogenetic movements after overexpression in embryos of Xenopus laevis. *Development* **119**, 97-111.

Moriguchi, T., Kawachi, K., Kamakura, S., Masuyama, N., Yamanaka, H., Matsumoto, K., Kikuchi, A. and Nishida, E. (1999). Distinct domains of mouse dishevelled are responsible for the c-Jun N-terminal kinase/stress-activated protein kinase activation and the axis formation in vertebrates. *J Biol Chem* **274**, 30957-30962.

Myers, D. C., Sepich, D. S. and Solnica-Krezel, L. (2002a). Bmp activity gradient regulates convergent extension during zebrafish gastrulation. *Dev Biol* **243**, 81-98.

Myers, D. C., Sepich, D. S. and Solnica-Krezel, L. (2002b). Convergence and extension in vertebrate gastrulae: cell movements according to or in search of identity? *Trends Genet* **18**, 447-455.

Nasevicius, A. and Ekker, S. C. (2000). Effective targeted gene 'knockdown' in zebrafish. *Nat Genet* **26**, 216-220.

Park, M. and Moon, R. T. (2002). The planar cell-polarity gene stbm regulates cell behaviour and cell fate in vertebrate embryos. *Nat Cell Biol* **4**, 20-25.

Penzo-Mendez, A., Umbhauer, M., Djiane, A., Boucaut, J. C. and Riou, J. F. (2003). Activation of Gbetagamma signaling downstream of Wnt-11/Xfz7 regulates Cdc42 activity during Xenopus gastrulation. *Dev Biol* **257**, 302-314.

Pyati, U. J., Webb, A. E. and Kimelman, D. (2005). Transgenic zebrafish reveal stage-specific roles for Bmp signaling in ventral and posterior mesoderm development. *Development* **132**, 2333-2343.

Schulte-Merker, S., Lee, K. J., McMahon, A. P. and Hammerschmidt, M. (1997). The zebrafish organizer requires chordino. *Nature* **387**, 862-863.

Sheldahl, L. C., Park, M., Malbon, C. C. and Moon, R. T. (1999). Protein kinase C is differentially stimulated by Wnt and Frizzled homologs in a G-protein-dependent manner. *Curr Biol* **9**, 695-698.

Shimizu, T., Yamanaka, Y., Nojima, H., Yabe, T., Hibi, M. and Hirano, T. (2002). A novel repressor-type homeobox gene, ved, is involved in dharma/bozozok-mediated dorsal organizer formation in zebrafish. *Mech Dev* **118**, 125-138.

Slack, J. M. W. (2001). Essential developmental biology. Malden, MA Abingdon, Oxon: Blackwell Science : Distributors Marston Book Services.

Slusarski, D. C., Yang-Snyder, J., Busa, W. B. and Moon, R. T. (1997). Modulation of embryonic intracellular Ca2+ signaling by Wnt-5A. *Dev Biol* **182**, 114-120.

Stickney, H. L., Imai, Y., Draper, B., Moens, C. and Talbot, W. S. (2007). Zebrafish bmp4 functions during late gastrulation to specify ventroposterior cell fates. *Dev Biol* **310**, 71-84.

Tada, M. and Smith, J. C. (2000). Xwnt11 is a target of Xenopus Brachyury: regulation of gastrulation movements via Dishevelled, but not through the canonical Wnt pathway. *Development* **127**, 2227-2238.

Thorpe, C. J., Weidinger, G. and Moon, R. T. (2005). Wnt/beta-catenin regulation of the Sp1-related transcription factor sp5l promotes tail development in zebrafish. *Development* **132**, 1763-1772.

Topczewski, J., Sepich, D. S., Myers, D. C., Walker, C., Amores, A., Lele, Z., Hammerschmidt, M., Postlethwait, J. and Solnica-Krezel, L. (2001). The zebrafish glypican knypek controls cell polarity during gastrulation movements of convergent extension. *Dev Cell* **1**, 251-264.

Tree, D. R., Shulman, J. M., Rousset, R., Scott, M. P., Gubb, D. and Axelrod, J. D. (2002). Prickle mediates feedback amplification to generate asymmetric planar cell polarity signaling. *Cell* **109**, 371-381.

Tucker, J. A., Mintzer, K. A. and Mullins, M. C. (2008). The BMP signaling gradient patterns dorsoventral tissues in a temporally progressive manner along the anteroposterior axis. *Dev Cell* **14**, 108-119.

Ulrich, F., Krieg, M., Schotz, E. M., Link, V., Castanon, I., Schnabel, V., Taubenberger, A., Mueller, D., Puech, P. H. and Heisenberg, C. P. (2005). Wnt11 functions in gastrulation by controlling cell cohesion through Rab5c and E-cadherin. *Dev Cell* **9**, 555-564.

Veeman, M. T., Axelrod, J. D. and Moon, R. T. (2003a). A second canon. Functions and mechanisms of beta-catenin-independent Wnt signaling. *Dev Cell* **5**, 367-377.

Veeman, M. T., Slusarski, D. C., Kaykas, A., Louie, S. H. and Moon, R. T. (2003b). Zebrafish prickle, a modulator of noncanonical Wnt/Fz signaling, regulates gastrulation movements. *Curr Biol* **13**, 680-685.

von Bubnoff, A. and Cho, K. W. (2001). Intracellular BMP signaling regulation in vertebrates: pathway or network? *Dev Biol* **239**, 1-14.

von der Hardt, S., Bakkers, J., Inbal, A., Carvalho, L., Solnica-Krezel, L., Heisenberg, C. P. and Hammerschmidt, M. (2007). The Bmp gradient of the zebrafish gastrula guides migrating lateral cells by regulating cell-cell adhesion. *Curr Biol* **17**, 475-487.

Wallingford, J. B. and Habas, R. (2005). The developmental biology of Dishevelled: an enigmatic protein governing cell fate and cell polarity. *Development* **132**, 4421-4436.

Wallingford, J. B., Fraser, S. E. and Harland, R. M. (2002). Convergent extension: the molecular control of polarized cell movement during embryonic development. *Dev Cell* **2**, 695-706.

Warga, R. M. and Kane, D. A. (2007). A role for N-cadherin in mesodermal morphogenesis during gastrulation. *Dev Biol* **310**, 211-225.

Weaver, M., Dunn, N. R. and Hogan, B. L. (2000). Bmp4 and Fgf10 play opposing roles during lung bud morphogenesis. *Development* **127**, 2695-2704.

Wu, J. and Mlodzik, M. (2008). The frizzled extracellular domain is a ligand for Van Gogh/Stbm during nonautonomous planar cell polarity signaling. *Dev Cell* **15**, 462-469.

Yamamoto, A., Amacher, S. L., Kim, S. H., Geissert, D., Kimmel, C. B. and De Robertis, E. M. (1998). Zebrafish paraxial protocadherin is a downstream target of spadetail involved in morphogenesis of gastrula mesoderm. *Development* **125**, 3389-3397.

Ye, L., Bokobza, S. M. and Jiang, W. G. (2009). Bone morphogenetic proteins in development and progression of breast cancer and therapeutic potential (review). *Int J Mol Med* **24**, 591-597.

Yin, C., Kiskowski, M., Pouille, P. A., Farge, E. and Solnica-Krezel, L. (2008). Cooperation of polarized cell intercalations drives convergence and extension of presomitic mesoderm during zebrafish gastrulation. *J Cell Biol* **180**, 221-232.

Yu, P. B., Hong, C. C., Sachidanandan, C., Babitt, J. L., Deng, D. Y., Hoyng, S. A., Lin, H. Y., Bloch, K. D. and Peterson, R. T. (2008). Dorsomorphin inhibits BMP signals required for embryogenesis and iron metabolism. *Nat Chem Biol* **4**, 33-41.

CHAPTER 2 - BMP and Noncanonical Wnt Signaling are Required to Inhibit Secondary Tail Formation in Zebrafish

Abstract

The role of Bone Morphogenetic Protein (BMP) signaling in specifying cell fate in the tailbud has been well-established. Among the lost ventral tissues like ventral tailfin and cloaca, embryos with compromised BMP signaling produce a curious phenotype-a ventrally located secondary tail containing both somitic muscle and notochord. This phenotype is proposed to be a fate-patterning defect when the BMP gradient is lowered to a precise level. However, this morphogen model is insufficient to explain secondary tail formation. BMP also regulates morphogenetic movements during gastrulation, promoting the convergence of lateral mesodermal cells towards the dorsal midline. Here, we provide evidence that BMP signaling continues to mediate cell movements during tail development. Our data indicate that BMP signaling is activated in the ventroposterior tailbud to promote cell migration during tailbud protrusion, and that it is the defective migration of these cells which ultimately leads to bifurcation of the chordoneural hinge (CNH) domain, a presumptive stem cell pool in the tailbud that results information of a secondary tail in BMP mutants. In parallel, the morphogenesis of tailbud cells is known to be under the control of noncanonical Wnt signaling, although the exact nature of the defect remains unclear. Additionally, we show that noncanonical Wnt signaling interacts with BMP signaling to maintain CNH integrity by affecting cadherin localization in CNH cells, possibly disrupting cell cohesion. We propose a model that BMP and a noncanonical Wnt pathway regulate tail morphogenesis by controlling cell migration and cell adhesion within the tailbud.

Introduction

The vertebrate tailbud is a mass of undifferentiated cells that gives rise to posterior tissues of the body during tail development. In zebrafish, the tailbud is derived from cells originating at both the dorsal and ventral margins, which come together at the vegetal pole of the embryo upon completion of epiboly (Kimmel et al., 1995). Ventrally-derived cells comprise the posterior portion of the tailbud, and are fated to develop into somitic muscle during tail

formation, while the dorsally-derived cells form the anterior tailbud and form primarily axial tissues such as notochord and floor plate (Kanki and Ho, 1997; Myers et al., 2002; Agathon et al., 2003).

Extensive genetic analyses have demonstrated roles for several conserved signaling pathways including the BMP, FGF, Nodal, and both the Wnt/β-catenin and noncanonical Wnt pathways in the specification, patterning, and morphogenesis of the tailbud and its derivatives (Schier and Talbot, 2005). Some of these pathways are required at distinct stages both for proper initial specification of the tailbud and for correct fate patterning of cells derived from it. For example, the BMP pathway is required (along with Wnt/β-catenin and Nodal signaling) during gastrulation for the formation of a tail organizer, located at the ventral margin (Agathon et al., 2003). In embryos completely lacking BMP activity during gastrulation, such as *swirl(swr)/bmp2b* mutants, tail development is essentially nonexistent (Mullins et al., 1996; Kishimoto et al., 1997). During gastrulation, BMP is thought to function as a morphogen, patterning cell fates along the dorsal-ventral (DV) axis, with higher BMP activity inducing the ventral-most fates, including tail mesoderm, intermediate levels specifying lateral fates such as trunk mesoderm, and with the absence of BMP activity allowing for the development of dorsal fates, such as the notochord (Little and Mullins, 2006). Later, during somitogenesis stages, BMP also acts to pattern cell fates derived from the tailbud (Pyati et al., 2005). Post-gastrula inhibition of BMP signaling using Dorsomorphin, a small molecule BMP inhibitor, or inducible overexpression of either a dominant-negative, truncated BMP receptor (dnBMPR) or the BMP antagonist Chordin, results in embryos showing reduced ventral tailfin and cloacal tissue (Pyati et al., 2005; Pyati et al., 2006; Tucker et al., 2008; Yu et al., 2008). Such embryos show a phenotype similar to that observed in embryos carrying mutations in several conserved components of the BMP pathway-*bmp4, minifin(mfn)/tolloid*, *lost-a-fin(laf)/Alk8*, as well as hypomorphic *smad5* alleles (Connors et al., 1999; Mintzer et al., 2001; Kramer et al., 2002; Stickney et al., 2007). Based on phenotypic analysis of embryos carrying certain combinations of *bmp4*, *bmp2*, and *bmp7* alleles, it has been suggested that a gradient of BMP signaling specifies distinct cell types in posterior tissues, with the highest levels of BMP activity being required for production of ventral tailfin and cloaca and a lower amount being sufficient for presomitic mesoderm and blood (Stickney et al., 2007). Further, *bmp4* has recently been shown to regulate tail development by promoting proliferation of cells that reside in the chordoneural

hinge (CNH) (Esterberg et al., 2008), a population of cells at the caudal end of the notochord which has been shown in other vertebrates to act as a pool of progenitor cells that can give rise to multiple tail tissues, including notochord, floor plate, and somitic muscle (Charrier et al., 1999; Davis and Kirschner, 2000; Cambray and Wilson, 2002; Cambray and Wilson, 2007).

Recent studies have shown that, independent of its role in fate patterning, BMP also regulates morphogenetic movements during gastrulation, promoting the convergence of lateral mesodermal cells towards the dorsal midline (Myers et al., 2002; von der Hardt et al., 2007). The BMP activity gradient is proposed to negatively regulate calcium-dependent cell adhesion, establishing distinct patterns of migratory behavior among mesodermal cells along the DV axis (von der Hardt et al., 2007). The ventral-most cells, exposed to the highest levels of BMP, exhibit very low levels of intercellular adhesion, and do not converge dorsally at all, but move vegetally to occupy the tailbud. In contrast, laterally positioned cells move preferentially towards regions of lower BMP/higher adhesion (dorsally). Presumably, simultaneous control of both cell fate patterning and of cell movements by BMP ensures the necessary tight coupling of these two essential processes. BMP's role in promoting dorsalward migration of mesodermal cells is independent of the role of noncanonical Wnt signaling, with BMP being required predominantly for migration of ventrolateral mesoderm and noncanonical Wnts functioning in more dorsolateral regions of the gastrula.

Cell tracing experiments have shown that the anterior and posterior portions of the tailbud undergo distinct morphogenetic movements during tail outgrowth (Kanki and Ho, 1997). Cells in the anterior (dorsally derived) tailbud continue the convergence and extension (CE) movements observed during gastrulation, with presomitic and somitic mesoderm converging to the midline, driving the posteriorward extension of the embryo. In contrast, posterior (ventrally derived) tailbud cells move laterally away from the midline and subduct beneath the posteriorly migrating anterior tailbud cells.

Relatively little is known concerning the signaling pathways that regulate morphogenetic movements during tail development. However, it is known that some genes that regulate cell movements during gastrulation have also been shown to contribute to proper tail morphogenesis. For example, when noncanonical Wnt signaling is disrupted, as in *pipetail(ppt)/wnt5* or *knypek(kny)/glypican* mutant embryos, posterior tailbud cells correctly undergo subduction and move laterally away from the midline, but tail extension is reduced, suggesting a requirement for

noncanonical Wnt signaling in promoting continued CE movements during tail development (Marlow et al., 2004). Further, in embryos deficient for both noncanonical Wnt signaling and the T-box transcription factor *no tail (ntl)*, posterior tailbud cells fail to undergo subduction movements, and tail extension is completely absent (Marlow et al., 2004). Clearly, noncanonical Wnt signaling is essential for proper morphogenesis during tail development, although the exact nature of the defect remains unclear.

As described above, recent studies have shown that post-gastrula BMP signaling is required for patterning of ventral mesoderm in the developing tail. A subset of embryos with compromised BMP signaling also produce a ventrally located secondary tail containing both somitic muscle and notochord (Connors et al., 1999; Pyati et al., 2005; Stickney et al., 2007; Yu et al., 2008). It has been proposed that these secondary tails form as a result of a mis-specification of cell fates due to a change in the slope of the postulated gradient of BMP activity in the tail (Stickney et al., 2007). According to this hypothesis, a mild reduction in BMP activity could lead to a shallower slope of the gradient such that it would be insufficient to specify ventral tailfin, which requires the highest level of BMP signaling, but would expose more cells to the intermediate level of activity sufficient for formation of tail mesoderm, leading to an expansion of this tissue.

However, this model does not explain why the excess tail mesoderm would form such a morphologically distinct structure or why the secondary tails observed in BMP-compromised embryos include notochord, which is not hypothesized to be responsive to the BMP gradient. Also, while *bmp4* mutant embryos show the loss of ventral tailfin and expansion of blood progenitors predicted by the gradient model, these embryos do not form secondary tails (Stickney et al., 2007). Further, in dnBMPR (transgenic line carrying dominant negative BMP receptor) embryos, when expression is induced at bud stage, the population of blood progenitors is not expanded, although approximately 15% of these embryos form secondary tails (Pyati et al., 2005). Taken together, these observations are inconsistent with the hypothesis that secondary tails form as a consequence of defects in fate patterning and raise questions about the BMP gradient model as it relates to secondary tail formation.

Earlier analysis of secondary tail formation in dnBMPR embryos had indicated that initial tailbud specification occurs normally, and that the secondary tail might be composed of cells that are inappropriately left behind by the tailbud during tail extension (Pyati et al., 2005). This

suggests that a defect in morphogenesis may be underlying secondary tail formation in BMP compromised embryos. To test this hypothesis, we undertook a detailed analysis of tail development in several BMP-defective backgrounds. We found that, contrary to the gradient hypothesis, secondary tails are formed in several BMP pathway mutants, irrespective of the severity of dorsalization observed. We further found that formation of secondary tails is presaged during early tail extension by bifurcation of the CNH, with the ectopic CNH cells contributing to the secondary tail. Time-lapse confocal videomicroscopy shows that BMP is required for anterior migration of ventral-posterior presomitic mesoderm that serves to lift the CNH away from the yolk. In the absence of this migration, the CNH remains closely associated with the yolk and gradually becomes bifurcated during tail elongation. We further demonstrate that noncanonical Wnt signaling functions in a parallel pathway to prevent secondary tail formation. We show that in *kny* embryos, the adhesion protein cadherin is mislocalized in CNH cells, suggesting that noncanonical Wnts may promote cohesion of CNH cells, in addition to their previously described role in CE movements.

Materials and methods

Zebrafish strains

Wild-type line AB was used. Mutant lines used were *mfn*^{tc263a} (a point mutation, undescribed) (Connors et al., 1999), *kny*^{fr6} (a nonsense mutation results in a truncated protein) (Topczewski et al., 2001), *smad5*^{m169} (an insertional mutation) (Kramer et al., 2002), *smad5*^{dty40} (a missense mutation) (Kramer et al., 2002) and *snh*^{ty68a} (a missense mutation leads to exchange from Val to Gly at amino acid position 130 in the proregion of Bmp7 protein) (Dick et al., 2000). *mfn*/+;*Tg(flh:EGFP)* and *kny*/+;*Tg(flh:EGFP)* strains were created by crossing *mfn* and *kny* heterozygotes to the *Tg(flh:EGFP)* transgenic line (Gamse et al., 2003).

In situ hybridization and antibody staining

Whole amount *in situ* hybridization was carried out using standard methods (Oxtoby and Jowett, 1993). The following probes were used: *col2a* (Yan et al., 1995), *myoD* (Weinberg et al., 1996), *neurog1*(Blader et al., 1997), *ntl* (Schulte-Merker et al., 1992), *gata1* (Detrich et al., 1995) and *flh* (Talbot et al., 1995). Fluorescent *in situ* hybridization (FISH) for *flh* expression was performed using a Fast Red color reaction (Hauptmann and Gerster, 1994), followed by an

incubation of 1:100 diluted P-Smad1/5/8 antibody (Cell Signaling Technology). β-catenin antibody (BD Transduction Laboratories) was applied at 1:400; pan-cadherin antibody (Sigma) was applied at 1:100; Tbx6 antibody (ZIRC) was applied at 1:1000. Appropriate Alexa Fluor conjugated (Molecular Probes) secondary antibodies were used.

Morpholino and RNA injection

Morpholino antisense oligonucleotides: (*dvl1* MO: 5'-ATATGATTTTAGTCTCCGCCATGAG-3') were purchased from Gene Tools. *mfn, dvl2, dvl3* and *cdh2* morpholinos have been previously described (Lele et al., 2002; Angers et al., 2006; Jasuja et al., 2006). The standard control morpholino by Gene Tools was used in some experiments. Morpholinos were diluted in Danieau's buffer before injection. *mfn* MO was injected at a concentration of 1 mg/ml; concentrations of 0.5 mg/ml and 1.5 mg/ml were injected as low and high dose. *dvl1, dvl2 and dvl3* MOs were injected at a sub-optimal concentration of 1 mg/ml each; a concentration of 1.5 mg/ml was injected as high dose; to fully inhibit *dvl2* and *dvl3*, the concentration was 3 mg/ml. *cdh2* MO was injected at a sub-optimal concentration of 0.1mg/ml and a high concentration of 0.25 mg/ml was injected to achieve strong synergistic effects. Standard deviation of three replicated experiments was calculated by Excel. Synthetic mRNA of membrane-bound RFP (mRFP) was made from pCS2+ constructs with mMessage mMachine kit (Ambion) and injected at a concentration of 25 mg/ml. In all experiments, a volume of 3-5 nl was injected in the yolk of one-cell stage embryos.

Time lapse confocal microscopy

Tg(flh:EGFP), *mfn*;*Tg(flh:EGFP)* and *kny*;*Tg(flh:EGFP)* embryos were injected with mRFP RNA. To analyze tail morphogenesis, embryos were mounted at 10 somites in 0.7% low-melt agarose in Ringer's solution. Agarose surrounding the posterior body was mechanically removed to ensure the free extension of the tailbud. Images were acquired using a Zeiss LSM 5 Pascal confocal microscope and a 20 × lens every 1.5 min. Videos were re-aligned by ImageJ.

Chemical treatment

To inhibit BMP signaling, embryos were treated with Dorsomorphin (AMPK Inhibitor, Compound C, Calbiochem) as described with slight modifications (Yu et al., 2008).

Dorsomorphin resuspended in DMSO was dissolved in fish water at 60 μM. Embryos were manually dechorionated and reared in the solution for the duration of the experiment.

Results

Mesoderm tissues produced in the secondary tail of mini fin

To develop a clearer understanding of the origin of secondary tails in BMP-compromised embryos, we carefully analyzed the process of secondary tail formation in the *mfn/tolloid* mutant, which, at the time we began this study, was the only reported mutant to consistently produce secondary tails (Connors et al., 1999). To determine which tissues are located in the secondary tail domain, we examined the expression of the notochord marker *col2a*, muscle marker *myoD,* neural marker *neurog1* and the notochord/tailbud marker *ntl* by *in situ* hybridization. In *mfn* embryos at 26 hpf, ectopic *col2α* expression (Fig. 2.1A, B) was observed in 53% of the embryos and ectopic *myoD* expression (Fig. 2.1C, D) was observed in 30% of the embryos (Table 2.1). Consistent with previous studies, no embryo showed ectopic *neurog1* expression (Fig. 2.1E, F), indicating that secondary tails do not contain neural tissue (Pyati et al., 2005). Ectopic *ntl* expression (Fig. 2.1G, H) was detected in 64% of the embryos. These data suggest that different mesodermal tissues are not equally represented in the secondary tail. The majority of the secondary tails contain ectopic notochord tissue, while only a subset of them have ectopic somitic muscle.

Secondary tail formation is not accompanied by changed mesoderm fates.

The BMP morphogen model in tail development suggests that secondary tail formation only occurs at a modestly reduced level of BMP signaling in the tailbud, while stronger reduction of BMP activity results in reduced ventral mesoderm, with no secondary tails formed (Stickney et al., 2007). Secondary tail formation is proposed to occur only in embryos with a phenotype intermediate between C1 (losing partial ventral fin) and C2 (slightly twisted tail) (Mullins et al., 1996), which is included in the range of phenotypes typically seen in *mfn* embryos (Stickney et al., 2007). To test this model, we examined *ntl* expression in mutants that more significantly reduce BMP signaling-*piggytail (smad5)* and *snailhouse (bmp7)*. These mutants display a range of dorsalized phenotypes from weak (C1) to severe (C4) (Mullins et al., 1996) (Also see Chapter 1, Fig1.2F). In the weak *piggytail (smad5^{m169})* allele, we observed that 49% of the C1 homozygotes had a secondary tail (Table 2.S1). In clutches of embryos from an incross of *piggytail (smad5^{dty40})* carriers, we observed a range of phenotypes spanning the C1, C2 and C3

classes. The overall penetrance of secondary tail formation in all the mutant embryos was 36% (Table 2.S1). Notably, we observed secondary tail formation in each phenotypic class (Fig. 2.2A-D). Further, in *snailhouse (bmp7^{ty68})* embryos, which are severly dorsalized (C4), 38% formed secondary tails (Fig. 2.2E, Table 2.S1). Taken together, we observed secondary tails in multiple BMP mutant lines independent of the severity of dorsalization. These results suggest that secondary tail formation does not require that BMP signaling is reduced to a specific level, and it is unlikely to result from expanded mesoderm since secondary tails can even be specified in embryos that have limited tail mesoderm. Further, our earlier observation that only a subset of secondary tails contain somitic mesoderm is also inconsistent with secondary tails forming as a consequence of an overproduction of presomitic mesoderm.

BMP signaling is required during early somitogenesis to inhibit secondary tail formation

A previous study using transgenic zebrafish carrying a heat shock inducible, dominant-negative BMP receptor construct (Tg:dnBMPR) had shown that inhibition of BMP signaling post-gastrulation can induce secondary tails in a subset of embryos (Pyati et al., 2005). To confirm this result, we used a small molecule BMP antagonist, Dorsomorphin (DM) (Yu et al., 2008). We treated embryos at progressively later stages, beginning at the 1 somite stage, then scored for the presence of a secondary tail at 24 hpf by fixing the embryos and staining with *ntl* probe. Nearly all embryos treated with DM beginning at 6 somites lacked ventral tailfin at 24 hpf, with about 30% also forming a secondary tail (Fig. 2.2F). Embryos treated with DM after 7 somites showed normal or slightly reduced ventral tail fin with only a few embryos forming a secondary tail (Fig. 2.2F). In rare cases, embryos treated with DM at 7 somites formed a secondary tail even in the presence of a fully formed ventral tail fin (Fig. 2.2F, G). Our data indicate that the critical periods for specifying ventral tailfin and for prevention of secondary tail formation overlap significantly. However, the two processes appear to be separable, indicating that secondary tails might be formed in the absence of overt fate patterning defects.

Blood and muscle fates are expanded in the tails of *bmp4* mutant embryos (Stickney et al., 2007). Although *bmp4* mutants do not form secondary tails, it has been suggested that these expanded tissues could contribute to their formation in other BMP-compromised embryos. To investigate whether expansion of blood and tail mesoderm is associated with secondary tail

formation, we examined *gata1* (a blood progenitor marker) and *myoD* expression in BMP-compromised embryos. First, we treated 60 embryos with DM beginning at 5-somite stage. We fixed half of these at the 13-somite stage and performed whole amount *insitu* hybridization with *gata1* probe. 27 embryos were indistinguishable from wild-type (Fig. 2.2H, I), while 3 showed weak expansion of *gata1* expression to the posterior end (data not shown). To get an estimate of the penetrance of secondary tails in this clutch of embryos, we stained the other 30 embryos with *ntl* at 24 hpf. 11/30 embryos showed a secondary tail in this assay, suggesting that secondary tails can form in the absence of *gata1* expansion.

To determine whether somitic muscle is expanded in embryos producing secondary tails, we stained *mfn* embryos at 22 hpf with *myoD*. Whereas *myoD* expression has been reported to be expanded across the midline of the caudal tail in *bmp4* embryos (Stickney et al., 2007), we observed no such expansion in *mfn* embryos (Fig. 2.2J, K). These observations suggest a lack of association between secondary tail formation and an expansion of somitic muscle and blood precursors. Our data suggest that BMP is required to regulate the integrity of the tailbud during early somitogenesis, and this function of BMP signaling is independent of its early role of establishing dorsoventral axis and late role of specifying ventral tail fin, somitic mesoderm and blood.

Noncanonical Wnt signaling functions with BMP in inhibiting secondary tail formation

Noncanonical Wnt signaling plays an essential role in governing morphogenesis of the posterior body (Veeman et al., 2003; Seifert and Mlodzik, 2007). *ppt/wnt5* and *kny/glypican4* mutants are defective in components of the noncanonical Wnt signaling pathway and have short tails due to impaired cell movements within the tailbud (Marlow et al., 2004). Strikingly, *kny* mutants have also been reported to exhibit ectopic *eve1* (a gene expressed in the tailbud) and *shh* (*sonic hedgehog*, a gene expressed in notochord and floorplate) expression domains in the tail (Solnica-Krezel et al., 1996; Marlow et al., 1998), resembling the expression pattern of these markers in secondary tails of dnBMPR embryos (Pyati et al., 2005). This suggested that *kny* embryos might also produce secondary tails, with the dramatic shortening of the axis perhaps precluding identification of the ectopic tissue in living embryos. In looking at later stage (72 hpf) *kny* embryos, we could observe clear bifurcations of the posterior notochord (Fig. 2.3C),

suggesting that a secondary tail may form in these embryos. We confirmed this by examining *ntl* expression at 24 hpf (Fig. 2.3D, E). Further, we observed ectopic expression of *col2α* (Fig. 2.3F, G) as well as *myoD* (Fig. 2.3H, I; Table 2.2). These results suggest that inhibition of non-canonical Wnt signaling results in secondary tail formation. We next tested whether this phenotype is unique to *kny* mutants, or might be common to other embryos in which noncanonical Wnt signaling is impaired. We screened the tail phenotype of *disheveled*, *strabismus* and *prickle* morphants by examining *ntl* expression at 22 hpf. Three *disheveled* homologs, *dvl1, dvl2 and dvl3* were knocked down systematically by morpholino (MO). Knockdown of each *dvl* gene individually did not result in a secondary tail phenotype (data not shown). However, we found that inhibition of *dvl2* and *dvl3* simultaneously did give rise to a secondary tail in a subset of embryos (Fig. 2.3A, B) in addition to the previously reported mild CE defect.

As described above, approximately 50% of *kny* embryos form secondary tails. To test whether this partial penetrance was due to residual activity of the noncanonical Wnt pathway or to genetic redundancy with another pathway, we injected *dvl2/dvl3* MOs into *kny* embryos. We did not observe any increased penetrance of secondary tail formation (data not shown) in these embryos, suggesting that even in embryos lacking most, if not all, noncanonical Wnt activity, other pathways such as the BMP pathway might partially compensate (see below). Lastly, we tested several known noncanonical Wnt ligands-*wnt5*, *wnt11*, and *wnt11r* for a role in secondary tail formation-knocking them down using morpholinos, singly and in combination, and observed no evidence for a role in this process for any of these genes (data not shown).

In contrast to our observations in *kny* or *dvl2/dvl3* MO embryos, we never observed secondary tail formation in embryos in which *strabismus*, *prickle 1a* and *prickle 2b* had been inhibited, separately or in combination (Table 2.S2). These data suggest that *prickle* and *strabismus* do not regulate secondary tail formation, and that secondary tail formation is not likely to be merely a secondary consequence of earlier defects in CE. Our data support the involvement of at least some elements of a non-canonical Wnt pathway in preventing secondary tail formation.

To investigate whether non-canonical Wnt signaling interacts with BMP signaling in inhibiting secondary tail formation, we tested for synergy between *mfn* and *dvl* by injecting suboptimal amounts of morpholinos for each gene and scoring embryos for secondary tail

formation by examining *ntl* expression (Fig. 2.3J). Partial knockdown of *mfn* showed a very low penetrance of secondary tail formation, while partial knockdown of either *mfn* and *dvl1* or *mfn* and *dvl2* did not affect the penetrance of secondary tail formation. Moderate enhancement of secondary tail penetrance was observed with partial knockdown of *mfn* and *dvl3* simultaneously, while partial knockdown of *mfn*, *dvl2* and *dvl3* greatly enhanced the secondary tail penetrance to over 50%.

Next, we confirmed this interaction by using *mfn* mutants. Injection of suboptimal amounts of *dvl2*/*dvl3* MO into *mfn* embryos also caused a robust enhancement (Fig. 2.3J). Lastly, to test whether *mfn* interacts with *kny*, we scored the penetrance of secondary tails in *mfn;kny* double mutant embryos. In *mfn;kny*, strong enhancement of secondary tail formation was observed (88% of double mutant embryos formed a secondary tail, Fig. 2.3K), approximately what one would expect for a simple additive effect on penetrance of this phenotype. Together, the genetic interactions are consistent with a model in which noncanonical Wnt signaling and BMP signaling function together to inhibit secondary tail formation.

BMP and noncanonical Wnt signaling are required to prevent bifurcation of the chordoneural hinge during tail outgrowth

The chordoneural hinge (CNH) is a stem cell pool lying posterior to the developing notochord in the tailbud. In *Xenopus*, progenitors of neural tube, notochord and somites reside in the CNH, and when the CNH is grafted to host embryos, it is able to produce ectopic tails (Gont et al., 1993). In mice, the CNH hosts both differentiating axial progenitors and self-renewing stem cells that contribute to differentiated tissues along the anterior/posterior axis (Cambray and Wilson, 2002). Our observation that secondary tails contain both notochord and somitic muscle suggested the possibility that a defect in CNH specification or morphogenesis could underlie the defect.

We first tested whether the secondary tails contained ectopic CNH cells by performing *in situ* hybridization with *flh*, which is expressed in the CNH during tail development. In both *mfn* and *kny* embryos at 24 hpf, *flh* was ectopically expressed in the region of the secondary tail, suggesting the existence of an extra CNH domain (Fig. 2.4A-C). We confirmed this result by observing ectopic expression of a second CNH marker *fgf4* (Fig. 2.S1).

The above experiments did not distinguish whether two distinct CNH domains were specified in these embryos or a single domain was initially specified that later split into two separate domains. In order to understand the emergence of the ectopic CNH domain, we performed a time-course experiment by fixing mutant embryos hourly during tail outgrowth and using *flh* expression to determine the onset of the secondary CNH domain. At 17 hpf, all *mfn* embryos showed one intact CNH domain in the tailbud (Fig. 2.4D). Over the next few hours, an increasing percentage of *mfn* embryos showed an elongated CNH stretched along the ventral side of the tailbud, with embryos showing two distinct CNH domains beginning to appear at 20 hpf (Fig. 2.4D). By 24 hpf, the penetrance of two CNH domains reached its peak and no stretched CNH were observed at this stage. In *snh* embryos, we observed similar progress of the onset of two CNH domains (Fig. 2.S2). In the case of *kny* embryos, the kinetics of secondary tail formation were roughly similar, with the onset of the appearance of two CNH domains beginning slightly later (23 hpf) (Fig. 2.4E). By 25 hpf, the formation of two CNH domains in *kny* embryos was close to completion (Fig. 2.4E). These results suggest that the CNH domain is specified normally in both *mfn* and *kny* embryos, but becomes split during tail extension, suggesting that a defect in morphogenetic movements could underlie the secondary tail phenotype.

N-Cadherin is required to maintain tailbud integrity.

Proper regulation of intercellular adhesion is important for proper cell movements (Halbleib and Nelson, 2006). Both the BMP pathway and noncanonical Wnt signaling have been demonstrated to regulate cell movements during gastrulation at least in part by regulation of the localization or activity of cadherins (Ulrich et al., 2005; von der Hardt et al., 2007). As a recent study has shown that a semidominant allele of N-cadherin (*cdh2)* perturbs cell cohesion in the tailbud (Harrington et al., 2007), we asked whether disruption of cell adhesion in the tailbud affects CNH morphogenesis. We performed genetic interaction assays between *dvl*2/3 and *cdh2*. Simultaneous injection of suboptimal amounts of *dvl2/3* MO and *cdh2* MO, which did not cause any tail defects when injected separately, induced secondary tail formation (Fig. 2.5A, C-E). At higher doses of *dvl2/3* MO and *cdh2* MO, we observed dramatically scattered tailbud cells rather than simple bifurcation (Fig. 2.5F). Interestingly, in *kny* embryos, we occasionally observed

embryos with three CNH domains, triple-branch notochords and peeled off hyphochord (Fig. 2.S3), which resemble these severe *dvl/cdh2* MO morphants (Fig. 2.5F).

To test for genetic interactions between BMP signaling and N-cadherin in secondary tail formation, we combined partial loss of BMP with partial loss of N-cadherin function. *cdh2* MO significantly enhanced the secondary tail penetrance in *mfn* morphants (Fig. 2.5B). Together, these results indicate that proper regulation of cell adhesion is essential for maintaining the coherence of the CNH during tail development, and suggests that BMP and the noncanonical Wnt pathway may act to prevent tail bifurcations by regulating intercellular adhesion in the tailbud.

During gastrulation, *wnt11* promotes coherence of the anteriorly migrating prechordal plate population of cells (Ulrich et al., 2005). In wild-type migrating prechordal plate cells, cadherin is believed to cycle between the plasma membrane and endosomes, but is found predominantly in endosomes. In embryos with impaired *wnt11* function, E-cadherin was localized more exclusively to the plasma membrane, suggesting that proper cycling of cadherin localization, regulated by noncanonical Wnts, is important for maintaining coherence of migrating prechordal plate cells (Ulrich et al., 2005). To determine whether cadherin localization is regulated by non-canonical Wnt signaling, we performed confocal imaging of embryos stained with a pan-cadherin antibody. In both *mfn* and wide-type embryos, cadherin was localized to the plasma membrane of CNH cells (Fig. 2.5H). In contrast, we observed a apparent shift to a more intracellular localization of cadherin within the CNH of *kny* embryos (Fig. 2.5I). We also analyzed the localization of β-catenin in *mfn* and *kny* embryos, and observed no defects in the normal membrane localization of β-catenin in tailbud cells (Fig. 2.S4). These results indicate that noncanonical Wnt signaling specifically affects the localization of cadherin without affecting the β-catenin.

CNH bifurcation occurs during tailbud protrusion.

Although BMP signaling clearly acts to promote the coherence of the CNH, it was unclear whether BMP acts directly on the CNH, or indirectly. The fact that known BMP ligands in the tailbud-*bmp2, bmp4,* and *bmp7*, are expressed most intensely in the posterior tailbud, away from the CNH, suggested that BMP's action could be indirect (Dick et al., 2000; Thisse et al., 2004). To determine more precisely where in the tailbud BMP is active, we performed

immunostaining with phosphorylated Smad1/5/8 (P-smad5) antibody in embryos at the 6-somite stage, and combined this assay with fluorescent *in situ* hybridization (FISH) using *flh* probe to visualize the CNH. Consistent with a recent study (Esterberg et al., 2008), we observed activation of BMP signaling in the posterior mesoderm of the tailbud, separate from the CNH (Fig. 2.6A). This localization of BMP activity to the posterior tailbud persisted at least until the 14-somite stage (Fig. 2.6B). In contrast, we observed no activation of BMP signaling in the tailbud of *mfn* embryos (Fig. 2.6C) although these embryos showed normal phosphorylation of Smad1/5/8 in the notochord. These results suggested that BMP regulates CNH morphogenesis indirectly.

To better understand how BMP signaling regulates CNH morphogenesis by its activation in the posterior mesoderm of the tailbud, we performed confocal time-lapse imaging of the developing tail in *Tg(flh:EGFP)* (Video 2.S1.) and *mfn*;*Tg(flh:EGFP)* embryos (Video 2.S2). In wild-type embryos, during tailbud extension stage, the CNH moved along the surface of the yolk cell in close association with Kupffer's vesicle (KV) (Fig. 2.6D). As the tailbud entered the protrusion phase at about the 12-somite stage, the most ventral posterior tailbud cells, coming from a region of high BMP activity (see Fig. 2.6B), moved anteriorly and started to undercut the KV (Fig. 2.6D'). Progressively, more cells from the ventral side moved in between the KV and yolk, and this was accompanied by notochord extension and yolk constriction (Fig. 2.6D''). As a result, the CNH together with the KV was lifted away from the surface of yolk and the tail began extending off of the yolk (Fig. 2.6D'''). In the case of *mfn* embryos, after a comparatively normal extension stage (Fig. 2.6E), the tailbud entered a protrusion phase also at the 12-somite stage. In contrast to wild type, the most ventral cells failed to undercut the KV. Instead, they moved inward, protruding into the yolk, often forming a very notable indentation (Fig. 2.6E'). This had the effect of drawing the KV and the CNH ventrally towards, or even into, the yolk. As tail extension continued, the lengthening notochord eventually caused the CNH to adopt the elongated "stretched" state during yolk constriction (Fig. 2.6E''). At the end of tailbud protrusion, the stretching of the CNH became more severe as the most ventral cells continued their irregular movements. This finally led to part of the CNH embedded into the yolk with the KV (Fig. 2.6E'''). Depending on the embryo, these ectopic CNH domains could either be completely 'left behind' during tail elongation, or remain connected to the main axis by a branching of the notochord (data not shown).

We also performed confocal time-lapse in vivo imaging with *kny*;*Tg(flh:EGFP)* transgenic line (Video 2.S3). We did not notice any change of CNH morphology until about the 14-somite stage, when the tailbud began to protrude off the yolk (Fig. 2.6F'). As the most ventral cells in *kny* undercut beneath the KV, we observed cells gradually detaching away from the CNH (Fig. 2.6F''). Over time, the ectopic CNH cells formed an elongated cluster nearly the size of the main CNH (Fig. 2.6F'''). Our observations suggest that stereotypical cell movements occur roughly normally in *kny* embryos, albeit at a reduced rate, and that the CNH, perhaps due to the mislocalization of cadherin, is unable to maintain coherence during tail extension and protrusion. Our confocal microscopy videos plus results of immunostaining experiments with pan-cadherin antibody suggest that non-canonical Wnt and BMP regulate CNH cohesion by direct and indirect mechanisms, respectively.

BMP regulates migration of posterior mesoderm cells in the tailbud

To determine the identity of the cells that undercut the KV and the CNH, we performed immunostaining with a Tbx6 antibody to label presomitic mesoderm cells (Szeto and Kimelman, 2004) in *Tg(flh:EGFP)* and *mfn*;*Tg(flh:EGFP)* embryos at several stages of tail development. In wild type, we observed a band of Tbx6-positive cells located beneath the CNH at the 16-somite stage (Fig. 2.7A), suggesting that those cells migrating along the ventral side of the CNH during tail protrusion are from the posterior mesoderm. Notably, cells in this region also show high levels of phospho-Smad staining (Fig. 2.S5). In *mfn* embryos, a cluster of Tbx6-positive cells is retained posteriorly in the tailbud, reflecting the defective movement of these undercutting cells (Fig. 2.7B). Consistent with our time-lapse video of *mfn* embryos, at least some of these posterior mesoderm cells eventually moved anteriorly and gradually surrounded the ectopic CNH domain, eventually ending up in the secondary tail domain (Fig. 2.7D). Taken together, our data suggest that split of the CNH upon loss of BMP signaling is likely a secondary consequence caused by the aberrant migration of a group of ventral-posterior presomitic mesoderm cells.

To determine whether blocking non-canonical Wnt signaling also affects the movement of posterior mesoderm cells, we performed a similar time course experiment in *kny*;*Tg(flh:EGFP)* embryos. Migration of the Tbx6-positive cells is delayed in *kny* embryos- these cells are retained posteriorly at 18 hpf (Fig. 2.7F). Only later, at the 21-somite stage do we observe some Tbx6-positive cells located ventrally beneath the CNH (Fig. 2.7H). At 23 hpf, we

observed Tbx6 positive cells colocalized with ectopic CNH cells (Fig. 2.7J), suggesting these Tbx6 cells were pushed along as the ectopic CNH cells drifted out from the main axis. Consistent with our time-lapse video (Fig. 2.6F'', also see Video 2.S3), the undercutting movement of the posterior mesoderm cells also occurred in *kny* embryos, though with delayed timing.

Discussion

The role of BMP signaling in specifying cell fate in the tailbud has been well-established. Here, we provide evidence that BMP signaling also mediates cell movements during tail development. Our data indicate that BMP signaling is activated in the ventroposterior tailbud to promote cell migration during tailbud protrusion, and that it is the defective migration of these cells which ultimately leads to bifurcation of the CNH domain and formation of a secondary tail in BMP mutants.

We also show that noncanonical Wnt signaling interacts with BMP signaling to maintain CNH integrity by affecting cadherin localization in CNH cells, possibly disrupting cell cohesion. Our data suggest a model in which BMP and noncanonical Wnt signaling regulate tail morphogenesis by controlling cell migration and cell adhesion within the tailbud.

BMP signaling inhibits secondary tail formation

It has been observed in previous investigations that reducing BMP signaling after gastrulation results in secondary tail formation (Connors et al., 1999; Pyati et al., 2005), and multiple explanations have been suggested to account for this unusual phenotype. Pyati and Kimelman proposed that after gastrulation, the role of BMP switches from that of promotion of tail development to one of inhibition, although a mechanism was not proposed (Pyati et al., 2005). In contrast, a recently proposed model suggests that post-gastrula BMP's continue to act as morphogens, patterning the fates of tail mesoderm, and that when BMP is inhibited mildly, ectopic presomitic mesoderm is produced that leads to formation of a secondary tail (Stickney et al., 2007). Two main lines of evidence indicate that the gradient model does not adequately explain the formation of secondary tails. First, our observation that secondary tails are produced by several BMP pathway mutants of widely varying strengths, spanning the strongly dorsalized *snh* mutants to the weakly dorsalized *mfn* mutant. The severity of the phenotype of mutants represents the level of loss of BMP signaling. The observation that secondary tail formation is

not restricted in a specific phenotypic category indicates that secondary tails are not a consequence of a precise adjustment of a BMP activity gradient within a narrow range (also see Fig 1.2F). Secondly, secondary tails are formed in the absence of the fate patterning defects predicted by the BMP gradient model. Thus, our findings do not support the BMP morphogen model as an explanation of secondary tail formation. Rather, we propose that BMP signaling independently regulates morphogenesis and cell fate patterning in the tailbud during early somitogenesis stages.

This model is similar to the proposed separable roles for BMP signaling during gastrulation in DV fate patterning and regulation of CE movements (von der Hardt et al., 2007). During gastrulation, BMP is thought to create a gradient of intercellular adhesion along the DV axis, from low levels on the ventral side, where BMP activity is highest, to high levels dorsally, where BMP activity is low. Migrating mesodermal cells therefore move away from regions of high BMP signaling/low adhesion towards regions of low BMP activity/higher adhesion (Myers et al., 2002; von der Hardt et al., 2007). While we observe a similar directionality (movement of mesodermal cells away from a region of high BMP activity), we do not know if an analogous gradient of adhesion is established in the tailbud by BMP. A key phenotypic distinction between the role of BMP in regulation of cell migration during gastrulation and the defects we observe here is that during gastrulation, dorsalward movement of lateral mesoderm is completely blocked in BMP-compromised embryos, while in the tailbud, posterior mesodermal cells still move anteriorly in *mfn* mutants, but move aberrantly into the yolk instead of undercutting Kupffer's vesicle. Precisely why these cells take this path remains unclear, though one possible explanation is that Kupffer's vesicle becomes more tightly associated with the yolk cell in BMP-compromised embryos, thereby blocking the movement of the presomitic mesoderm cells. However, in embryos where the dorsal organizer region was surgically removed near the end of gastrulation, and also in embryos where formation of Kupffer's vesicle was blocked by blastula-stage injection into the yolk of *ntl* and *spt* MOs, we still observed ectopic *tbx6*-postive cells associated with yolk extension (data not shown), indicating that these cells migrate aberrantly even in the absence of Kupffer's vesicle or the CNH. Therefore, we favor the hypothesis that BMP signaling is required for ventroposterior mesodermal cells to undertake a migratory path between the surface of the yolk cell and Kupffer's vesicle. When these cells move inappropriately into the yolk when BMP signaling is blocked, Kupffer's vesicle and the CNH

can be drawn at least partially into the yolk as well. As tail elongation proceeds, the CNH can become bifurcated, resulting in a branched notochord (see Fig. 2.1B, 1G). In some cases the ectopic CNH cells remain associated with the yolk extension, sometimes generating a short stretch of notochord that does not connect with the main notochord at all (data not shown). In general, such embryos do not form any morphologically obvious secondary tail and can only be detected by staining with the appropriate marker.

Our results are consistent with observations of dnBMPR embryos by Pyati and Kimelman, which led them to suggest that some population of mesodermal progenitors were being left behind during tail extension, and subsequently formed the secondary tail (Pyati et al., 2005). Our observations confirm and extend their hypothesis by identifying the population of mesodermal progenitors whose migration is regulated by BMP, by showing that defective migration of these cells leads to a bifurcation of the CNH, and by demonstrating that BMP signaling genetically interacts with N-cadherin and noncanonical Wnt signaling to regulate tail morphogenesis.

During gastrulation, BMP is proposed to regulate cell adhesion in a cadherin-dependent manner. For example, when BMP signaling is abrogated, as in *alk8* MO embryos, mesodermal cells exhibit behaviors (high stability of intercellular contacts) consistent with an increase in intercellular adhesion (von der Hardt et al., 2007). When cadherin function is also blocked via coinjection of a dominant negative Cadherin, cells show decreased stability of intercellular contacts, indicating that cell-cell adhesion is reduced (von der Hardt et al., 2007). These and other data led to a model in which BMP signaling negatively regulates an as yet unknown aspect of cadherin function.

We observed a strong enhancement of the secondary tail phenotype when *cdh2*/N-cadherin was knocked down in conjunction with partial knockdown of BMP. While this result indicates that regulation of cell adhesion is important for proper morphogenesis of the tailbud, whether BMP functions in this process via regulation of cadherin function, as it does during gastrulation, is unclear. For example, *cdh2* is expressed in the notochord as well as the tailbud (Lele et al., 2002; Harrington et al., 2007), raising the possibility that the synergy we observe is due to separate effects of BMP on the posterior tailbud and N-cadherin on the notochord/CNH. Alternatively, *cdh2* and BMP might both regulate migration of posterior mesoderm without necessarily functioning in the same pathway. More work, including a detailed examination of

morphogenetic movements occurring in the tailbuds of *mfn;cdh2* MO embryos will be required to address these possibilities more definitively.

Noncanonical Wnt signaling and Cadherin localization

Our results are the first to demonstrate that secondary tails are formed in embryos deficient for noncanonical Wnt signaling, although we note that the first published report of the *kny* mutant presciently described the presence of ectopic *eve1*-expressing cells near the yolk (Solnica-Krezel et al., 1996). As tail extension in *kny* embryos is so dramatically reduced, the presence of ectopic tail structures is generally not nearly as obvious as in *mfn* embryos. Indeed, we first observed secondary tails due to defective noncanonical Wnt signaling in the course of earlier experiments on *dvl2/dvl3* MO embryos (Angers et al., 2006), which have a much milder tail extension defect, allowing for easier identification of secondary tails.

We observed secondary tails in *kny* and *dvl2/dvl3* MO embryos, although the ligand for this putative noncanonical Wnt pathway remains unidentified at this time. Our observation that other genes that are required for CE movements during gastrulation, such as *stbm*, *pk1*, and *pk2*, do not appear to play a role in secondary tail formation, suggests that secondary tails are not formed merely as a by-product of earlier defects in morphogenesis. This, along with the defects in cadherin localization in CNH cells of *kny* embryos (see below), suggests a role for noncanonical Wnt signaling specifically during tail development to govern morphogenetic movements.

As the CNH moves posteriorly during tail extension, it encounters a continuous stream of anteriorly-migrating mesodermal progenitors from the tailbud, which move around the CNH via subduction and by moving laterally away from the midline (Kanki and Ho, 1997). We hypothesize that the CNH experiences some shear stress as the result of moving through this field of tailbud cells, and that, in the absence of noncanonical Wnt signaling, is unable to maintain sufficient cohesion to support CNH integrity during tail extension. Our time-lapse imaging of *kny* embryos shows that the ectopic CNH cells slough off the ventral portion of the CNH during tail extension, consistent with this group of cells being less cohesive. Our observation that partial inhibition of *cdh2*, which has previously been shown to be important in maintaining cohesion of the notochord (Harrington et al., 2007), synergizes strongly with

inhibition of noncanonical Wnt signaling, is consistent with cell-cell adhesion playing a key role in maintaining the integrity of the CNH.

Noncanonical Wnt signaling promotes plasma membrane localization of cadherin

During gastrulation, Wnt11 has been proposed to promote the cycling of E-cadherin between the plasma membrane and endosomes in migrating prechordal plate cells (Ulrich et al., 2005). In the absence of Wnt11, E-cadherin is predominantly localized at the plasma membrane, while in Wnt11-overexpressing cells, E-cadherin is observed most often in endosomes. Wnt11-deficient cells were also shown to adhere more weakly to an E-cadherin coated substrate, indicating that the noncanonical Wnt signaling promotes intercellular adhesion among prechordal plate cells as they migrate past other cells, such as the overlying epiblast (Ulrich et al., 2005). Curiously, in the CNH, we observe the opposite effect on cadherin localization-cadherin becomes more intracellularly localized in the absence of Wnt signaling, rather than in its presence. The significance of this difference remains unclear. One possibility is that prechordal plate cells, being actively migrating across a substrate of other cells and extracellular matrix, need to constantly remodel adhesion complexes in order to both move over their substrate and remain associated with other prechordal plate cells. It is not clear if CNH cells behave in the same way-posteriorward extension of the CNH appears more passive, driven predominantly by CE movements occurring more anteriorly. Perhaps in this situation, more static localization of cadherin to the plasma membrane is sufficient to maintain coherence of CNH cells as they move posteriorly through a stream of anteriorly migrating posterior tailbud cells.

A model for the roles of BMP and noncanonical Wnt signaling in tail morphogenesis

Our genetic and phenotypic data suggest that BMP and noncanonical Wnt signaling function independently of each other to ensure integrity of the CNH and proper morphogenesis of the tail (Fig. 2.8). First, BMP signaling, acting on ventroposterior mesodermal prescursors, promotes the anteriorward migration of these cells, undercutting Kupffer's vesicle and disrupting the association of the CNH with the yolk prior to tail protrustion. When BMP signaling is blocked, aberrant migration of the mesodermal progenitors into the yolk can capture the CNH, leading to its bifurcation as tail development proceeds. Meanwhile, noncanonical Wnt signaling promotes the localization of cadherin to the plasma membrane in CNH cells, increasing intercellular adhesion among these cells and allowing them to remain associated as CE

movements push them posteriorly into the tailbud. When noncanonical Wnt signaling is impaired, cohesion of the CNH is reduced, leading to a sloughing off of CNH cells and formation of a secondary tail. When both pathways are blocked, nearly all embryos form a secondary tail, possibly because a less cohesive CNH will nearly always split when 'caught' in the yolk. Thus, we propose that these two pathways, which function independently to regulate convergence-extension during gastrulation, work in separate pathways later in development in distinct regions of the tailbud to govern proper morphogenetic movements.

Figures and Tables

Figure 2.1 Mesoderm tissues are mis-specified in the secondary tails of *mfn*.

(A-G) Lateral view of expression of *col2*α (A,B), *myoD* (C,D), *neurog1* (E,F) and *ntl* (F,G) in the posterior tail of wild-type and *mfn* embryos fixed at 26 hpf. *col2*α (B), *myoD* (D) and *ntl* (G) are ectopically expressed in the secondary tail, but not *neurog1* (F). Embryos in all images are mounted with anterior to the left.

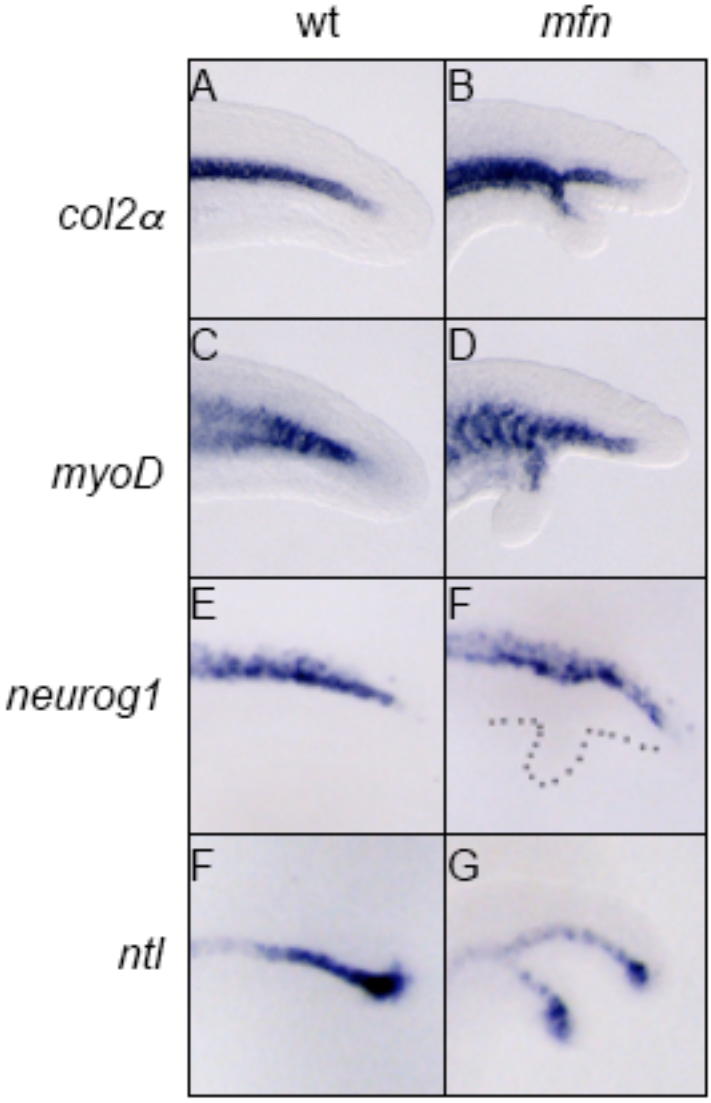

Figure 2.2 Secondary tail formation is independent of the role of BMP signaling in fate patterning.

(A-E) Lateral view of tails in wild-type and dorsalized embryos of indicated genotypes at 24 hpf, after whole amount *in situ* with *ntl*. Primary and secondary tails are marked with arrowheads.

(F) Distribution of secondary tail phenotype in embryos following DM treatment at indicated time points. Secondary tails were scored by the presence of ectopic *ntl* expression.

(G) Lateral view of the tail of a live embryo at 24 hpf, after DM treatment at 7 somites. Note the secondary tail with fully developed ventral fin.

(H,I) Dorsal view of *gata1* expression in embryos at 12-somite stage, after treatment with DMSO (H) and DM (I) at 5-somite stage.

(J,K) Dorsal view of *myoD* expression in the tails of wt (J) and *mfn* (K) embryos at 22 hpf. Inset shows the lateral view.

Expression of *gata1* (I) and *myoD* (K) is unaffected.

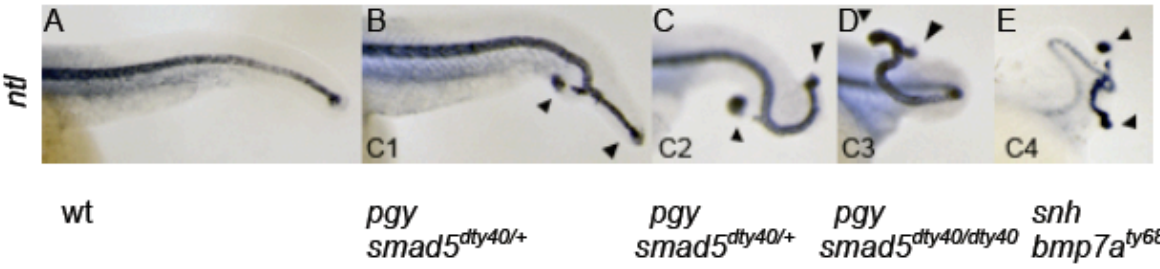
ntl
A
B
C
D
E
C1
C2
C3
C4
wt
pgy
smad5dty40/+
pgy
smad5dty40/+
pgy
smad5dty40/dty40
snh
bmp7ata68a/ty68a

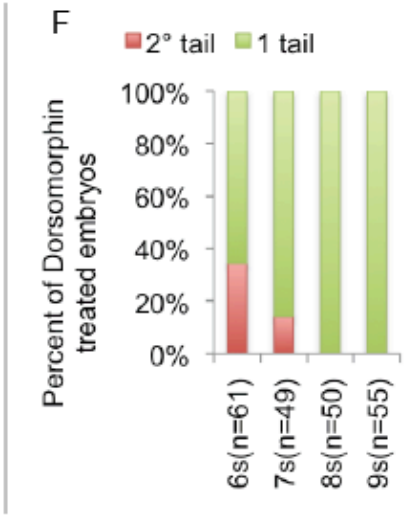
F
2° tail
1 tail
Percent of Dorsomorphin treated embryos
100%
80%
60%
40%
20%
0%
6s(n=61)
7s(n=49)
8s(n=50)
9s(n=55)

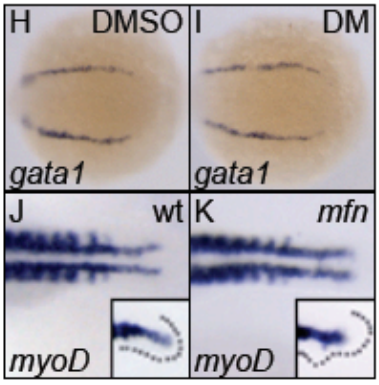
H
DMSO
I
DM
gata1
gata1
J
wt
K
mfn
myoD
myoD


DM 7s
G

Figure 2.3 Noncanonical Wnt signaling functions with BMP in inhibiting secondary tail formation.

(A-C) Lateral view of wild-type (A, 24 hpf), *dvl2/3* morphant (B, 24 hpf) and *kny* mutant (C, 72 hpf). Insets of (A) and (B) show *ntl* expression in the posterior tail. Inset of (C) shows a close-up of posterior tail. Primary and secondary tails are marked with arrowheads.

(D-I) Lateral view of expression of *ntl* (D,E), *col2*α (F,G), and *myoD* (H,I) in the tail of wild-type and *kny* embryos fixed at 24 hpf. *ntl* (E), *col2*α (G), and *myoD* (I) exhibit ectopic expression within the tails of *kny*.

(J) Percentages of secondary tail formation in embryos injected with indicated combination of morpholinos (1 mg/ml each, except for 'dvl2/dvl3 MO' condition, where a concentration of 3 mg/ml for each MO was injected). For each column embryos from at least three separate experiments were scored.

(K) Percentages of secondary tail formation in embryos from incross of *mfn/+*;*kny/+* double mutants carriers. Embryos are categorized by phenotypes.

Secondary tails in (J) and (K) were scored by *ntl* expression. Percentage of secondary tail of each separate experiment is calculated. Then the arithmetic mean of percentage of all replicates is calculated by dividing the sum of percentages with numbers of replicates. Then the variation from the mean is represented by calculated standard deviation. Error bars represent standard deviations of at least 3 replicates. Number of embryos scored for each column is shown in figures.

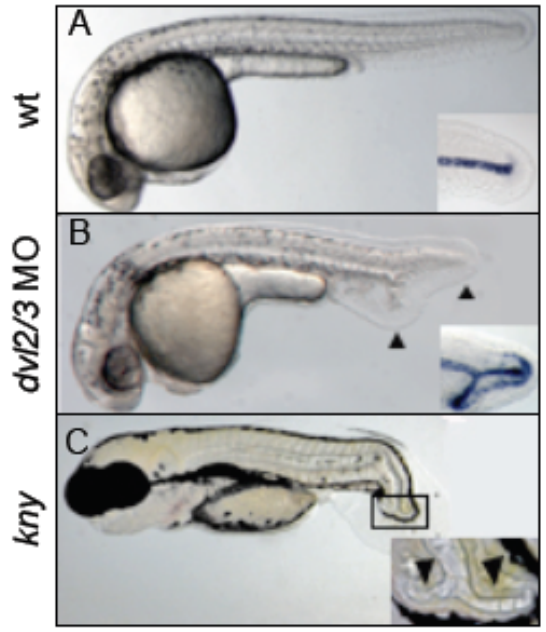
A
B
C
wt
dvl2/3 MO
kny

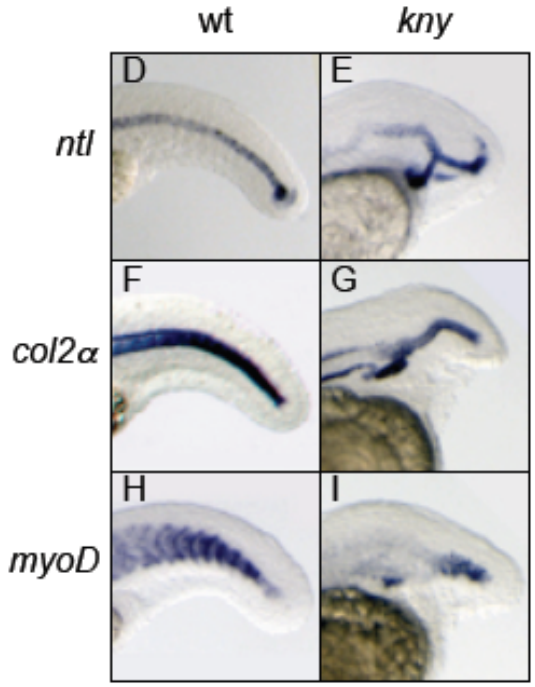
wt
kny
D
E
F
G
H
I
ntl
col2α
myoD

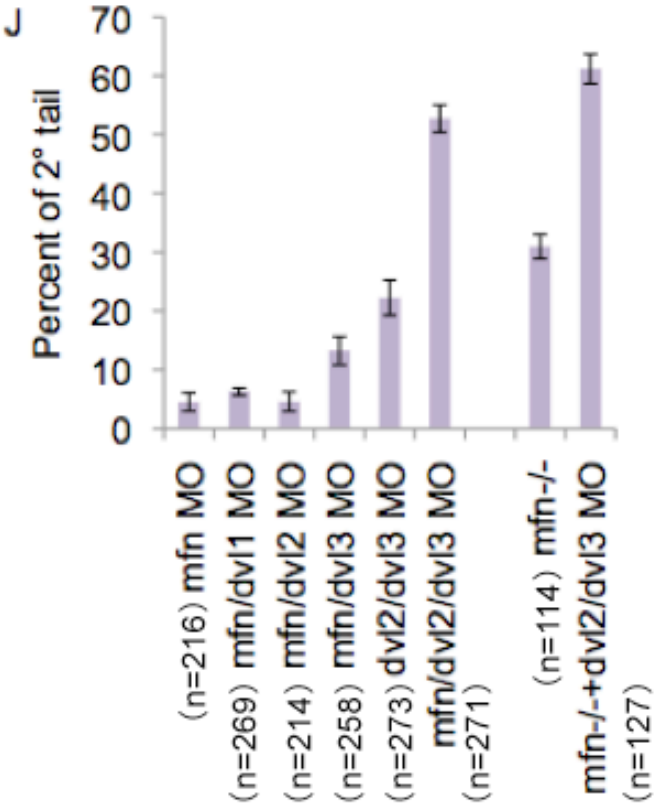
J
Percent of 2° tail
0
10
20
30
40
50
60
70
(n=216) mfn MO
(n=269) mfn/dvl1 MO
(n=214) mfn/dvl2 MO
(n=258) mfn/dvl3 MO
(n=273) dvl2/dvl3 MO
mfn/dvl2/dvl3 MO
(n=271)
(n=114) mfn-/-
mfn-/-+dvl2/dvl3 MO
(n=127)

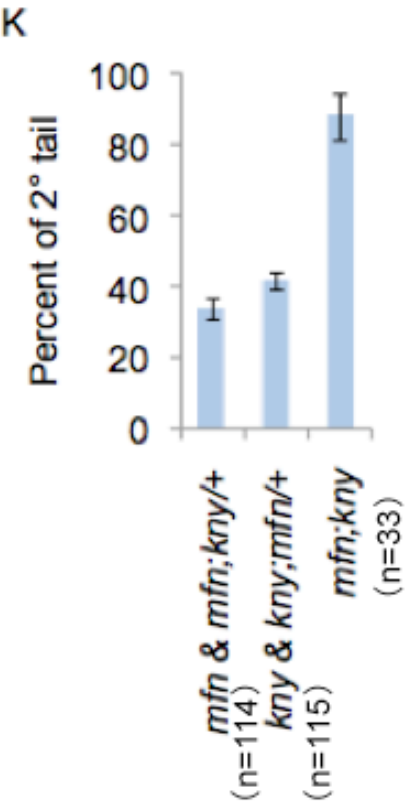
K
Percent of 2° tail
0
20
40
60
80
100
mfn & mfn;kny/+
(n=114)
kny & kny;mfn/+
(n=115)
mfn;kny
(n=33)

Figure 2.4 Bifurcation of the chordoneural hinge (CNH) in BMP and noncanonical Wnt mutants during tail outgrowth.

(A-C) Lateral view of expression of CNH marker, *flh* in the tail of wild-type, *mfn* and *kny* embryos fixed at 24 hpf. *flh* is expressed in the secondary tail of *mfn* (B) and *kny* (C).

(D,E) Distribution of morphological phenotypes of *flh*-expressing CNH in *mfn* (D) and *kny* (E) embryos fixed at indicated time points. Right panel shows the lateral view of representative embryo in each phenotypic class; inset, close-up of posterior tail of *kny*. For each time point around 40 embryos were scored.

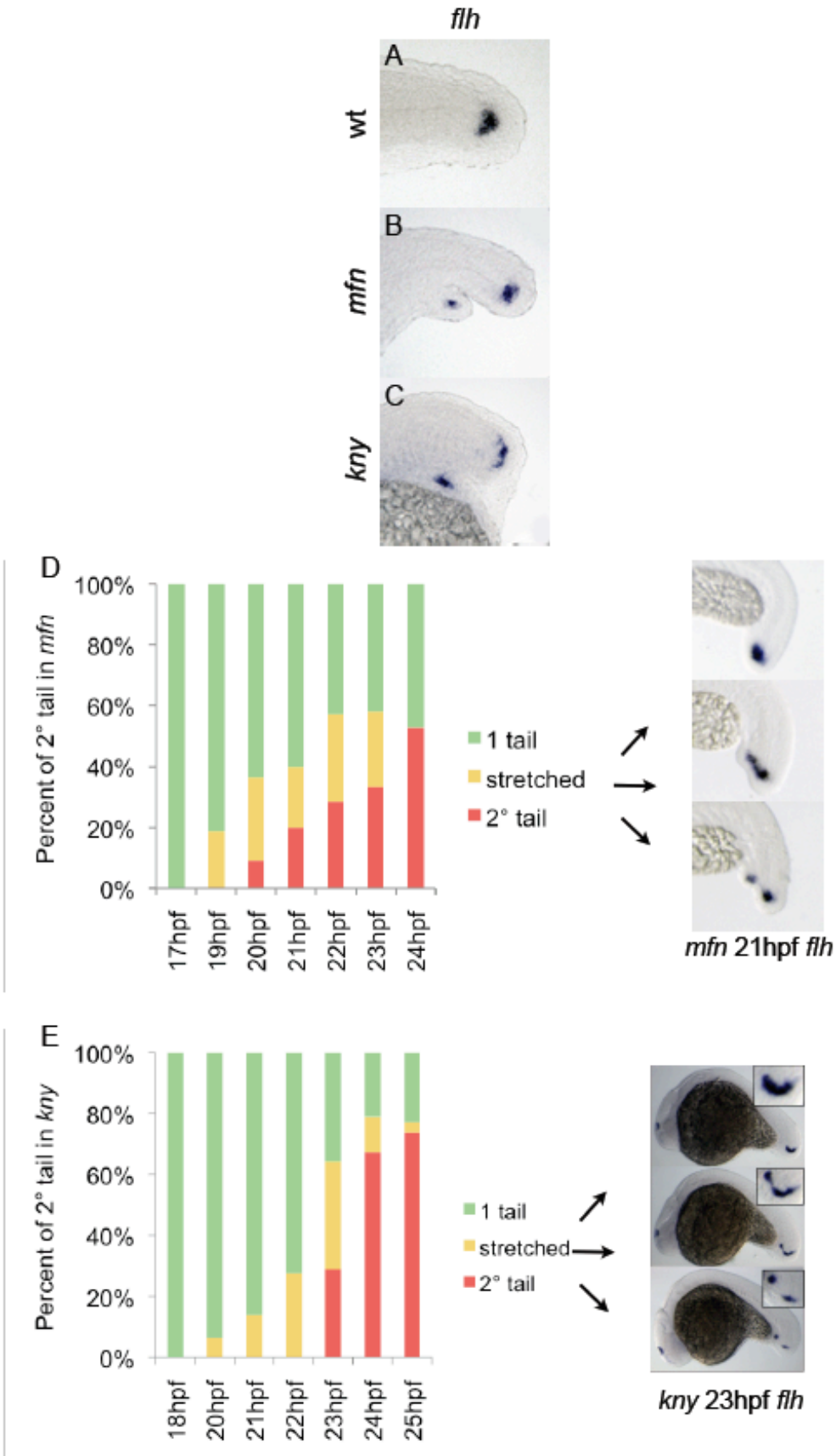
flh
A
wt
B
mfn
C
kny
D
Percent of 2° tail in mfn
100%
80%
60%
40%
20%
0%
17hpf
19hpf
20hpf
21hpf
22hpf
23hpf
24hpf
1 tail
stretched
2° tail
mfn 21hpf flh
E
Percent of 2° tail in kny
100%
80%
60%
40%
20%
0%
18hpf
20hpf
21hpf
22hpf
23hpf
24hpf
25hpf
1 tail
stretched
2° tail
kny 23hpf flh

Figure 2.5 N-cadherin synergizes with BMP and noncanonical Wnt signaling to prevent secondary tail formation.

(A, B) Percentages of secondary tail formation in embryos injected with indicated combination of morpholinos. For low concentration, *dvl2/3* (1 mg/ml each), *mfn* (0.5 mg/ml) and *chd2* (0.1 mg/ml) MOs were injected. Embryos from three separate experiments were scored. Percentage of secondary tail of each separate experiment is calculated. Then the arithmetic mean of percentage of all replicates is calculated by dividing the sum of percentages with numbers of replicates. Then the variation from the mean is represented by calculated standard deviation. Error bars represent standard deviations of at least 3 replicates. Number of embryos scored for each column is shown in figures.

(C-G) Lateral view of tails of embryos at 24 hpf injected with indicated combination of morpholinos, after *in situ* hybridization with *ntl*. *ntl* expression in *cdh2* and *dvl2/3* MO morphants (C,D) is similar to wide-type. Note that co-injection of high concentration of *chd2* and *dvl2/3* MOs further enhanced the *ntl* expression from a single fork shaped pattern in (E) to a multi-fork pattern in (F), and co-injection of high concentration of *chd2* and *mfn* MOs in embryo (G) did not result in similar phenotype. This difference is consistent with our following antibody staining results (see below). For high concentration, *dvl2/3* (1.5 mg/ml each), *mfn* (1.5 mg/ml) and *chd2* (0.25 mg/ml) MOs were injected.

(H-J) Representative confocal microscopy images of tailbud in wild-type, *kny* and *mfn* embryos stained with pan-cadherin antibody at 21 somites; inset, close-up of CNH region. Membrane staining pattern in CNH is shown in wild-type (H) and *mfn* (J), while diffused staining pattern is shown in *kny* (I).

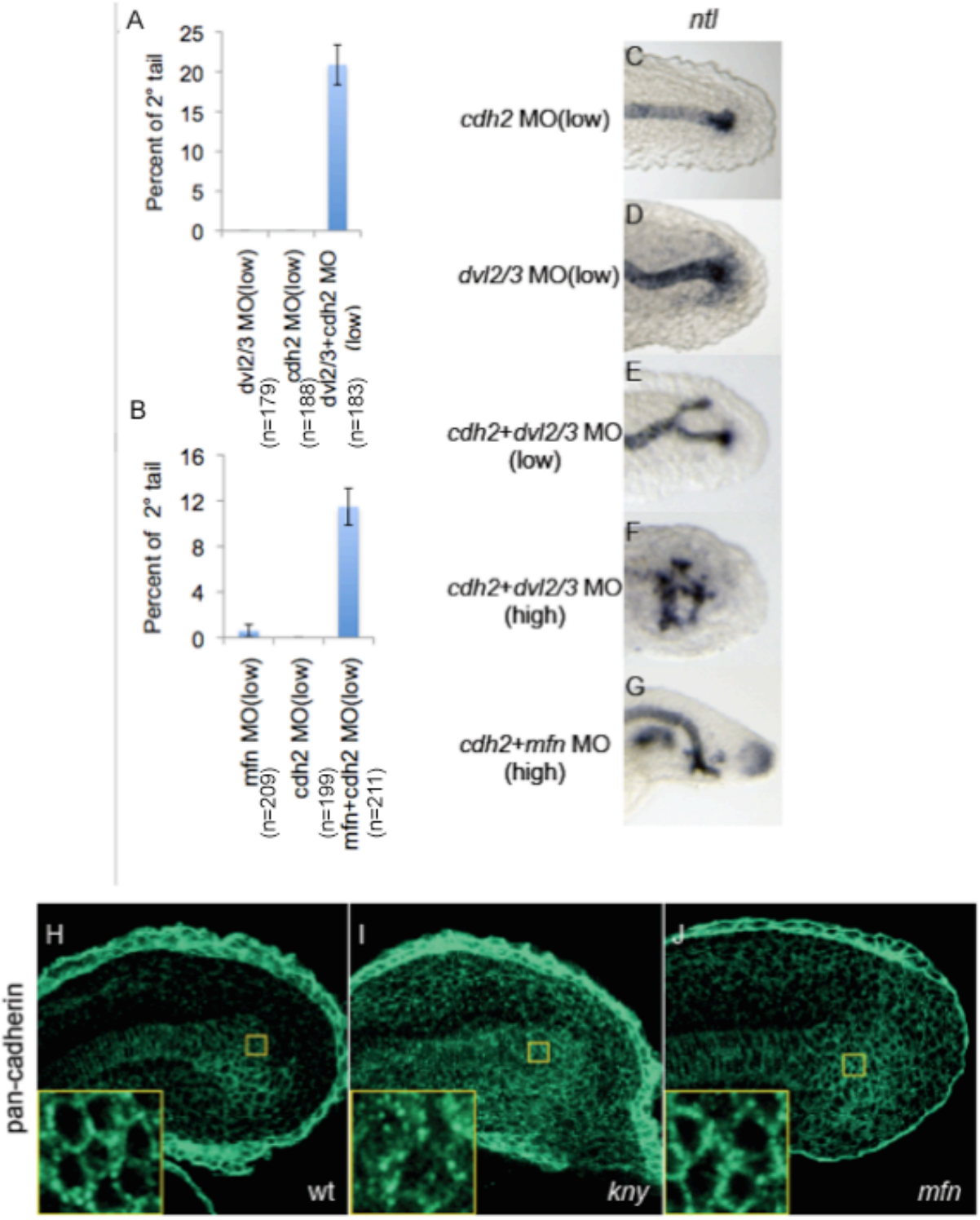
A
Percent of 2° tail
25
20
15
10
5
0
dvl2/3 MO(low) (n=179)
cdh2 MO(low) (n=188)
dvl2/3+cdh2 MO (low) (n=183)
B
Percent of 2° tail
16
12
8
4
0
mfn MO(low) (n=209)
cdh2 MO(low) (n=199)
mfn+cdh2 MO(low) (n=211)
ntl
C
cdh2 MO(low)
D
dvl2/3 MO(low)
E
cdh2+dvl2/3 MO (low)
F
cdh2+dvl2/3 MO (high)
G
cdh2+mfn MO (high)
pan-cadherin
H
wt
I
kny
J
mfn

Figure 2.6 Defects of CNH in *mfn* and *kny* initiate during tailbud protrusion.

(A) Dorsal view of flat-mounted tailbud of 6-somite wild-type embryo, after FISH with *flh* (red) and antibody staining with P-Samd5 (green), and no colocalization (merge) is seen.

(B,C) Lateral view of tails of 14-somite wild-type and *mfn* embryos exposed to P-Smad5 (green) and β-catenin (red) antibodies. P-Smad5 staining is absent in the posterior tailbud of *mfn* (C, merge). Arrowheads indicate the ventroposterior cells in the tailbud that are normally positive for P-Smad5 (B, merge).

(D-F’’’) Confocal time-lapse recording of tailbuds in embryos expressing *Tg(flh:EGFP)* transgene (green) and mRFP (red) from 10-somite stage. Shown are wild-type embryo (D-D’’’), *mfn* (E-E’’’) and *kny* mutants (F-F’’’). Note that besides CNH transgenic EGFP is retained in notochord, floorplate and periphery of Kupffer’s vesicle (KV), marked by white line. Ends of stretched CNH are indicated by blue line in (E’’’) and (F’’’). Arrowheads mark the ventroposterior cells in the tailbud. Embryos were all mounted laterally.

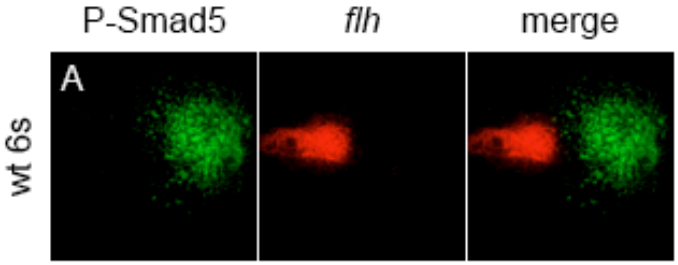
P-Smad5
flh
merge
A
wt 6s

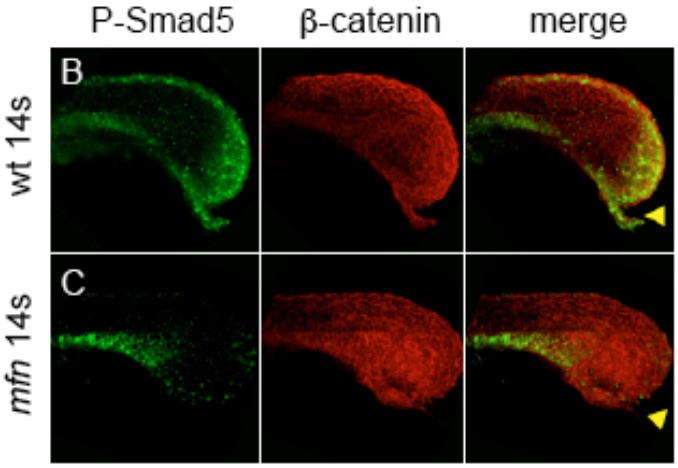
P-Smad5
β-catenin
merge
B
wt 14s
C
mfn 14s

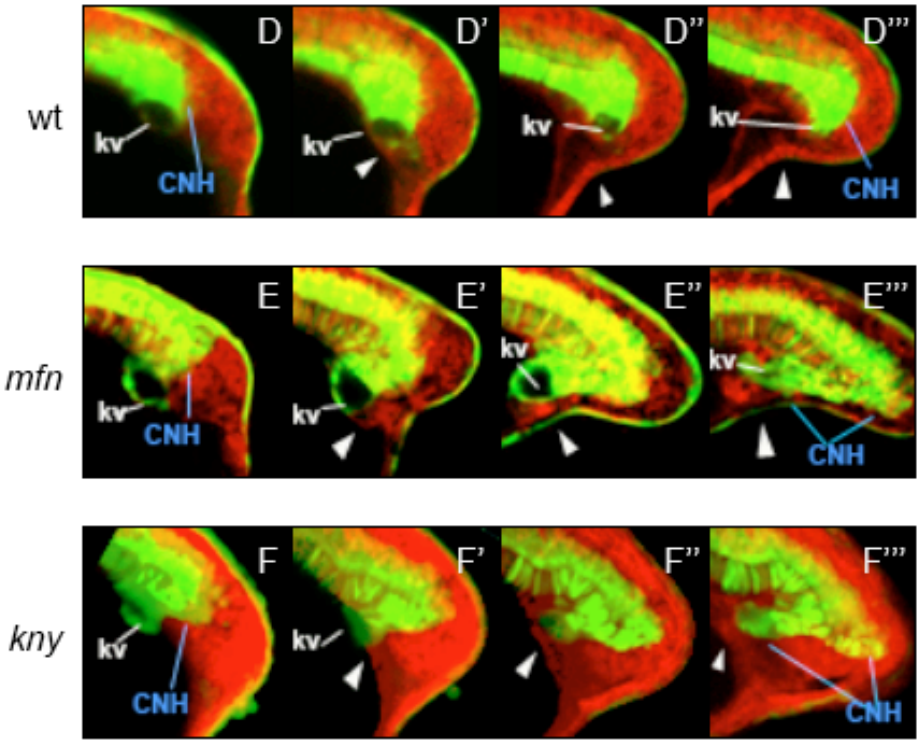
wt
mfn
kny
D
D'
D''
D'''
E
E'
E''
E'''
F
F'
F''
F'''
kv
CNH

Figure 2.7 BMP regulates posterior mesoderm cells of tailbud to inhibit secondary tail formation.

(A-J) all panels show the midline section of tails of *Tg(flh:EGFP)* expressing embryos (green) at indicated time points after anti-Tbx6 (red) immunostaining. Tbx6 positive mesoderm cells in *mfn* embryo (B) displays a detention in the posterior tailbud, when compared to wild-type embryo (A) at the same stage. Ectopic A more wild-type like movement of posterior mesoderm cells in *kny* embryo is shown in (F) and (H). Note eventually ectopic Tbx6 positive mesoderm cells are shown in the secondary tail domain of *mfn* (D) and *kny* embryos (J). Arrowheads mark the ventroposterior mesoderm cells in the taillbud. All tails are flat mounted laterally.

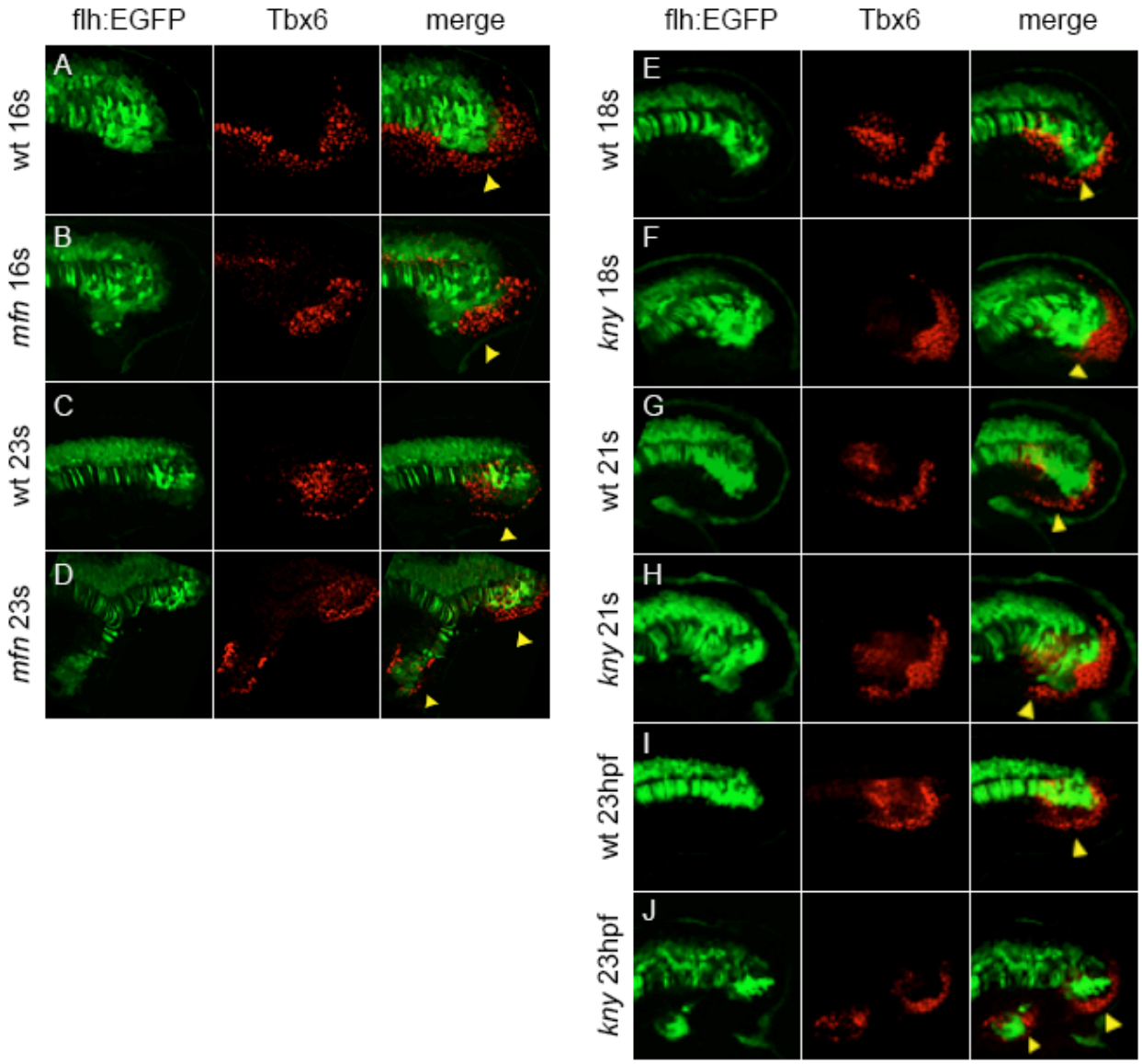

Figure 2.8 A model for the roles of BMP and noncanonical Wnt signaling in regulating tail development.

Depiction of the tailbud of a 10-somite wild-type embryo. During tailbud protrusion, BMP signaling in the posterior tailbud plays a crucial role in guiding the ventroposterior mesoderm cells to move beneath the Kupffer's vesicle properly. Noncanonical Wnt signaling promotes intercellular adhesion in CNH cells, allowing them to maintain cohesion during tail elongation. nt: notochord; PM: posterior mesoderm; KV: Kupffer's vesicle.

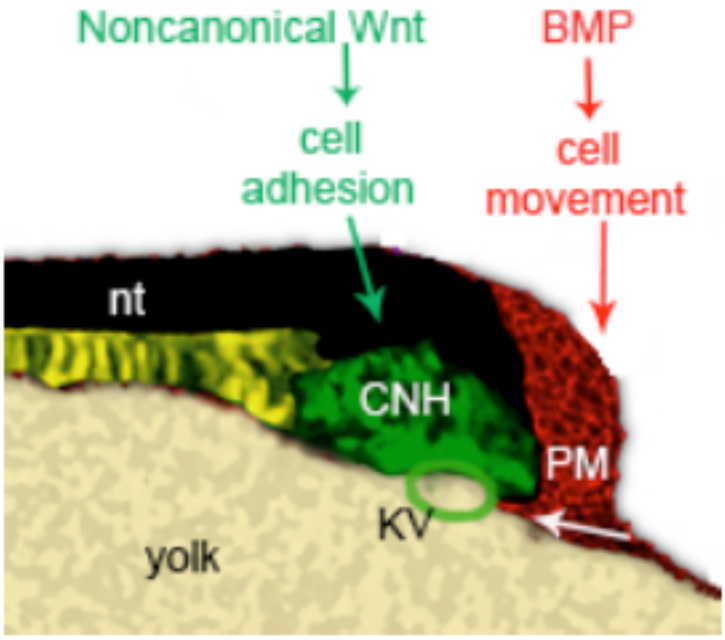

Table 2.1 Ectopic tail tissues produced in *mini fin* mutants

	col2α	*myoD*	*neurog1*	*ntl*
mfn embryos scored (n)	77	83	69	70
ectopic tissue (%)	53.2	30.1	0	64

Table 2.2 Ectopic tail tissues produced in *knypek* mutants

	col2α	*myoD*
kny embryos scored (n)	112	107
2° tail (%)	56.3	51.4

References

Agathon, A., Thisse, C. and Thisse, B. (2003). The molecular nature of the zebrafish tail organizer. *Nature* **424**, 448-452.

Angers, S., Thorpe, C. J., Biechele, T. L., Goldenberg, S. J., Zheng, N., MacCoss, M. J. and Moon, R. T. (2006). The KLHL12-Cullin-3 ubiquitin ligase negatively regulates the Wnt-beta-catenin pathway by targeting Dishevelled for degradation. *Nat Cell Biol* **8**, 348-357.

Blader, P., Fischer, N., Gradwohl, G., Guillemot, F. and Strahle, U. (1997). The activity of neurogenin1 is controlled by local cues in the zebrafish embryo. *Development* **124**, 4557-4569.

Cambray, N. and Wilson, V. (2002). Axial progenitors with extensive potency are localised to the mouse chordoneural hinge. *Development* **129**, 4855-4866.

Cambray, N. and Wilson, V. (2007). Two distinct sources for a population of maturing axial progenitors. *Development* **134**, 2829-2840.

Charrier, J. B., Teillet, M. A., Lapointe, F. and Le Douarin, N. M. (1999). Defining subregions of Hensen's node essential for caudalward movement, midline development and cell survival. *Development* **126**, 4771-4783.

Connors, S. A., Trout, J., Ekker, M. and Mullins, M. C. (1999). The role of tolloid/mini fin in dorsoventral pattern formation of the zebrafish embryo. *Development* **126**, 3119-3130.

Davis, R. L. and Kirschner, M. W. (2000). The fate of cells in the tailbud of Xenopus laevis. *Development* **127**, 255-267.

Detrich, H. W., 3rd, Kieran, M. W., Chan, F. Y., Barone, L. M., Yee, K., Rundstadler, J. A., Pratt, S., Ransom, D. and Zon, L. I. (1995). Intraembryonic hematopoietic cell migration during vertebrate development. *Proc Natl Acad Sci U S A* **92**, 10713-10717.

Dick, A., Hild, M., Bauer, H., Imai, Y., Maifeld, H., Schier, A. F., Talbot, W. S., Bouwmeester, T. and Hammerschmidt, M. (2000). Essential role of Bmp7 (snailhouse) and its prodomain in dorsoventral patterning of the zebrafish embryo. *Development* **127**, 343-354.

Esterberg, R., Delalande, J. M. and Fritz, A. (2008). Tailbud-derived Bmp4 drives proliferation and inhibits maturation of zebrafish chordamesoderm. *Development* **135**, 3891-3901.

Gamse, J. T., Thisse, C., Thisse, B. and Halpern, M. E. (2003). The parapineal mediates left-right asymmetry in the zebrafish diencephalon. *Development* **130**, 1059-1068.

Gont, L. K., Steinbeisser, H., Blumberg, B. and de Robertis, E. M. (1993). Tail formation as a continuation of gastrulation: the multiple cell populations of the Xenopus tailbud derive from the late blastopore lip. *Development* **119**, 991-1004.

Halbleib, J. M. and Nelson, W. J. (2006). Cadherins in development: cell adhesion, sorting, and tissue morphogenesis. *Genes Dev* **20**, 3199-3214.

Harrington, M. J., Hong, E., Fasanmi, O. and Brewster, R. (2007). Cadherin-mediated adhesion regulates posterior body formation. *BMC Dev Biol* **7**, 130.

Hauptmann, G. and Gerster, T. (1994). Two-color whole-mount *in situ* hybridization to vertebrate and Drosophila embryos. *Trends Genet* **10**, 266.

Jasuja, R., Voss, N., Ge, G., Hoffman, G. G., Lyman-Gingerich, J., Pelegri, F. and Greenspan, D. S. (2006). bmp1 and mini fin are functionally redundant in regulating formation of the zebrafish dorsoventral axis. *Mech Dev* **123**, 548-558.

Kanki, J. P. and Ho, R. K. (1997). The development of the posterior body in zebrafish. *Development* **124**, 881-893.

Kimmel, C. B., Ballard, W. W., Kimmel, S. R., Ullmann, B. and Schilling, T. F. (1995). Stages of embryonic development of the zebrafish. *Dev Dyn* **203**, 253-310.

Kishimoto, Y., Lee, K. H., Zon, L., Hammerschmidt, M. and Schulte-Merker, S. (1997). The molecular nature of zebrafish swirl: BMP2 function is essential during early dorsoventral patterning. *Development* **124**, 4457-4466.

Kramer, C., Mayr, T., Nowak, M., Schumacher, J., Runke, G., Bauer, H., Wagner, D. S., Schmid, B., Imai, Y., Talbot, W. S. et al. (2002). Maternally supplied Smad5 is required for ventral specification in zebrafish embryos prior to zygotic Bmp signaling. *Dev Biol* **250**, 263-279.

Lele, Z., Folchert, A., Concha, M., Rauch, G. J., Geisler, R., Rosa, F., Wilson, S. W., Hammerschmidt, M. and Bally-Cuif, L. (2002). parachute/n-cadherin is required for morphogenesis and maintained integrity of the zebrafish neural tube. *Development* **129**, 3281-3294.

Little, S. C. and Mullins, M. C. (2006). Extracellular modulation of BMP activity in patterning the dorsoventral axis. *Birth Defects Res C Embryo Today* **78**, 224-242.

Marlow, F., Gonzalez, E. M., Yin, C., Rojo, C. and Solnica-Krezel, L. (2004). No tail co-operates with non-canonical Wnt signaling to regulate posterior body morphogenesis in zebrafish. *Development* **131**, 203-216.

Marlow, F., Zwartkruis, F., Malicki, J., Neuhauss, S. C., Abbas, L., Weaver, M., Driever, W. and Solnica-Krezel, L. (1998). Functional interactions of genes mediating convergent extension, knypek and trilobite, during the partitioning of the eye primordium in zebrafish. *Dev Biol* **203**, 382-399.

Mintzer, K. A., Lee, M. A., Runke, G., Trout, J., Whitman, M. and Mullins, M. C. (2001). Lost-a-fin encodes a type I BMP receptor, Alk8, acting maternally and zygotically in dorsoventral pattern formation. *Development* **128**, 859-869.

Mullins, M. C., Hammerschmidt, M., Kane, D. A., Odenthal, J., Brand, M., van Eeden, F. J., Furutani-Seiki, M., Granato, M., Haffter, P., Heisenberg, C. P. et al. (1996). Genes establishing dorsoventral pattern formation in the zebrafish embryo: the ventral specifying genes. *Development* **123**, 81-93.

Myers, D. C., Sepich, D. S. and Solnica-Krezel, L. (2002). Bmp activity gradient regulates convergent extension during zebrafish gastrulation. *Dev Biol* **243**, 81-98.

Oxtoby, E. and Jowett, T. (1993). Cloning of the zebrafish krox-20 gene (krx-20) and its expression during hindbrain development. *Nucleic Acids Res* **21**, 1087-1095.

Park, M. and Moon, R. T. (2002). The planar cell-polarity gene stbm regulates cell behaviour and cell fate in vertebrate embryos. *Nat Cell Biol* **4**, 20-25.

Pyati, U. J., Webb, A. E. and Kimelman, D. (2005). Transgenic zebrafish reveal stage-specific roles for Bmp signaling in ventral and posterior mesoderm development. *Development* **132**, 2333-2343.

Pyati, U. J., Cooper, M. S., Davidson, A. J., Nechiporuk, A. and Kimelman, D. (2006). Sustained Bmp signaling is essential for cloaca development in zebrafish. *Development* **133**, 2275-2284.

Schier, A. F. and Talbot, W. S. (2005). Molecular genetics of axis formation in zebrafish. *Annu Rev Genet* **39**, 561-613.

Schmid, B., Furthauer, M., Connors, S. A., Trout, J., Thisse, B., Thisse, C. and Mullins, M. C. (2000). Equivalent genetic roles for bmp7/snailhouse and bmp2b/swirl in dorsoventral pattern formation. *Development* **127**, 957-967.

Schulte-Merker, S., Ho, R. K., Herrmann, B. G. and Nusslein-Volhard, C. (1992). The protein product of the zebrafish homologue of the mouse T gene is expressed in nuclei of the germ ring and the notochord of the early embryo. *Development* **116**, 1021-1032.

Seifert, J. R. and Mlodzik, M. (2007). Frizzled/PCP signalling: a conserved mechanism regulating cell polarity and directed motility. *Nat Rev Genet* **8**, 126-138.

Solnica-Krezel, L., Stemple, D. L., Mountcastle-Shah, E., Rangini, Z., Neuhauss, S. C., Malicki, J., Schier, A. F., Stainier, D. Y., Zwartkruis, F., Abdelilah, S. et al. (1996). Mutations affecting cell fates and cellular rearrangements during gastrulation in zebrafish. *Development* **123**, 67-80.

Stickney, H. L., Imai, Y., Draper, B., Moens, C. and Talbot, W. S. (2007). Zebrafish bmp4 functions during late gastrulation to specify ventroposterior cell fates. *Dev Biol* **310**, 71-84.

Szeto, D. P. and Kimelman, D. (2004). Combinatorial gene regulation by Bmp and Wnt in zebrafish posterior mesoderm formation. *Development* **131**, 3751-3760.

Talbot, W. S., Trevarrow, B., Halpern, M. E., Melby, A. E., Farr, G., Postlethwait, J. H., Jowett, T., Kimmel, C. B. and Kimelman, D. (1995). A homeobox gene essential for zebrafish notochord development. *Nature* **378**, 150-157.

Thisse, B., Heyer, V., Lux, A., Alunni, V., Degrave, A., Seiliez, I., Kirchner, J., Parkhill, J. P. and Thisse, C. (2004). Spatial and temporal expression of the zebrafish genome by large-scale *in situ* hybridization screening. *Methods Cell Biol* **77**, 505-519.

Topczewski, J., Sepich, D. S., Myers, D. C., Walker, C., Amores, A., Lele, Z., Hammerschmidt, M., Postlethwait, J. and Solnica-Krezel, L. (2001). The zebrafish glypican knypek controls cell polarity during gastrulation movements of convergent extension. *Dev Cell* **1**, 251-264.

Tucker, J. A., Mintzer, K. A. and Mullins, M. C. (2008). The BMP signaling gradient patterns dorsoventral tissues in a temporally progressive manner along the anteroposterior axis. *Dev Cell* **14**, 108-119.

Ulrich, F., Krieg, M., Schotz, E. M., Link, V., Castanon, I., Schnabel, V., Taubenberger, A., Mueller, D., Puech, P. H. and Heisenberg, C. P. (2005). Wnt11 functions in gastrulation by controlling cell cohesion through Rab5c and E-cadherin. *Dev Cell* **9**, 555-564.

Veeman, M. T., Axelrod, J. D. and Moon, R. T. (2003). A second canon. Functions and mechanisms of beta-catenin-independent Wnt signaling. *Dev Cell* **5**, 367-377.

von der Hardt, S., Bakkers, J., Inbal, A., Carvalho, L., Solnica-Krezel, L., Heisenberg, C. P. and Hammerschmidt, M. (2007). The Bmp gradient of the zebrafish gastrula guides migrating lateral cells by regulating cell-cell adhesion. *Curr Biol* **17**, 475-487.

Weinberg, E. S., Allende, M. L., Kelly, C. S., Abdelhamid, A., Murakami, T., Andermann, P., Doerre, O. G., Grunwald, D. J. and Riggleman, B. (1996). Developmental regulation of zebrafish MyoD in wild-type, no tail and spadetail embryos. *Development* **122**, 271-280.

Yan, Y. L., Hatta, K., Riggleman, B. and Postlethwait, J. H. (1995). Expression of a type II collagen gene in the zebrafish embryonic axis. *Dev Dyn* **203**, 363-376.

Yu, P. B., Hong, C. C., Sachidanandan, C., Babitt, J. L., Deng, D. Y., Hoyng, S. A., Lin, H. Y., Bloch, K. D. and Peterson, R. T. (2008). Dorsomorphin inhibits BMP signals required for embryogenesis and iron metabolism. *Nat Chem Biol* **4**, 33-41.

Supplement

Materials and methods (supplementary)

In situ hybridization and antibody staining

Whole amount *in situ* hybridization with *fgf4* (Thisse et al., 2004) , and other mentioned probes and antibody staining were performed as described previously in the Chapter 2.

Morpholino injection

pk1a, *pk2b* and *stbm* morpholinos have been previously described (Park and Moon, 2002; Carreira-Barbosa et al., 2003) and are injected at a concentration of 1 mg/ml each in embryo at one cell stage.

Figures and tables (supplementary)

Figure 2.S1

Ectopic expression of CNH marker, *fgf4* in the secondary tail of *mfn* embryo (B) and *dvl2/3* morphant (C) fixed at 24 hpf. Lateral view with anterior to the left.

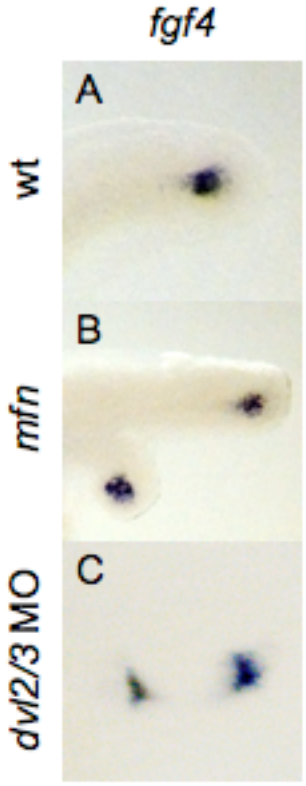

Figure 2.S2

Distribution of morphological phenotypes of *flh*-expressing CNHs in *snh* embryos fixed at indicated time points. Right panel shows the lateral view of representative embryo in each phenotypic class. For each time point around 40 embryos were scored.

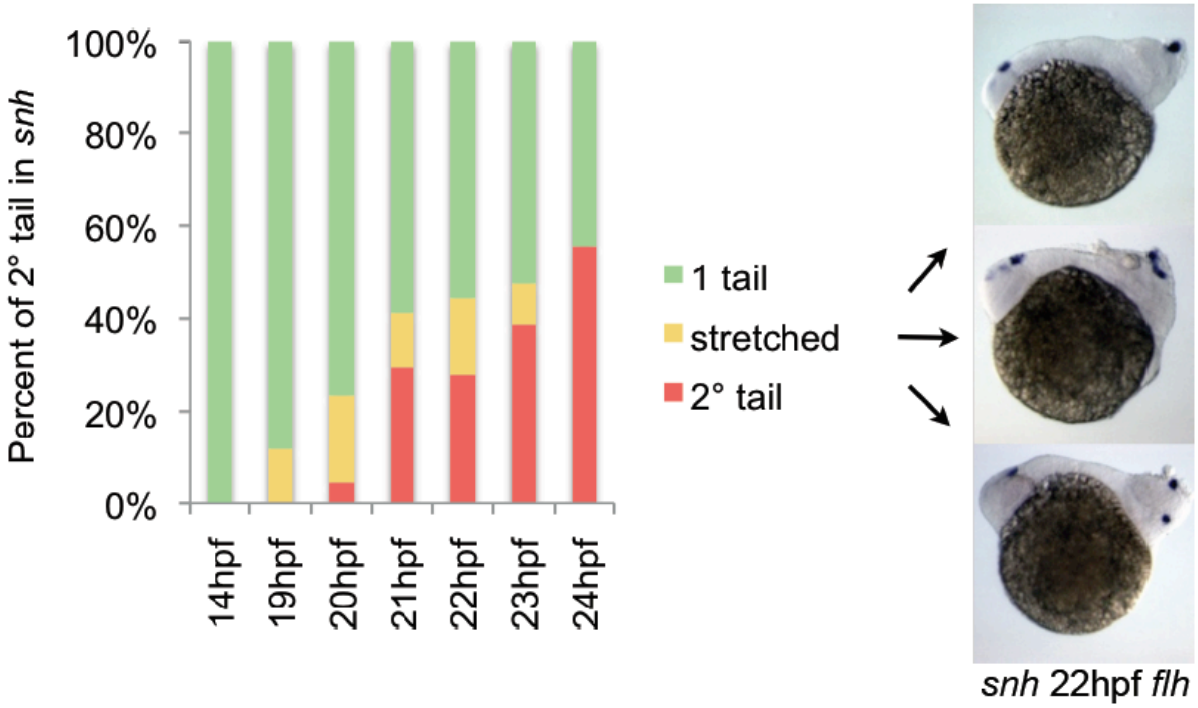

Figure 2.S3

(A-E) Lateral view of expression of *ntl* (A,B) and *col2α* (C-E) in the tail of wild-type and *kny* embryos fixed at 24 hpf. Note the three separate *flh*-expressing CNH domains in (B), triple-branched notochord (nt) in (D) and birfurcated notochord with detached hypochord (hc) (the tissue that is localized immediately ventral to the notochord) in (E). Each region is indicated by arrowheads.

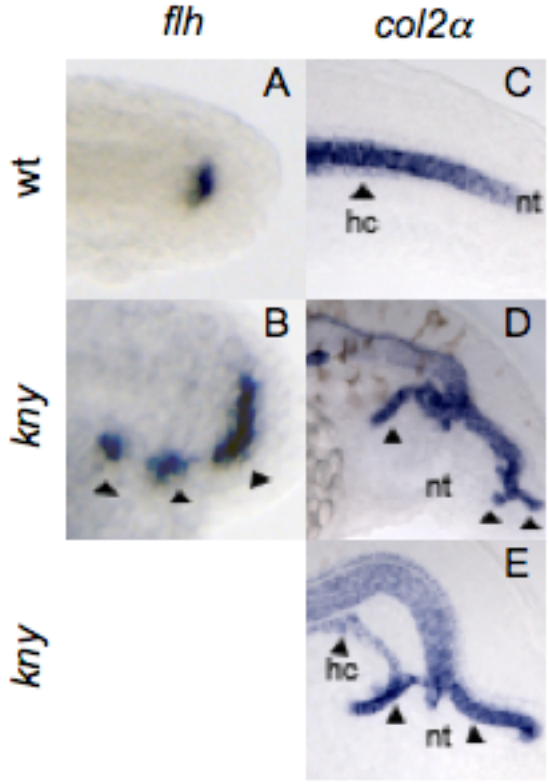

Figure 2.S4

(A-C) Confocal microscopy images of tailbud in wild-type, *kny* and *mfn* embryos labeled with β-catenin antibody at 21 somites; inset, close-up of CNH region. Lateral view with anterior to the left.

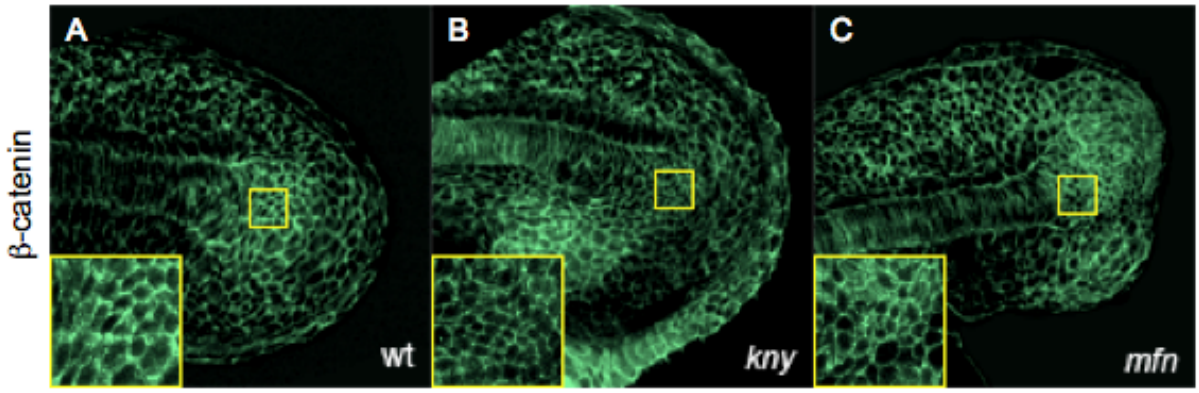

Figure 2.S5

(A,B) Confocal microscopy images of tailbud in wild-type and *mfn* embryos labeled with β-catenin (red) and P-Smad5 (green) antibody at 21 somites. Note in wild-type embryo (A) P-Smad5 staining is expressed in the posterior tailbud and extends under the notochord, while absent in *mfn* (B).

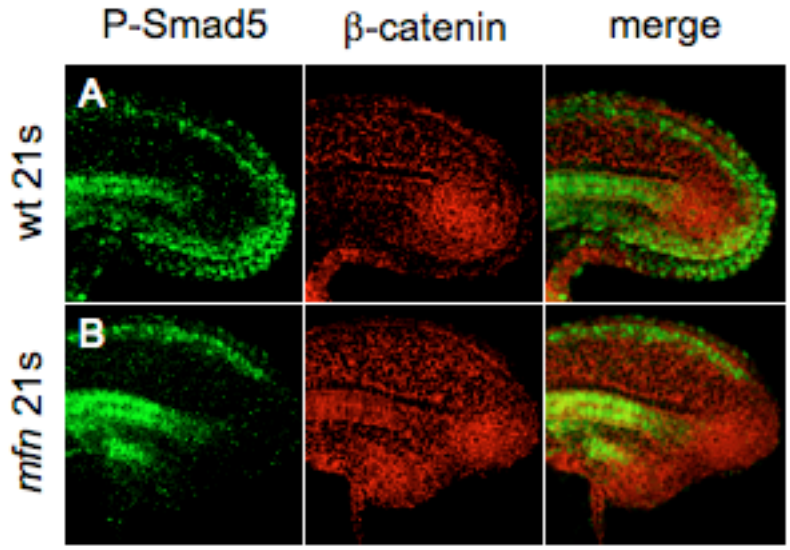

Video 2.S1

Time-lapse video of normal tailbud morphogenesis in mRFP-labled alive *Tg(flh:EGFP)* embryo starting at 10-somite stage. Lateral view, anterior to the left.

Video 2.S2

Time-lapse video of defective tailbud morphogenesis in mRFP-labled alive *mfn*;*Tg(flh:EGFP)* embryo starting at 10-somite stage. Lateral view, anterior to the left.

Video 2.S3

Time-lapse video of defective CNH morphogenesis in mRFP-labled alive *kny;tg(flh:EGFP)* embryo starting at 10-somite stage. Lateral view, anterior to the left.

Table 2.S1 Penetrance of secondary tail in BMP mutants

Mutants	*smad5*^{m169}	*smad5*$^{dty40/+}$, *smad5*$^{dty40/dty40}$	*bmp7a*^{ty68a}
2° tail	49% (n=84)	36% (n=186)	38% (n=95)

Table 2.S2 Penetrance of secondary tail in embryos injected with prickle1a, prickle 2b and strabismus morpholinos

MOs	*pk1a*	*pk2b*	*stbm*	*pk1a+ pk2b*	*pk1a+ stbm*	*pk2b+ stbm*	*pk1a+ pk2b+stbm*
2° tail	0% (n=70)	0% (n=82)	0% (n=79)	0% (n=75)	0% (n=69)	0% (n=84)	0% (n=77)

References (supplementary)

Carreira-Barbosa, F., Concha, M. L., Takeuchi, M., Ueno, N., Wilson, S. W. and Tada, M. (2003). Prickle 1 regulates cell movements during gastrulation and neuronal migration in zebrafish. *Development* **130**, 4037-4046.

Park, M. and Moon, R. T. (2002). The planar cell-polarity gene stbm regulates cell behaviour and cell fate in vertebrate embryos. *Nat Cell Biol* **4**, 20-25.

Thisse, B., Heyer, V., Lux, A., Alunni, V., Degrave, A., Seiliez, I., Kirchner, J., Parkhill, J. P. and Thisse, C. (2004). Spatial and temporal expression of the zebrafish genome by large-scale in situ hybridization screening. *Methods Cell Biol* **77**, 505-519.

CHAPTER 3 - Smad6 Influences Dorsoventral Patterning by Inhibiting BMP Activity in Zebrafish

Abstract

Bone morphogenetic protein (BMP) signaling is crucial for the patterning of embryonic dorsoventral axis in vertebrates. BMPs transduce signals by serine/theronine kinase receptor mediated phosphorylation of designated Smad proteins (Smad1/5/8). This process is negatively regulated by a subclass of Smad proteins, inhibitory Smads including Smad6 and Smad7. In this study, we have characterized two zebrafish homologs of *smad6* (*smad6.1 and smad6.2*) that share high structural similarity. We show that *smad6.1* and *smad6.2* are broadly expressed throughout early development and their expression patterns are largely overlapped by 24 hpf. Also, we show that *smad6.1* and *smad6.2* expression is mediated by BMP signaling during gastrulation. By examining the gain-of-function phenotypes, we determine that both genes function as BMP inhibitors. In addition, knockdown of *smad6.1* and *smad6.2* by morpholinos (MO) results in mild dorsoventral patterning defects at the mid-gastrula stage, suggesting that *smad6.1* and *smad6.2* fine tune BMP signaling to ensure proper dorsoventral patterning by negatively regulate the BMP activity in the zebrafish embryo during gastrulation.

Introduction

Bone morphogenetic proteins (BMPs) belong to the transforming growth factor-β (TGF-β) superfamily and play a central role in specifying cell fate during embryogenesis (Little and Mullins, 2006). As demonstrated in *Xenopus* and zebrafish, BMP signals act as morphogens and form an activity gradient along the dorsal-ventral (DV) axis of the embryo during gastrulation (Schier and Talbot, 2005; Kimelman, 2006; Little and Mullins, 2006). On the ventral side, the highest level of BMP activity is found to induce ventral cell fates, and on the dorsal side, the BMP activity is eliminated by a series of secreted inhibitory proteins such as as Chordin, Noggin and Follistatin to promote the dorsally expressed genes (Schier and Talbot, 2005; Kimelman, 2006; Little and Mullins, 2006). Activation of BMP signaling requires BMP ligands binding to type I and type II serine/theronine kinase receptors, which leads to the phosphorylation of receptor-regulated transcription factors Smad1/5/8 (R-Smads) (Feng and Derynck, 2005;

Massague et al., 2005). This phosphorylation allows R-Smads to translocate nucleus with cofactor Smad4 to propagate the signal (Feng and Derynck, 2005; Massague et al., 2005).

In contrast to the R-Smads, another class of Smad proteins known as inhibitory Smads (I-Smads), including Smad6 and Smad7 in vertebrates, function as intracelluar antagonists to inhibit BMP signaling (Feng and Derynck, 2005; Massague et al., 2005). The I-Smads share a conserved C-terminal MH2 (Mad-homology 2) domain present in all Smad proteins but lack the N-terminal MH1 (Mad-homology 1) domain that is highly conserved in all R-Smads and Smad4 (Massague et al., 2005). I-Smads. Although Smad6 and Smad7 both function to negatively regulate BMP, Smad7 displays additional inhibition of TGF-β/activin signaling (Hayashi et al., 1997; Imamura et al., 1997; Nakao et al., 1997; Hata et al., 1998). Smad6 has been proposed to inhibit BMP signaling by physically binding to type I receptors to prevent the phosphorylation of R-Smads (Imamura et al., 1997) and by binding to Smad1 in competition with Smad4 (Hata et al., 1998), which consequently interferes signal transduction. Additionally, Smad6 has also been suggested to act as a transcriptional corepressor to inhibit BMP signaling by recruiting other components such as corepressor C-terminal binding protein (CtBP) (Lin et al., 2003), class I histone deacetylase (HDAC) (Bai et al., 2000) and homeobox (Hox) c-8 proteins (Bai and Cao, 2002).

In vitro studies using mouse and human cell lines have shown that Smad6 expression can be induced by BMP signaling (Afrakhte et al., 1998; Ishida et al., 2000). In chick embryos, it has been shown that Smad6 is strongly expressed in the cardiogenic region and developing limb where high amount of BMPs are expressed (Yamada et al., 1999; Vargesson and Laufer, 2009). BMP2 protein can induce the ectopic expression of Smad6 in explant culture and Noggin protein treatment reduces the expression of Smad6 in cardiogenic cells (Yamada et al., 1999). Activating BMP signaling by retrovirus-mediated expression of a constitutively-active form of type I BMP receptor in the limb tissues induces the expression of Smad6 while expressing of dominant negative BMP receptor or Noggin reduces Smad6 expression in limb tissues (Vargesson and Laufer, 2009). These results suggest Smad6 functions in a negative feedback loop to limit the BMP signal (Park, 2005). In *Xenopus* Smad6 is expressed through the gastrulation, and overexpression of Smad6 in ventral cells forms a partial secondary axis which phenocopies the embryos with suppressed BMP signaling, while overexpression of Smad6 in dorsal cells result in no patterning defect (Nakayama et al., 1998). This suggests in *Xenopus* Smad6 has a potential

role in DV patterning during gastrulation. However, since there are limited loss-of-function studies of Smad6, the exact role of Smad6 in fish development is still unclear. Insertion of a *LacZ* reporter to the MH2 domain of Smad6 in mice demonstrates Smad6 expression is largely restricted to the heart and blood vessels (Galvin et al., 2000). These Smad6 mutant mice exhibit multiple cardiovascular defects suggesting a specific role of Smad6 in regulating endocardial cushion transformation and homeostasis of adult cardiovascular system (Galvin et al., 2000), but do not show any obvious gastrulation defects (Zhao, 2003). In zebrafish, the role of Smad6 has yet to be addressed. Here we provide evidence to show that two homologs of *smad6* in zebrafish, *smad6.1* and *smad6.2* are broadly expressed throughout early development and their expression patterns are similar to each other. Also, we show that *smad6.1* and *smad6.2* expression is mediated by BMP signaling during gastrulation. By examining the phenotypes after overexpression of *smad6.1* and *smad6.2*, we determine that both genes are able to inhibit BMP signaling. Lastly, inhibition of *smad6.1* and *smad6.2* results in mild dorsoventral patterning defects at the mid-gastrula stage, suggesting that *smad6.1* and *smad6.2* fine tune BMP signaling to ensure proper DV patterning by negatively regulate the BMP activity in the zebrafish embryo during gastrulation.

Results

Clone and sequence analysis of zebrafish Smad6.1 and Smad6.2

One of our hits from a yeast two hybrid screen for proteins interacting Spork (homolog of human ARHGAP21 in zebrafish) was charaterized as zebrafish Smad6.2 (also named Smad6b) on the linkage group 18 (Fig. 3.1A red letters). The paralog of Smad6.2, Smad6.1 (also named Smad6a) on linkage group 7 was found in the BLAST results with mRNA sequence of Smad6.2. Multi-alignments with amino acid sequences of Smad6.1, Smad6.2 and zebrafish Smad7, together with Smad6 and Smad7 in *Xenopus*, mouse and human showed the position of MH2 domain (predicted by Prosite) is conserved (Fig. 3.1C). The conserved domain analysis showed this domain is highly conserved. Smad6.1 and Smad6.2 showed higher similarity and identity scores when comparing amino acids sequences with *Xenopus*, mouse and human Smad6 than those scores when comparing with listed Smad7 sequences (Fig. 3.1 D). Phylogenetic tree of amino acid sequences of Smad6.1, Smad6.2 and zebrafish Smad7, together with Smad6 and Smad7 in frog, mouse and human clearly show Smad6.1 and Smad6.2 are more closely related to

other Smad6 homologs than Smad7 (Fig. 3.1E) and this result is supported by those representative amino acids that differentiate Smad6 and Smad7 in conserved MH2 domain (Fig. 3.1C, red box). To get a more percise phylogenetic tree we built a tree by only aligning the MH2 domains, which showed Smad6.2 is closely related to Smad6 in mammals while Smad6.1 is more distantly related. Considering the possible functional redundancy, we began study of these two Smad6 homologs by isolating full-length cDNAs of Smad6.1 and Smad6.2 from a 24hpf zebrafish cDNA library (Fig.3.1A, B). For Smad6.2 an alternative ORF (in frame of annotated ORF, based on the sequences from our yeast two hybrid screening data) was cloned (Fig. 3.1B).

Comparison of spatial expression patterns of smad6.1 and smad6.2 in early development

To determine the expression patterns of *smad6.1* and *smad6.2*, we performed *in situ* hybridization analysis in embryos at multiple stages during early development. At the shield stage, in contrast to other BMP antagonists such as *chordin*, which is exclusively expressed on the dorsal margin, *smad6.1* and *smad6.2* were both ubiquitously expressed throughout the embryo (Fig. 3.2A,B,A',B'). At bud stage, both *smad6* homologs were expressed broadly, with more intense expression in the midline axis and tailbud (Fig. 3.2C,D,C',D'). At the 10-somite stage, *smad6.1* and *smad6.2* transcripts were evenly distributed all over the embryo (Fig. 3.2E,F,E',F'). At 24 hpf, *smad6.2* was more intensly expressed in the posterior tail compared to *smad6.1*, while both genes were strongly expressed in the anterior region (Fig. 3.2G,G'). In the head, both *smad6* homologs showed strong expression in the eye and throughout the brain (Fig. 3.2H,H'). In addition, *smad6.2* was more clearly expressed on the periphery of the otic vesicle (Fig. 3.2H'). At 48 hpf, we observed expression of *smad6.1* and *smad6.2* in the head, heart, pectoral fin and somites (Fig. 3.2I,J,I',J'). We also observed unique expression of *smad6.1* near the hindbrain (Fig. 3.2I), and high expression levels of *smad6.2* in the lens (Fig. 3.2J'). Our data shows that both *smad6s* have a comparatively broad and largely overlapping expression pattern during early development, suggesting that these two homologs could be functionally redundant.

Expression of smad6.1 and smad6.2 is regulated by BMP signaling during gastrulation

The BMP expression gradient is established from shield stage: high ventrally and low dorsally. This expression pattern resembles that of the concurrently expressed *smad6.1* and *smad6.2*, which led us to determine whether *smad6* expression is controlled by BMP signaling in

zebrafish. At early gastrula stage (60% eipobly), we analyzed the *smad6.1* and *smad6.2* expression patterns by *in situ* hybridization when down- and up-regulating BMP signaling. Consistent with the expression profile of *smad6* in *Xenopus* during gastrulation (Nakayama et al., 1998) (also see Fig. 3.2A,A'), *smad6.1* showed ubiquitous expression in the embryo with slightly more intensive signal on the dorsal versus the ventral side at 60% epiboly (Fig 3.3A,B). Knocking down *admp* (encoding anti-dorsalizing morphogenetic protein, ADMP) and *mfn* (encoding BMP agonist Tolloid) was previously shown to result in weakly dorsalized embryos due to mild loss of BMP signaling. Here, we found inhibiting *mfn* or *admp* causes absence of *smad6.1* expression from the ventral side (Fig. 3.3C-F). However, this effect is weak and penetrance is very low: around 8% (10/122) in *mfn* morphants and 15% (16/105) in *admp* morphants. However, we did not find any apparent change in *smad6* expression in *snh/bmp7 and* Dorsomorphin (a chemical inhibitor of BMP pathway)-treated embryos (data not shown). Enhancing BMP signaling by inhibiting the BMP antagonist *chordin* by morpholino resulted in a moderate enhancement of *smad6.1* expression level in 52% (46/88) of the embryos (Fig. 3.3G,H). Overexpression of a constitutively active form of the BMP receptor (caBMPR) potently enhanced BMP signaling and resulted in severely ventralized embryo at 24 hpf (data not shown). We observed strong induction of *smad6.1* transcripts in 80% (90/112) of embryos injected with caBMPR mRNA (Fig. 3.3I,J). Enhancing BMP signaling by injecting Smad5 mRNA, also induced expression of *smad6.1* in 65% (70/108) of embryos (Fig. 3.3K,L). So far, our data suggests the expression of *smad6.1* is regulated, at least in part, by BMP signaling. To test the possibility that expression of *smad6.1* is partially regulated by a second family member in TGFβ signals, Nodal signaling, we knocked down *oep* (encoding Nodal co-receptor) and then checked *smad6.1* expression. We did not observe a significant change in *smad6.1* expression, suggesting that *smad6.1* expression is independent of Nodal signaling (Fig. 3.3M,N). The concentrated signal along the margin is likely due to accumulation of un-internalized marginal cells resulting from the loss of Nodal signaling (Fig. 3.3M). Our parallel experiments with *smad6.2* display the same changes in expression pattern as *smad6.1* (data not shown) and the penetrance is similar to that of *smad6.1* (Fig. 3.3O). Together, we show that enhancing BMP signaling induces the expression of *smad6.1* and *smad6.2* and suppressing BMP signaling slightly reduces their expression. The result that *smad6.1* and *smad6.2* are responsive to both up- and down-regulation of BMP signaling suggests that they may act cooperatively as feedback inhibitors.

Overexpression of smad6.1 and smad6.2 inhibits BMP signaling

Overexpression of *smad6* in *Xenopus* embryos has previously been shown to result in secondary axis formation, a patterning defect due to loss of BMP signaling (Nakayama et al., 1998). In order to test whether *smad6* can function as a BMP inhibitor in zebrafish, we examined the effect of overexpression of *smad6.1* and *smad6.2* on DV patterning during early gastrulation (60% epiboly). Embryos injected with either *smad6.1* and *smad6.2* mRNAs showed reduced expression domain of the ventral marker *eve1* (Fig. 3.4A-C), and expanded expression of two dorsal markers: *flh*, expressed in the chordamesoderm (Fig. 3.4E-G), and *chd*, expressed in axial mesoderm (Fig. 3.4I-K). Combined injection of *smad6.1* and *smad6.2* mRNA showed slightly stronger effect in restricting the expression of *eve1* (Fig. 3.4D). However, no further expansion of *flh* and *chd* is detected (Fig. 3.4H,L). At shield stage, *chd* is expressed in a comparatively smaller domain and we observed significant expansion of *chd* in embryos injected with both *smad6.1* and *smad6.2* mRNAs (Fig. 3.4M,N). The ventrally shifted expression patterns of *eve1*, *flh* and *chd* resulting from overexpression of *smad6.1* and *smad6.2* reflect disrupted DV patterning during gastrulation, a typical early defect expected in BMP-compromised embryos (Schier and Talbot, 2005). Consistent with this result, embryos injected with *smad6.1* and *smad6.2* mRNA at one-cell stage exhibited a noted dorsalization phenotype at 24 hpf evidenced by reduced ventral tail tissues, which phenocopies the BMP mutants *piggytail* and *minifin* (data not shown). To confirm that overexpression of both *smad6.1* and *smad6.2* perturbs transduction of BMP signaling, we performed antibody staining with P-Smad5 as readout of BMP activity. Overexpressing *smad6.1* and *smad6.2* together resulted in a moderately reduced domain of active BMP signaling (Fig. 3.4O,P). In addition, the overall signal intensity in these injected embryos is comparatively weaker than in wild type (Fig. 3.4O,P). The numbers of embryos injected are given in Table 3.1. Overall, our results suggest that *smad6.1* and *smad6.2* both act as antagonists of BMP signaling in zebrafish embryos.

Inhibition of smad6.1 and smad6.2 impacts dorsoventral patterning

To further investigate the function of *smad6.1* and *smad6.2* in early gastrulation, we used antisense morpholino oligonucleotides (MO) to knock down both *smad6* homologs. In embryos injected with *smad6.1* MO and *smad6.2* MO respectively, expression of *eve1* exhibited little, if any, lateral expansion (Fig. 3.5A-C), and expression domains of *flh* (Fig. 3.5E-G) and *chd* were

reduced (Fig. 3.5I-K). Comparing to single knockdown, double knockdown of *smad6.1* and *smad6.2* resulted in a further reduction of *chd* expression (Fig. 3.5L), but no stronger change in *eve1* and *flh* expression (Fig. 3.5D,H). The more dorsally shifted expression of *flh* and *chd* indicates slight ventralization (Schier and Talbot, 2005). This result is consistent with an increase in BMP signaling in *smad6.1* and *smad.2* knockdown embryos. However, we did not observe apparently ventralized embryos at 24 hpf (data not shown). To confirm that knockdown of *smad6.1* and *smad6.2* could increase the activity of BMP signaling during gastrulation, we performed immunostaining assay using P-Smad5 antibody in embryos injected with both *smad6.1* MO and *smad6.2* MO. We observed a mild expansion of the BMP-active domain in *smad6.1*/*2* MO morphants (Fig. 3.5M,N). This result further supports the idea that *smad6.1* and *smad6.2* antagonize BMP signaling. The ventralization phenotype observed early during gastrulation in our loss-of-function assay suggests one function of *smad6.1* and *smad6.2* is to help establish proper DV patterning by inhibiting BMP signaling. The numbers of embryos injected are given in Table 3.2.

Discussion

In this study, we have charaterized two homologs of Smad6 in zebrafish and provide evidence that they share high sequence similarity with Smad6 in other species (human, mouse and *Xenopus*) and both function as inhibitory Smads that antagonize BMP signaling during gastrulation. This is consistent with the role of Smad6 proteins as BMP inhibitors previously described in other systems (Afrakhte et al., 1998; Nakayama et al., 1998; Ishida et al., 2000). The spatial expression patterns of *smad6.1* and *smad6.2* are largely overlapping during early development. Besides a broad early expression pattern, both *smad6* homologs exhibit high expression in the brain, eye and heart, which is consistent with the expression pattern of *smad6* in chick embryos (Yamada et al., 1999; Vargesson and Laufer, 2009). This expression pattern also overlaps with the expression of *bmp* genes (Dick et al., 1999; Stickney et al., 2007; Shawi and Serluca, 2008) suggesting that Smad6 may function in those BMP-responsive cells to adjust the strength or duration of the BMP signaling. Unlike Chordin, which is expressed locally to abolish BMP activity (Schulte-Merker et al., 1997), Smad6 has a much broader expression pattern suggesting it may be an inhibitor used to fine-tune overall BMP signaling.

In line with the ubiquitous expression of *Xenopus smad6* during gastrulation as previously reported (Nakayama et al., 1998), we observe that both *smad6* homologs are expressed broadly in zebrafish embryos at early gastrula stage with a perceivably increasing intensity from ventral to dorsal pole. This expressing pattern suggests Smad6 may help major inhibitors like Chordin to establish the DV axis by suppressing BMP signaling along the margin of embryo, and this idea is supported by our results from gain- and loss-of-function assays. Interestingly, we find *smad6* expression is more responsive to up-regulated BMP signaling while showing less response to down-regulated BMP signaling, suggesting a partial dependence of BMP signaling in *smad6* expression. In contrast, suppressing BMP signaling by viral expression of Noggin in chick limb tissue abolishes *smad6* expression and directly applying Noggin protein to chick cardiogenic tissues results in significant reduction of *smad6* expression. This discrepancy might suggest *smad6* is differentially regulated by BMP signaling depending on the system. It has been shown that expression of mouse *smad6* is regulated by a Smad binding element (SBE) in the promoter region, and this SBE is preferentially recognized by BMP-activated Smad1/5 (Ishida et al., 2000). In the putative promoter region of *smad6.1* (1k bp

upstream of the coding sequence), we found one DNA motif was identical to the Smad5 SBE (TGTCTAGAC) identified in the mouse *smad7* promoter (Li et al., 2001), however we did not find such motif in the similar region upstream of *smad6.2* (data not shown). Possible cross-talk of Smad6 to TGF-β signaling may interfere our results as well. It has been shown that TGF-β and activin can transiently induce the expression of *smad6* while BMP results in comparatively stable expression of *smad6* (Afrakhte et al., 1998).

Inhibiting *smad6.1* and *smad6.2* simultaneously results in slightly futher expansion of *eve1* expression, which suggests the two genes work somewhat redundantly. Our P-Smad5 antibody staining assays show the active BMP region is reduced/increased in size as well as in amplitude when expressing/suppressing *smad6*. This suggests *smad6* is utilized to finely adjust and strength of BMP gradient along the DV axis during gastrulation. *smad6* may also regulate BMP signaling by adjust its duration. Smad6 knockout mice are reported to have phenotypes in cardiovascular system but no gastrulation defect (Galvin et al., 2000; Zhao, 2003). Here we observe a slight shifting in the DV markers in *smad6.1/2*-MO morphants during gastrulation, though no overtly ventralized phenotypes at 24 hpf. This difference may be due to varied biological activity of Smad6 among organisms, considering *Xenopus* Smad6 could inhibit activin but human Smad6 could not (Hata et al., 1998; Nakayama et al., 1998). The weak effect of *smad6* on DV patterning in zebrafish indicates it may function transiently to suppress BMP activity during gastrulation. Another possible explanation is the loss of Smad6 function could be compensated by closely related Smad7, since in chick limb tissue Smad7 exhibits similar response to down- and up-regulated BMP signaling as Smad6 (Vargesson and Laufer, 2009). It will be necessary to perform comparative studies between Smad6 and Smad7 in future to see how these I-Smads work together to regulate the gastrulation process in zebrafish.

Materials and methods

Cloning of smad6.1 and smad6.2

Smad6.2 was originally identified from a yeast two hybrid screen for Spork (homolog of human ARHGAP21) interactive protein (screening service was provided by Hybrigenics). This sequence was used to BLAST the zebrafish Ensembl genome database. These approaches identified two *smad6* paralogs, *smad6.2* on linkage group 18 and *smad6.1* on linkage group 7. PCR primers designed to clone *smad6.2* were 5'-

GCGGATCCAAATTCCCAAGACGGAGTTC-3' (forward) and 5'-CCCTCGAGATTGTTTGTGGAGTCTCTCG-3' (reverse). Primers designed to clone *smad6.1* were 5'-GCGGATCCCGTATGTTCAGGACGAGAC-3' (forward) and 5'-CCCTCGAGAAGGTGGATTGGTTATCTGT-3' (reverse). The *Bam*HI and *Xho*I enzymatic sites were introduced in the forward and reverse primers respectively for subsequent clone to pCS2+ vector. We used these primers to amplify full-length cDNAs of *smad6.1* and *smad6.2* from a 24 hpf cDNA library made using the SMART cDNA kit (Clontech) (see Fig. 3.1A,B for cloned sequences). The PCR product was inserted the PGEM vector (Promega) for sequencing as well as into the vector pCS2+ for mRNA synthesis (Turner and Weintraub, 1994).

Phylogenetic analysis

Amino acid sequences were aligned using ClustalW algorithm with the default parameters performed by MacVector® software. The phylogenetic trees were built using the method UPGMA (Unweighted Pair Group Method with Arithmetic Mean, assuming the rate of divergence is constant in different evolutionary lineages). Distance is estimated by total number of differences between sequences and confidence of particular nodes in a tree is estimated by bootstrap resampling approach. Other parameters were set at default values.

In situ hybridization and antibody staining

In situ hybridization with digoxigenin-labeled mRNA probes was performed as described previously (Oxtoby and Jowett, 1993). The *smad6.1* probe recognizes a 675 bp sequence beginning at the 298bp nucleotides from the 5' ends of *smad6.1* cDNA. The *smad6.2* probe recognizes a 612 bp sequence beginning from the start codon of *smad6.2* cDNA. The exact sequences used to design *in situ* probes are indicated in Figure 3.1A,B. The hybridization temperature was set to 65 ℃ to minimize non-specific binding. Other probes used have been previously described: *chd* (Miller-Bertoglio et al., 1997), *eve1* (Joly et al., 1993), and *flh* (Talbot et al., 1995). For antibody staining, embryos were fixed, then dechorionated and incubated with 1:100 diluted P-Smad1/5/8 antibody (Cell Signaling Technology), and then followed by 488 Alexa Fluor conjugated to secondary antibody (Molecular Probes). Embryos were mounted in 3% methylcellulose and scanned by a Zeiss LSM 5 Pascal confocal microscope.

Morpholino and RNA injection

Morpholino antisense oligonucleotides: (*smad6.1* MO: 5'-TAACTTAAACTACTTACTCAGTGGC-3'; *smad6.2* MO: 5'-TCGACAGGACCTTCGCTTACCTGGC-3') were purchased from Gene Tools. *mfn, admp, chd* and *oep* morpholinos have been previously described (Miller-Bertoglio et al., 1997; Feldman and Stemple, 2001; Willot et al., 2002; Jasuja et al., 2006). Morpholinos were diluted in Danieau's buffer before injection. Morpholinos were injected at a concentration of 3 mg/ml. Synthetic mRNAs of *caBMPR* (1 mg/ml), *smad5* (120 mg/ml), *smad6.1* (50 mg/ml) and *smad6.2* (50 mg/ml) made from pCS2+ constructs with mMessage mMachine kit (Ambion) were injected except for when Smad6.1 and Smad6.2 mRNA were co-injected, a concentration of 25 mg/ml each were used. In all experiments, a volume of 3-5 nl was injected in the yolk of one-cell stage embryos.

Figures and Tables

Figure 3.1 Clone and sequence analysis of Smad6.1 and Smad6.2.

(A,B) Complete mRNA sequences of Smad6.2 (on linkage group 18) and Smad6.1 (on linkage group 7). The sequence characterized in yeast two hybrid screen for proteins interacting Spork is marked red. The open reading frame (ORF) is indicated by bold letters. Note, for *smad6.2* cDNA an alternative ORF is cloned (in frame with the larger ORF). The nucleotides where PCR primers bind to amplify cDNA are indicated by underline. The start codon of cloned cDNA is indicated by green capitalized letter. The sequences used to make *in situ* hybridization RNA probe is indicated by gray shade. lg, linkage group.

(C) Clustal alignment of amino acid sequences of zebrafish Smad6.1, Smad6.2 and Smad7 together with Smad6/Smad7 in mouse, *Xenopus* and humans. Outlined gray shading indicates identity. The conserved MH2 domains is indicated by underline. The representative amino acids in MH2 domains that distinguish Smad6 and Smad7 are indicated by red box.

(D) Similarity and indentity matrix of alignments of amino acid sequences of zebrafish Smad6.1, Smad6.2 and Smad7 together with Smad6/Smad7 in mouse, *Xenopus* and humans.

(E) Phylogenetic tree software built using UPGMA upon the amino acid sequences of zebrafish Smad6.1, Smad6.2 and Smad7 together with Smad6/Smad7 in mouse, *Xenopus* and humans by MacVector®.

(F) Phylogenetic tree built using UPGMA upon the amino acid sequences of the MH2 domains of zebrafish Smad6.1, Smad6.2 and Smad7 together with Smad6/Smad7 in mouse, *Xenopus* and humans by MacVector® software.

In (E) and (F), the method UPGMA (assuming the rate of divergence is constant in different evolutionary lineages) is used to build phylogenetic tree. Distance is estimated by total number of differences between sequences and confidence of particular nodes in a tree is estimated by bootstrap resampling approach.

A

Smad6.2 (lg18) complete mRNA

```
   1 aaaaaaaaaa aaaagggaga gaaacggaga aagagagaga gatctgggtt gcagtttgac
  61 caggtctgaa cacggaacca ggagcacatt ataagtctac ggattgttcc ttttctggcc
 121 ccggcgcgcg cacaaggata tttttggatc gcaaaaaaga gagcgcgctg gaattgtgga
 181 aaaacgaccg gaatagtgaa ttctgcaagg aattgtctgt ggatttaatt cgccgaggag
 241 cagcttcatt catgtctcca gacccgctgt tgaagagtgg atttgaacgt gtttcaaagt
 301 ccgaaaacat ttaagagcgc gcgactagag tagattttcg cctggggttt tttgacatca
 361 catttatttg atgtagttaa aacccgtagt gcattttaaa tctggaaaaa aatatcatcg
 421 gactcttggt ccactttcca aacatggttc acatgtaggc ttcttgacag cgttcttgta
 481 aaatgaatgc gtttcgctat gcggtagttt gacgatttct gtttttaatg caatatagca
 541 ttgtgccttc caaactaatg ttgtggcttt gccaccgata tacggtgctc ggctgtgcac
 601 gcgctgcacg gcattcggcc aacattaatg ttgcacgagc tcagaaatag tttcaaatcg
 661 ctgagatctg aacgtaaata actcatctag agtttcaagt tgtcgtatgt tcaggacgaa
 721 acgctcaggt cttgtgcggc gactctggag aagccgtttg attccagata aagaggggag
 781 cgatggatat ggcaaaagcg gcgaggggtc tcgagacgat ctgcttggca ccaacccaga
 841 gaaaattccc aagacggagt tcagaccgAT Gaccccgagc gggtcgccta gcgtggacta
 901 tggggaagtg tgtacgagga atcccgctga gagcagcggc ggtggcacct caggggcttt
 961 tttggaccaa gatgggggta cggtatgtac ggtgggaagc cctcggtctg tgcaggacag
1021 cgattgtaga acagtcactt gctgtttatt caaagatcgg gaccatcatt ctggatctag
1081 aagtccggag ccaggctcgt gccagtttgt gctgaggaac attggctctt cacgggaccc
1141 cggtcctctg gagagccagg agtcgaaacc tcgctccgtc atggagcagg agctcaagac
1201 cgccacctat tcactattaa aaaggctaaa ggagaaaacc ttggatactt tgttggaagc
1261 tgtggagtca ggcgggatgc cgagcgactg tgtgatggta tcgcggaccg agctgcggtt
1321 aggcggccac atggctcctc cacaactgct tatctgtaag ctttaccggt ggtcagacct
1381 gcagcacacg gcccagctaa aagcgctctg tgagtgcaag agcttcggag ctcaggacgg
1441 tccggtagtg tgctgcaatc catatcatta cagccgactc tgtgggccag agtcaccccc
1501 tcctccatac tcaagacttt cccccagcga agaacacaag ccactggatc tgtcagattc
1561 cacactgtct tacactgaaa cggaggctgc cagctcacca aacgccaccc aaggggaatt
1621 ctcagatgcc agtctgtcac ctgatgcccc caagcagagt cactggtgta acgtggcgta
1681 ctgggagcat cggacacggg tgggccgcct ctatacggtg taccagcctg ccgtcagcat
1741 tttctatgac ctacctcaag gtacgggctt ctgccttggc cagctgagcc tggaccagcg
1801 cagcagcacc gtgcagcgga cgcgtggcaa gatcggctac ggcttgctcc tgagcaaaga
1861 gccggatgga gtctgggctt acaaccgcag ccagcacccc atcttcgtca actctccgac
1921 tctggatgtc ccagggagcc gaagcctggt ggtgcgcaaa gtgatgcctg gatactccat
1981 taaagtgttt gactacgaac gctcgtccat gctcaggcaa ggagccgagt cggagctgct
2041 agacggaccc tatgacccga acagtgtgcg catcagtttc gcgaagggct ggggcccttg
2101 ttactcccgc cagttcatca cttcgtgccc ctgttggctg gagatcctcc tcaacaacca
2161 cagataacac atggataaac acatggactc gctcatgccg agagactcca caaacaatcc
2221 caaatatcat ctacttagat ttaatataaa gttttatata ttataagaaa tatatattat
2281 acttgtaaat actggagtca tttttacgat gtaattattt atgtatggtg caatgtgtac
2341 atggacaaga ggaaaaaaaa cgggaaatgc actttggctt atatattata tatataaata
2401 tctataaaga taaagaatct ttcaatacca atttgaaaaa ttatacagca aaaataggaa
2461 gagcctggtt ttggtgtata gttttcatat actattaata tccagatgaa aagctaacac
2521 cattcacaca ttgataataa agtattcgca taataaaaaa aaaaaaaaaa aa
```

B

Smad6.1 (lg7) complete mRNA

```
   1 ctctcctcag gggccccgtg tgtgtgtatc tgaagaagaa agagagtgaa acggcgaaag
  61 aagccatcga agaattctat taatctcacc cgaaacacgg aacgaaacct caagacaaca
 121 tatgtccgtc tatccgccta gaacgaccac tttgccgtcg caacgtaagc attttcatcc
 181 gccaggagcg cgcggaacgt gaacggggat tatagtgagc tccattcatg tgctcggcgt
 241 cattaacccg ctgcagaagg tttgcttgaa aacggggatc cgttacggac gctatcgaag
 301 atttttttc tgcataccgt gcatttcgag gagagtaaag tttcacatgt ttacggggca
 361 tgtttacaga ctggatgcaa cgctccacac gtagtgcact atcattatta catcaagccc
 421 tttgctacag tgttgatata ttgtagcagc ggagtctaat gttgggcttc gcgcaggctc
 481 tgctcggctg tgcatgtgag cacagatcat tgatgtcgga cagcgagcgc acgagcgttt
 541 ggagtctccg cggttctgac caaacatagg aaaaacggat gcaaactgtt taaactgtcg
 601 tATGttcagg acgagacgca cgggtctggt tcggcgactc tggagaagcc gtttagtcac
 661 cgcaggtaaa gagggggcg atggaggtcc ggatgactgg agtgacagca acccagagaa
 721 gatccccaga acggaatacg caccgggaaa caacgcgggc tcgtgcggca gacgcgtaga
 781 ggagcgcggg gaaccggggg tccttattga acacgatgga cctctcaacg atgggagcga
 841 aggcaggacg gtgacatgct gtttgtttaa agacctcccc agaagcaaaa acagactcgc
 901 ttgccgtgtg gaacatagga accacaacaa ctatagcagt ttgagtggca gggaacggaa
 961 aactggtgcc gtgaccgagc aagaactcaa gaagtgcact tatgcctttc tcaaaaagtt
1021 gaaagacaag tctctggatg ttttactgga agctgttgag tctcaaggcg ggatgccaag
1081 tggatgtgtt ctggtatcgc agactgaggt gcgaatcggg ggtcatctag tgtctccaca
1141 gtacctgctg tgtcgacttt tccgctggcc agacctacga ttatcctctc tcctcaaacc
1201 actctgtcat tgtcagagct tcagggcaga ggacagccag accctctgct gcaaccccca
1261 tcattacagc cgcctctgtg gaccagtaaa ggatgataca ccaccacctc cttattctca
1321 tctctccccc ttaccagaac acaagccact gaattcttcc cttccaatgc tgccttacat
1381 agaaaccgaa gccactcgat ccgctggcgg cctgtcccag gactattcag atgccagtat
1441 gtctccctcc tcgctggcgc agaaccactg gtgtaatgtg gcttactggg agcttcgcac
1501 ccgtgtgggc cgcctgtacc cagttcacga cgcctctctc agcatcttct acgacctacc
1561 tcagggtaca ggcctatgtt tgggcctgct gcccctctct ccgcgctcca cttccgtcca
1621 gcgcacccgc ggcaagatcg gccacggcat cctcctcagc aaagagcccg atggagtttg
1681 ggcctacaac cgcagtcagc accctatatt tgtcaactcg cccactctgg agcatcaccc
1741 ctacctgagt ctgacggtga ggagagtaat gccaggctac tccataaagg tgtttgacta
1801 tgagaagtcg tgccaaatgc aaccggccag tcatccggta cacccggaag ggccatacga
1861 cccgaacagt gtgaggatca gttttgccaa gggttgggga ccgtgctatt ccagacagtt
1921 catcacatcg tgtccatgct ggctggagat tttactcaac aaccacagat aaccaatcca
1981 ccttttcct acaccacaat gatgctttga gttagctatg ggagtcactt cctttaaatt
2041 aagtgttttt aaaaatagtt tttgaggtgc tgttattctc tttatggttc atctatcaaa
2101 tatttaagaa aaaaatttta agtagaccac gactaacccc caaatgactt ctcacagcaa
2161 tataatgggt gtatattgac tattacttta ctgtagtgaa ttctgagaga cagtgaactc
2221 aaaggagcat tgacagacat gcttgtgtta aaataatata aataaaagca taattttcta
2281 tcaagtataa aaaataaagc acaaaaccag acatacctct tccacagttt ttactaagaa
2341 tattggaata tgaatataat aaaggaattt caaaattcct ttgaaaatcc ctaaagctag
2401 aagtgcaacc cataatttag aacacaatca tcacgtgtgg aaaaaggtgg ataaacaaca
2461 aacaaacaca aactcaatac gaactctcag agacccgcag ccaccatccc aaatgtaatc
2521 tatctaaatt taatataaag ttttatataa acgtattata tggaatactt gtaaatactg
2581 agtcattttt acagcataat tatttatgta tggtgcaatg tcttcatgga tggacaggaa
2641 ataaaaaaga aaaaaagaaa aaaaaaaaaa aaaaaaaaaa aaaa
```

C

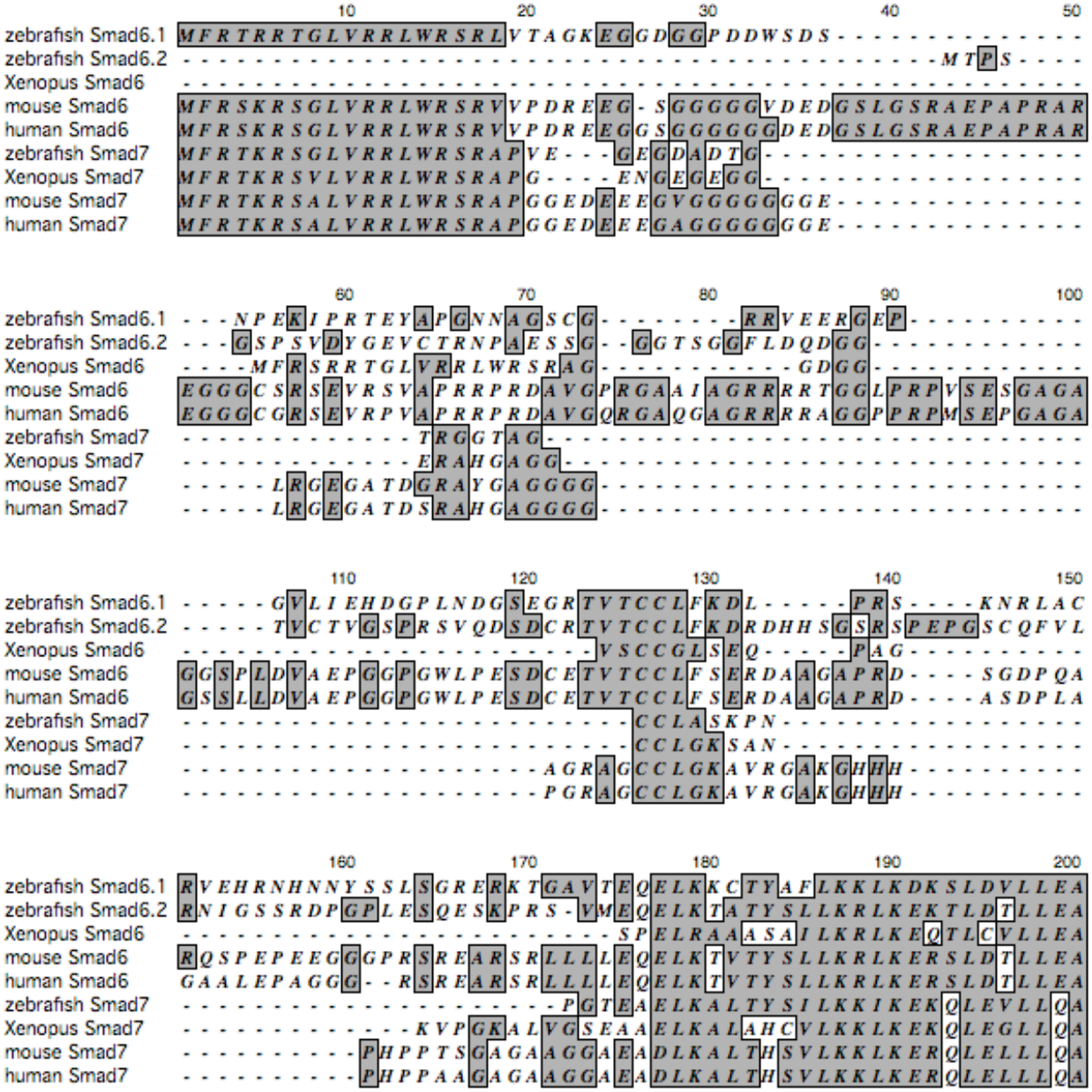
Formatted Alignments
zebrafish Smad6.1
zebrafish Smad6.2
Xenopus Smad6
mouse Smad6
human Smad6
zebrafish Smad7
Xenopus Smad7
mouse Smad7
human Smad7

(continued)

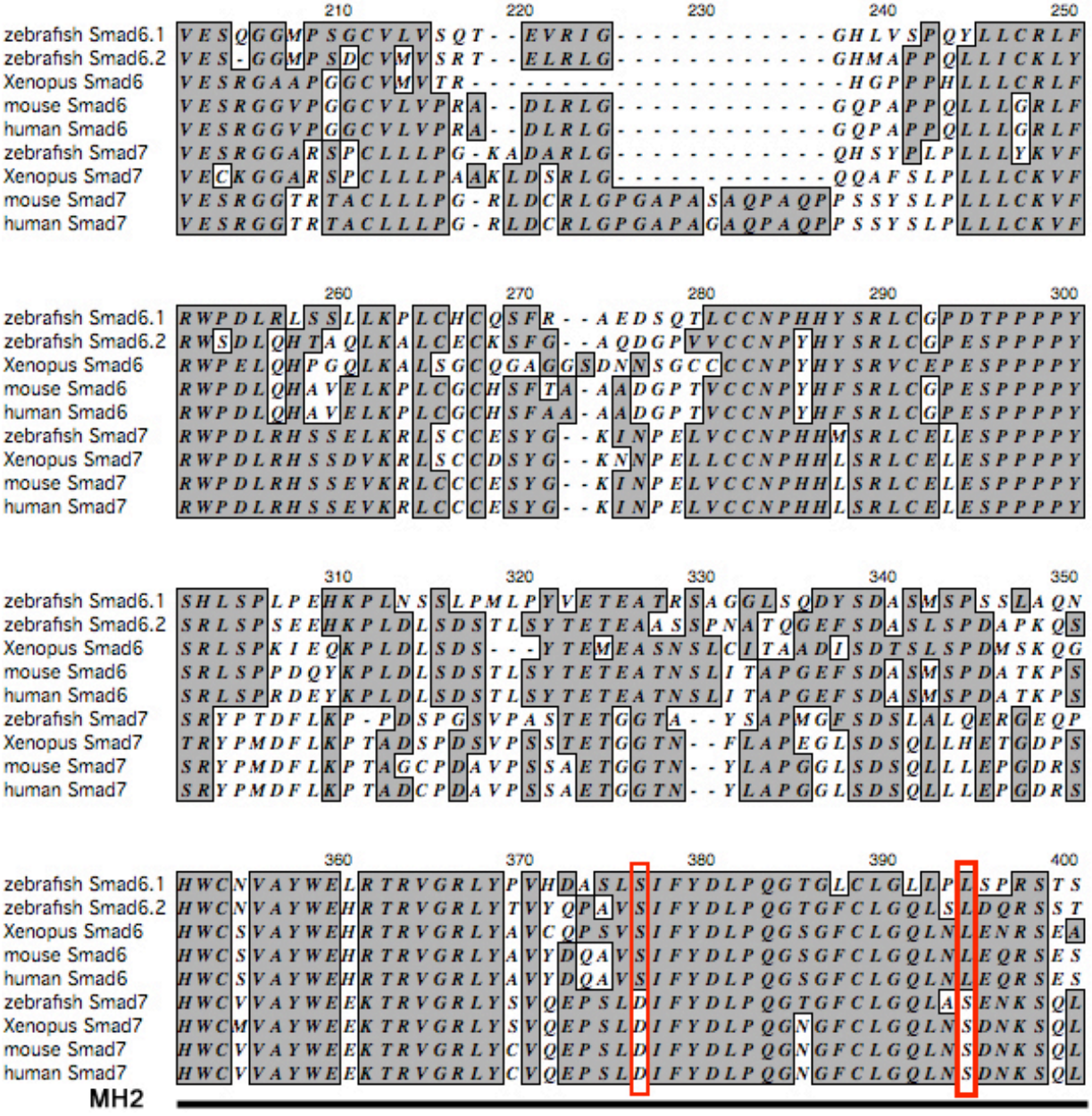
zebrafish Smad6.1
zebrafish Smad6.2
Xenopus Smad6
mouse Smad6
human Smad6
zebrafish Smad7
Xenopus Smad7
mouse Smad7
human Smad7
MH2

(continued)

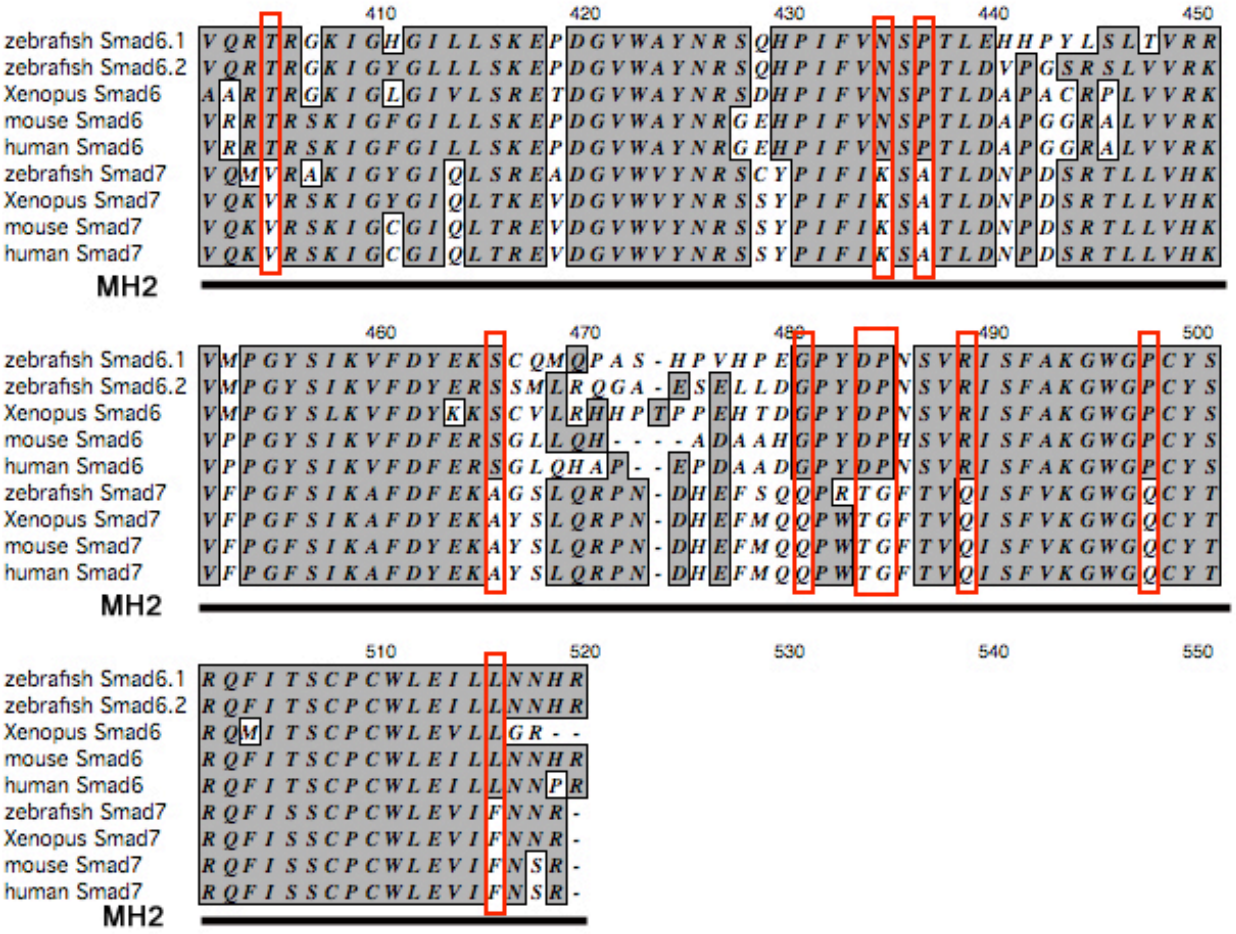

D

Identity Scores (%)

	zebrafish Smad6.1	zebrafish Smad6.2	Xenopus Smad6	mouse Smad6	human Smad6	zebrafish Smad7	Xenopus Smad7	mouse Smad7	human Smad7
zebrafish Smad6.1	100.0	52.5	44.5	51.7	51.9	40.4	38.8	37.5	37.5
zebrafish Smad6.2	63.3	100.0	52.3	56.8	56.7	37.6	37.1	35.7	36.0
Xenopus Smad6	54.2	61.9	100.0	45.8	46.3	41.4	39.6	36.5	36.7
mouse Smad6	61.7	67.7	54.4	100.0	92.8	39.1	37.9	38.6	38.8
human Smad6	61.7	66.8	54.7	94.4	100.0	39.1	37.9	38.6	38.8
zebrafish Smad7	51.8	50.3	53.1	50.1	49.9	100.0	77.8	70.4	70.7
Xenopus Smad7	51.8	50.6	52.3	50.5	50.5	85.6	100.0	76.1	76.6
mouse Smad7	51.1	49.0	49.5	49.7	49.3	76.5	82.0	100.0	98.1
human Smad7	51.3	49.4	49.8	50.1	49.7	77.0	82.4	98.6	100.0

Similarity Scores (%)

E

Method: UPGMA; Bootstrap (100 reps); tie breaking = Systematic
Distance: Absolute (# differences)
Gaps distributed proportionally

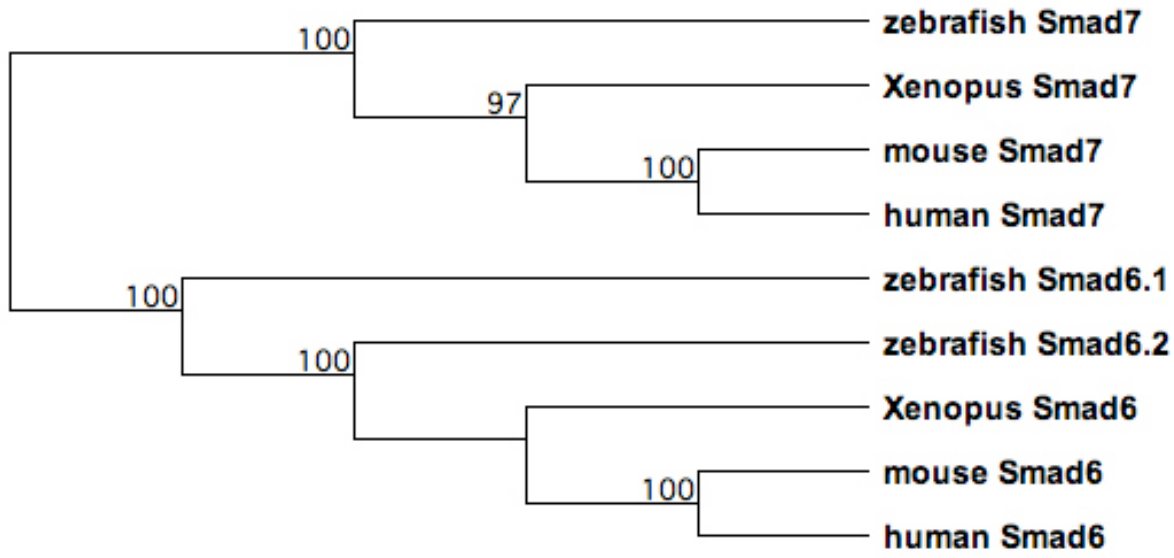

F

Method: UPGMA; Bootstrap (100 reps); tie breaking = Systematic
Distance: Absolute (# differences)
Gaps distributed proportionally

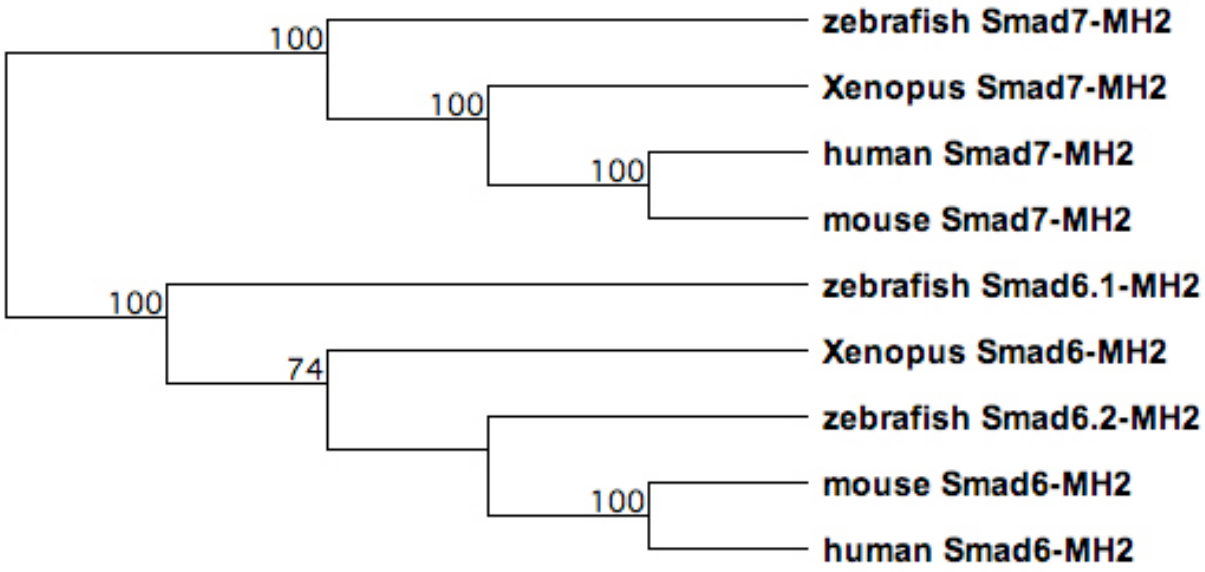

Figure 3.2 *smad6.1* and *smad6.2* show redundant and unique domains of expression during development.

(A,B,A',B') Shield stage, (A,A') lateral view, (B,B') animal pole view, dorsal towards the right. (C,D,C',D') Bud stage, (C,C') lateral view, anterior towards the top and dorsal towards the right; (D,D') caudal view, dorsal towards the top. (E,F,E',F') 10-somite stage, (E,E') lateral view and (F,F') dorsal view with anterior towards the top. (G,H,G',H') 24 hpf, (G,G') lateral view and (H,H') dorsal anterior view. (I,J,I',J') 48 hpf, (I, I') lateral view and (J,J') dorsal anterior view. tb, tailbud. ml, midline. ey, eye. br, brain. pt, posterior tail. ht, heart. so, somites. pf, pectoral fin. ov, otic viscle, le, lens. Open arrow indicates the unique expression of *smad6.1* near the hindbrain.

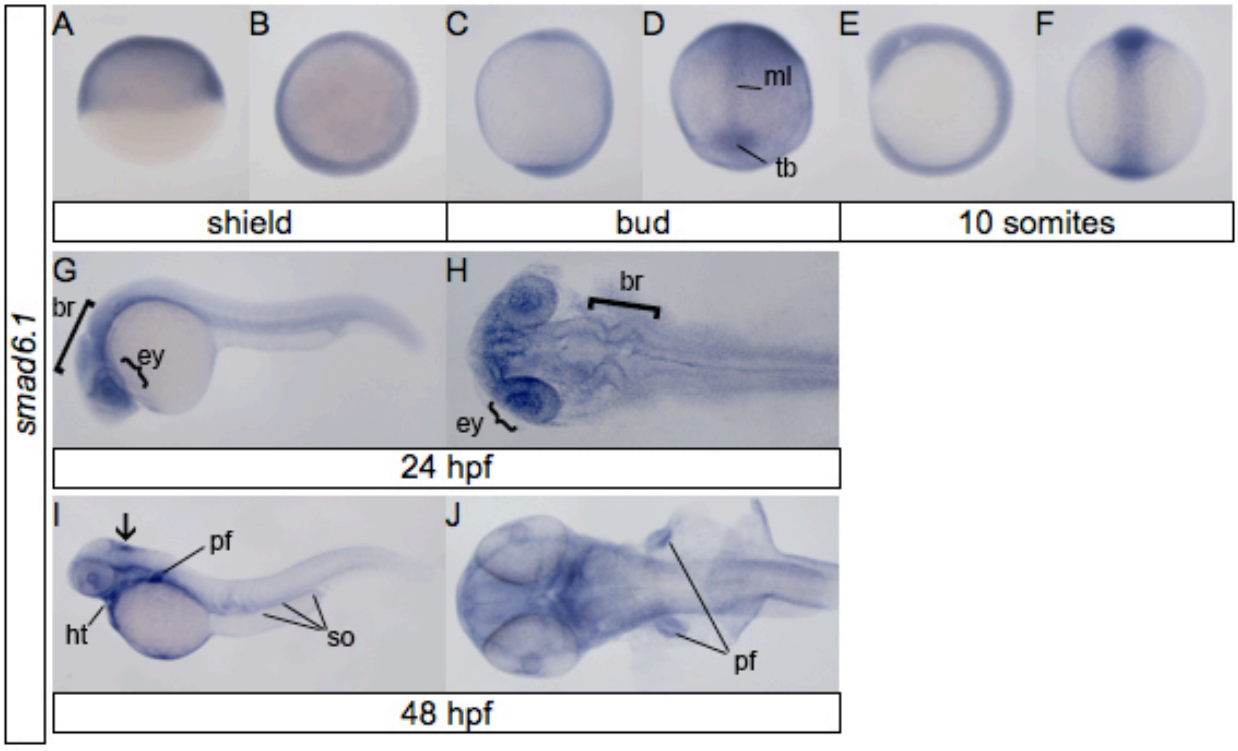
smad6.1
A
B
C
D
E
F
ml
tb
shield
bud
10 somites
G
H
br
ey
br
ey
24 hpf
I
J
pf
ht
so
pf
48 hpf

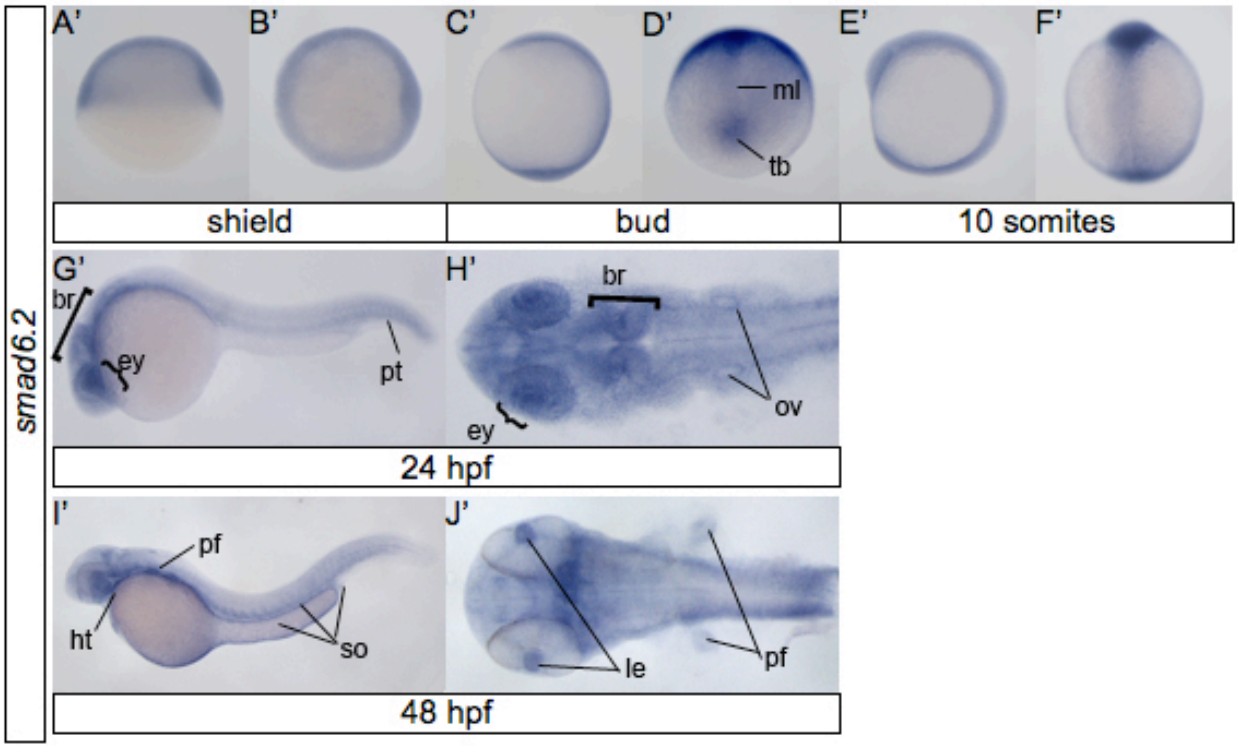
smad6.2
A'
B'
C'
D'
E'
F'
ml
tb
shield
bud
10 somites
G'
H'
br
ey
pt
br
ey
ov
24 hpf
I'
J'
pf
ht
so
le
pf
48 hpf

Figure 3.3 Decreased and increased expression of *smad6.1* in response to down and up regulated BMP signaling at early gastrula stage.

(A-N) Common spatial expression of *smad6.1* in representative embryos at 60% epiboly, (A,C,E,G,I,K,M) lateral view and (B,D,F,H,J,L,N) animal pole view with dorsal towards the right. Embryos were injected with *mfn* MO (C,D), *admp* MO (E,F), *chd* MO (G,H), *caBMPR* RNA (I,J), *smad5* RNA (K,L) and *oep* MO (M,N). Decreased expression of *smad6.1* is indicated by arrowheads while increased expression is indicated by open arrow heads. Belt shaped expression pattern along the margin is indicated by arrow. (O) Penetrance of altered *smad6.1* and *smad6.2* expression in response to changed BMP signaling. Wild type like expression is denoted as value zero. Positive percentage represents the penetrance of increased expression and negative percentage represents the penetrance of decreased expression.

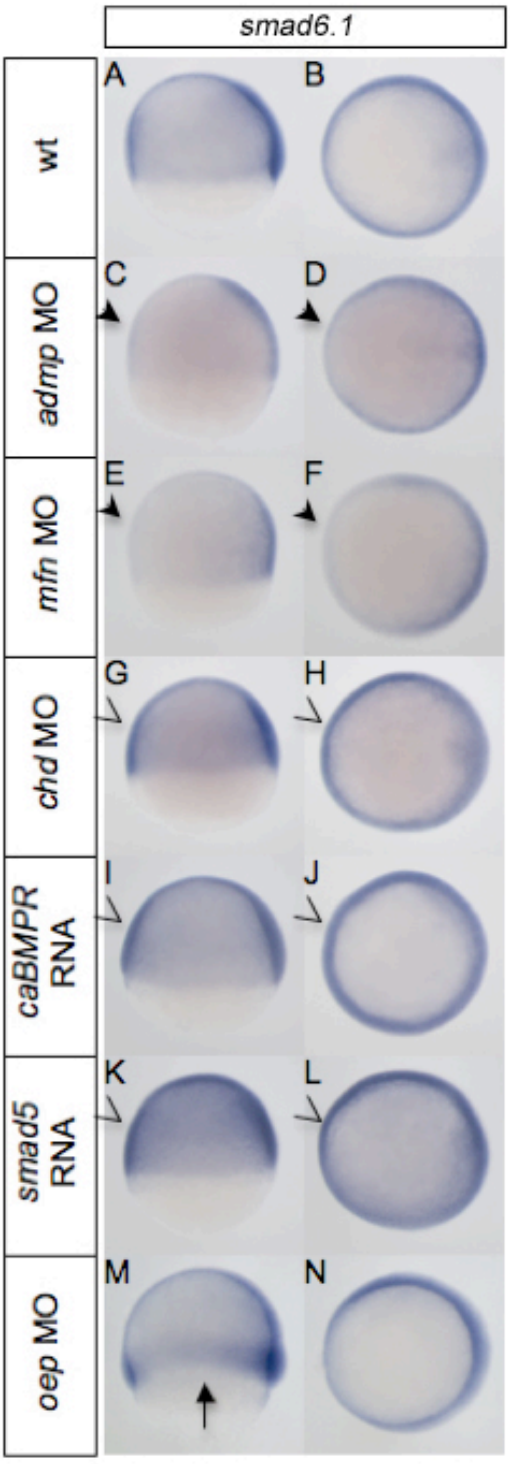
smad6.1
wt
admp MO
mfn MO
chd MO
caBMPR RNA
smad5 RNA
oep MO
A
B
C
D
E
F
G
H
I
J
K
L
M
N

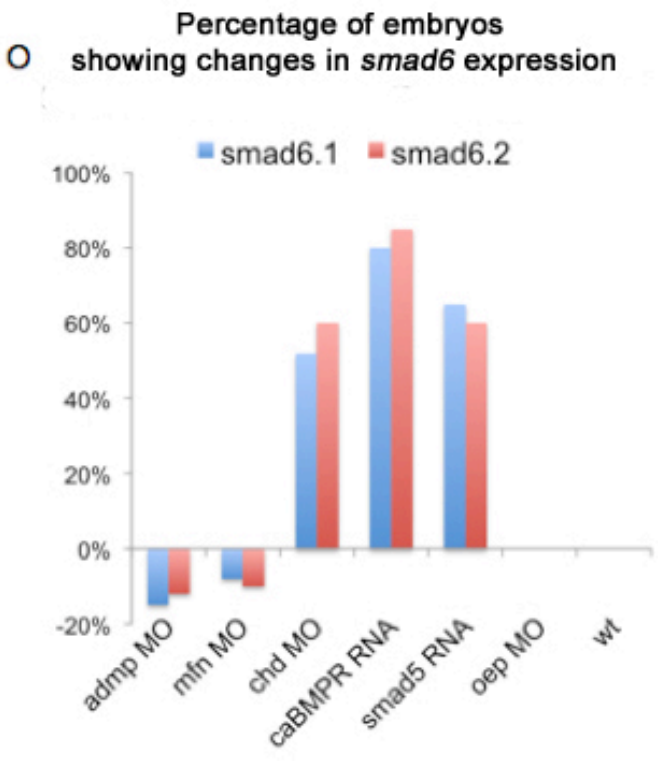
O
Percentage of embryos showing changes in smad6 expression
smad6.1
smad6.2
100%
80%
60%
40%
20%
0%
-20%
admp MO
mfn MO
chd MO
caBMPR RNA
smad5 RNA
oep MO
wt

Figure 3.4 Overexpressing *smad6.1* and *smad6.2* dosalizes embryo by inhibiting BMP signaling.

(A-L) Embryos after whole mount *in situ* hybridization at 60% epiboly; animal pole views, dorsal towards the right. Reduced ventral domain of *eve1* expression (A-D) and expanded *flh* (E-H) and *chd* expression in dorsal regions (I-L) in injected compared with uninjected embryos was observed. (M,N) Dorsal view of expansion of *chd* expression in embryos at shield stage. (O,P) Animal pole view of embryos at 60% epiboly after P-Smad5 antibody staining, dorsal towards the right. Expression domain is delineated by arrowheads.

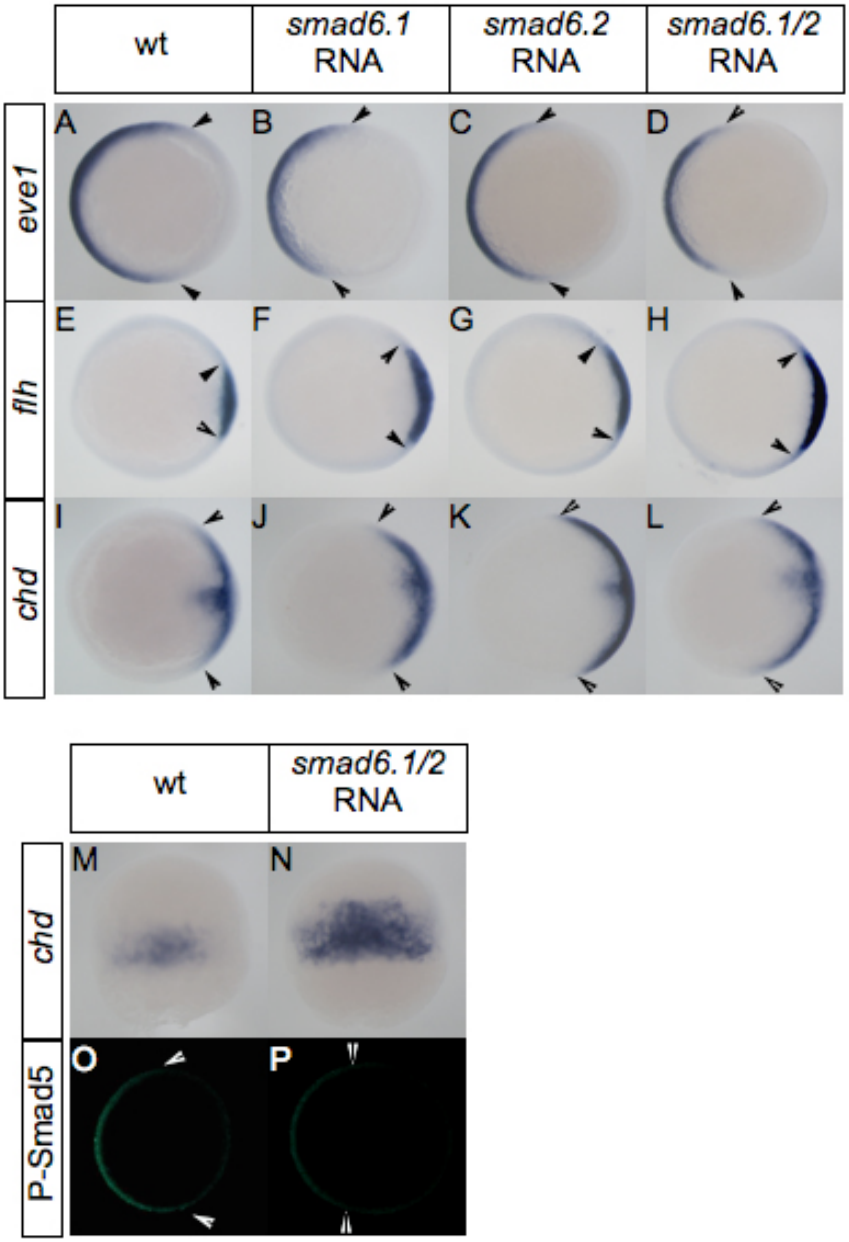

Figure 3.5 Inhibiting *smad6.1* and *smad6.2* ventralizes embryo as increasing BMP signaling.

(A-L) Embryos after whole mount *in situ* hybridization at 60% epiboly; animal pole views, dorsal towards the right. Expanded ventral domain of *eve1* expression (A-D) and reduced *flh* (E-H) and *chd* expression in dorsal regions (I-L) in injected compared with uninjected embryos was observed. (M,N) Animal pole view of embryos at 60% epiboly after P-Smad5 antibody staining, dorsal towards the right. Arrowheads indicates the expression region.

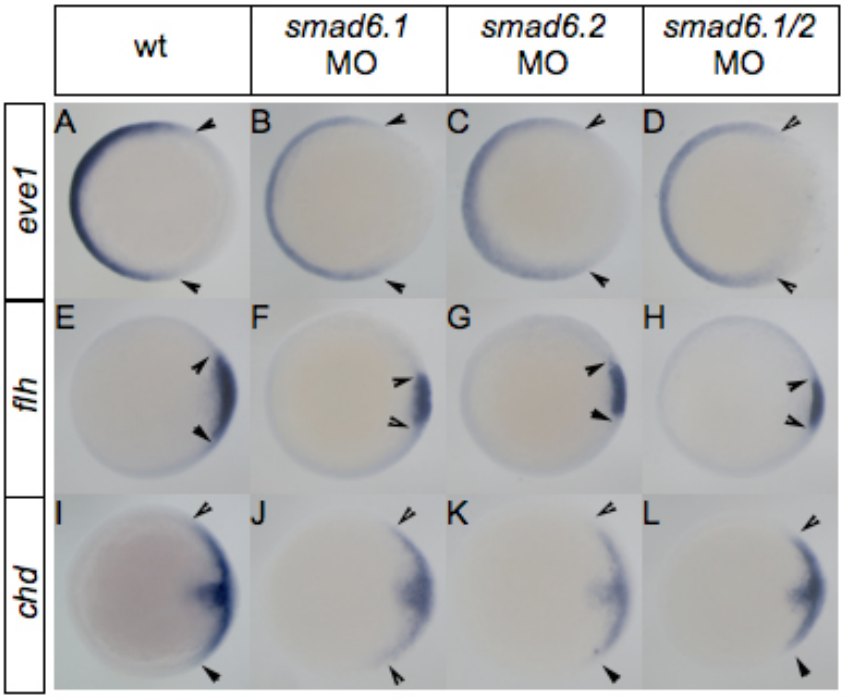

Table 3.1 Percentage of embryos showing changes of designated markers after injection of RNAs

	smad6.1 RNA	*smad6.2* RNA	*smad6.1/2* RNA	
eve1	50% (n=102)	49% (n=87)	60% (n=91)	
flh	43% (n=85)	44% (n=90)	55% (n=82)	
chd	40% (n=95)	45% (n=107)	50% (n=98)	55% (n=72),shield
P-Smad5	--	--	49% (n=35)	

Table 3.2 Percentage of embryos showing changes of designated markers after injection of morpholinos.

	smad6.1 MO	*smad6.2* MO	*smad6.1/2* MO
eve1	0%(n=110)	0% (n=112)	0% (n=118)
flh	38% (n=115)	35% (n=118)	42% (n=120)
chd	32% (n=115)	28% (n=104)	34% (n=122)
P-Smad5	--	--	35% (n=32)

References

Afrakhte, M., Moren, A., Jossan, S., Itoh, S., Sampath, K., Westermark, B., Heldin, C. H., Heldin, N. E. and ten Dijke, P. (1998). Induction of inhibitory Smad6 and Smad7 mRNA by TGF-beta family members. *Biochem Biophys Res Commun* **249**, 505-511.

Bai, S. and Cao, X. (2002). A nuclear antagonistic mechanism of inhibitory Smads in transforming growth factor-beta signaling. *J Biol Chem* **277**, 4176-4182.

Bai, S., Shi, X., Yang, X. and Cao, X. (2000). Smad6 as a transcriptional corepressor. *J Biol Chem* **275**, 8267-8270.

Dick, A., Meier, A. and Hammerschmidt, M. (1999). Smad1 and Smad5 have distinct roles during dorsoventral patterning of the zebrafish embryo. *Dev Dyn* **216**, 285-298.

Feldman, B. and Stemple, D. L. (2001). Morpholino phenocopies of sqt, oep, and ntl mutations. *Genesis* **30**, 175-177.

Feng, X. H. and Derynck, R. (2005). Specificity and versatility in tgf-beta signaling through Smads. *Annu Rev Cell Dev Biol* **21**, 659-693.

Galvin, K. M., Donovan, M. J., Lynch, C. A., Meyer, R. I., Paul, R. J., Lorenz, J. N., Fairchild-Huntress, V., Dixon, K. L., Dunmore, J. H., Gimbrone, M. A., Jr. et al. (2000). A role for smad6 in development and homeostasis of the cardiovascular system. *Nat Genet* **24**, 171-174.

Hata, A., Lagna, G., Massague, J. and Hemmati-Brivanlou, A. (1998). Smad6 inhibits BMP/Smad1 signaling by specifically competing with the Smad4 tumor suppressor. *Genes Dev* **12**, 186-197.

Hayashi, H., Abdollah, S., Qiu, Y., Cai, J., Xu, Y. Y., Grinnell, B. W., Richardson, M. A., Topper, J. N., Gimbrone, M. A., Jr., Wrana, J. L. et al. (1997). The MAD-related protein Smad7 associates with the TGFbeta receptor and functions as an antagonist of TGFbeta signaling. *Cell* **89**, 1165-1173.

Imamura, T., Takase, M., Nishihara, A., Oeda, E., Hanai, J., Kawabata, M. and Miyazono, K. (1997). Smad6 inhibits signalling by the TGF-beta superfamily. *Nature* **389**, 622-626.

Ishida, W., Hamamoto, T., Kusanagi, K., Yagi, K., Kawabata, M., Takehara, K., Sampath, T. K., Kato, M. and Miyazono, K. (2000). Smad6 is a Smad1/5-induced smad

inhibitor. Characterization of bone morphogenetic protein-responsive element in the mouse Smad6 promoter. *J Biol Chem* **275**, 6075-6079.

Jasuja, R., Voss, N., Ge, G., Hoffman, G. G., Lyman-Gingerich, J., Pelegri, F. and Greenspan, D. S. (2006). bmp1 and mini fin are functionally redundant in regulating formation of the zebrafish dorsoventral axis. *Mech Dev* **123**, 548-558.

Joly, J. S., Joly, C., Schulte-Merker, S., Boulekbache, H. and Condamine, H. (1993). The ventral and posterior expression of the zebrafish homeobox gene eve1 is perturbed in dorsalized and mutant embryos. *Development* **119**, 1261-1275.

Kimelman, D. (2006). Mesoderm induction: from caps to chips. *Nat Rev Genet* **7**, 360-372.

Li, W., Chen, F., Nagarajan, R.P., Liu, X. and Chen, Y. (2001). Characterization of the DNA-binding property of Smad5. *Biochem Biophys Res Commun* **286,** 1163–1169.

Lin, X., Liang, Y. Y., Sun, B., Liang, M., Shi, Y., Brunicardi, F. C. and Feng, X. H. (2003). Smad6 recruits transcription corepressor CtBP to repress bone morphogenetic protein-induced transcription. *Mol Cell Biol* **23**, 9081-9093.

Little, S. C. and Mullins, M. C. (2006). Extracellular modulation of BMP activity in patterning the dorsoventral axis. *Birth Defects Res C Embryo Today* **78**, 224-242.

Massague, J., Seoane, J. and Wotton, D. (2005). Smad transcription factors. *Genes Dev* **19**, 2783-2810.

Miller-Bertoglio, V. E., Fisher, S., Sanchez, A., Mullins, M. C. and Halpern, M. E. (1997). Differential regulation of chordin expression domains in mutant zebrafish. *Dev Biol* **192**, 537-550.

Nakao, A., Afrakhte, M., Moren, A., Nakayama, T., Christian, J. L., Heuchel, R., Itoh, S., Kawabata, M., Heldin, N. E., Heldin, C. H. et al. (1997). Identification of Smad7, a TGFbeta-inducible antagonist of TGF-beta signalling. *Nature* **389**, 631-635.

Nakayama, T., Gardner, H., Berg, L. K. and Christian, J. L. (1998). Smad6 functions as an intracellular antagonist of some TGF-beta family members during Xenopus embryogenesis. *Genes Cells* **3**, 387-394.

Oxtoby, E. and Jowett, T. (1993). Cloning of the zebrafish krox-20 gene (krx-20) and its expression during hindbrain development. *Nucleic Acids Res* **21**, 1087-1095.

Park, S. H. (2005). Fine tuning and cross-talking of TGF-beta signal by inhibitory Smads. *J Biochem Mol Biol* **38**, 9-16.

Schier, A. F. and Talbot, W. S. (2005). Molecular genetics of axis formation in zebrafish. *Annu Rev Genet* **39**, 561-613.

Schulte-Merker, S., Lee, K. J., McMahon, A. P. and Hammerschmidt, M. (1997). The zebrafish organizer requires chordino. *Nature* **387**, 862-863.

Shawi, M. and Serluca, F. C. (2008). Identification of a BMP7 homolog in zebrafish expressed in developing organ systems. *Gene Expr Patterns* **8**, 369-375.

Stickney, H. L., Imai, Y., Draper, B., Moens, C. and Talbot, W. S. (2007). Zebrafish bmp4 functions during late gastrulation to specify ventroposterior cell fates. *Dev Biol* **310**, 71-84.

Talbot, W. S., Trevarrow, B., Halpern, M. E., Melby, A. E., Farr, G., Postlethwait, J. H., Jowett, T., Kimmel, C. B. and Kimelman, D. (1995). A homeobox gene essential for zebrafish notochord development. *Nature* **378**, 150-157.

Turner, D. L. and Weintraub, H. (1994). Expression of achaete-scute homolog 3 in Xenopus embryos converts ectodermal cells to a neural fate. *Genes Dev* **8**, 1434-1447.

Vargesson, N. and Laufer, E. (2009). Negative Smad expression and regulation in the developing chick limb. *PLoS One* **4**, e5173.

Willot, V., Mathieu, J., Lu, Y., Schmid, B., Sidi, S., Yan, Y. L., Postlethwait, J. H., Mullins, M., Rosa, F. and Peyrieras, N. (2002). Cooperative action of ADMP- and BMP-mediated pathways in regulating cell fates in the zebrafish gastrula. *Dev Biol* **241**, 59-78.

Yamada, M., Szendro, P. I., Prokscha, A., Schwartz, R. J. and Eichele, G. (1999). Evidence for a role of Smad6 in chick cardiac development. *Dev Biol* **215**, 48-61.

Zhao, G. Q. (2003). Consequences of knocking out BMP signaling in the mouse. *Genesis* **35**, 43-56.

Appendix A - *strabismus* and *prickle* interact with Noncanonical Wnt and BMP Signaling to Affect the Secondary Tail Formation in Zebrafish

Abstract

Based on our resuls that inhibition of noncanonical Wnt and BMP singling leads to secondary tail formation in zebrafish, we studied the genetic interactions between *pk* and *stbm*, two genes involved in noncanonical Wnt signaling, and other players in secondary tail formation. By morpholino-induced gene knockdown, we found that inhibiting *stbm* and *pk1* suppresses the secondary tails induced by losing *kny* or *dvl2/dvl3*. This genetic interaction is consistent with the Planar Cell Polarity (PCP) signaling pathway in *Drosophila* where *pk* and *stbm* genetically antagonize *dsh*. Although we do not know whether there is corresponding asymmetrical localization of these proteins in tailbud cells, our data suggest that in tail development, noncanonical Wnt signaling functions similar to PCP signaling in *Drosophila*. We tested the genetic interactions between *stbm/pk* and BMP signaling in secondary tail formation. Surprisingly, knocking down *stbm* enhances the secondary tail phenotype when losing BMP signaling, whereas knocking down *pk1* suppresses the secondary tail phenotype in BMP mutants.

Introduction

In zebrafish, tail development is shaped by two forces: convergence and extension (CE) movements of the anterior (dorsally derived) tailbud, which converge the presomitic and somitic mesoderm to the midline and drive the posteriorward extension of the embryo, and the lateral subductive movements of the posterior (ventrally derived) tailbud cells, which avoids the posteriorly migrating anterior tailbud cells by diverging from the midline and moving anteriorly beneath them (Kanki and Ho, 1997).

Noncanonical Wnt signaling, the equivalent of *Drosophila* planar cell polarity (PCP) cascades that establish polarity in planar epithelial cells, is required in zebrafish tail morphogenesis. Two noncanonical Wnt signaling components, the heparan sulfate proteoglycan encoded by *glypican4*/*knypek* (*kny*) and the secreted glycoprotein of Wnt family encoded by

wnt5/*pipetail* (*ppt)*, control cell movements within the tailbud (Marlow et al., 2004). Zebrafish mutants of *kny* and *wnt5* have shortened tails and thinner and wider somites due to reduced CE and impaired laterad divergence movements (Topczewski et al., 2001; Kilian et al., 2003). We previously reported that inhibiting two *dvl* homologs, *dvl2* and *dvl3*, which are involved in noncanonical Wnt signaling, results in secondary tail phenotype (described in Chapter 2). We further confirmed this phenotype in the *kny* mutant, suggesting that one role of noncanonical Wnt signaling is regulating the integrity of the tailbud. We found that *kny* is required in the CNH domain of the tailbud to positively regulate the membrane localization of N-cadherin. Upon loss of noncanonical Wnt signaling, the CNH cells become less tightly associated with each other, which results in aberrant cell movement. This serves as the initiation of subsequent secondary tail formation. In parallel to the noncanonical Wnt signaling pathway, BMP signaling is required in the posterior mesoderm that surrounds the CNH to prevent secondary tail formation.

Whether other components of noncanonical Wnt signaling involved in maintaining the integrity of the tailbud is largely unknown. Most of the work in vertebrates concentrates on the role of noncanonical Wnt signaling in regulating CE movements during gastrulation, suggesting this process shares much similarity in the mechanism of PCP signaling in *Drosophila* (Veeman et al., 2003). In the *Drosophila* wing epithelium, asymmetrical localization of the core PCP components provides the cue for the establishment of cell polarity. When PCP signaling is activated, transmembrane receptor Frizzled brings the cytoplasmic docking protein Dishevelled (Dsh/Dvl) to the distal membrane and activated Dsh can transduce the signal to its downstream effectors. Strabismus (Stbm) recruits the intracellular protein Prickle (Pk) to the proximal cell membrane to suppress Frizzled and Dsh. Since the tailbud is a different context from the epithelium and gastrula cells, how genes involved in noncanonical Wnt signaling interact with each other needs to be clarified.

Here, we studied the genetic interactions between *pk* and *stbm* and the other players (*mfn*, *kny*, *dvl2* and *dvl3*) in secondary tail formation. By morpholino-induced gene knockdown, we found that inhibiting *stbm* and *pk1* suppresses the secondary tails induced by losing *kny* or *dvl2/dvl3*. This genetic interaction fits the PCP pathway in *Drosophila* that *pk* and *stbm* genetically antagonize *dsh*. Although we do not know whether there is corresponding asymmetrical localization of these proteins in tailbud cells, our data suggest that in tail development, noncanonical Wnt signaling functions similar to *Drosophila* PCP. We tested the

genetic interactions between *stbm/pk* and BMP signaling in secondary tail formation. Surprisingly, knocking down *stbm* enhances the secondary tail phenotype when losing BMP signaling, whereas knocking down *pk1* suppresses the secondary tail phenotype in BMP mutants.

Material and Methods

Morpholino Injections experiments were carried out as mentioned in the supplementary section of Chapter 2.

Results and Discussion

In *Drosophila*, *dsh* is genetically inhibited by *stbm* and *pk*. Interfering with the function of Dsh leads to disoriented wing hairs (Axelrod et al., 1998). Knocking down *stbm* or *pk* rescues the *dsh* loss of function phenotype (Jenny et al., 2005). As for the secondary tail phenotype in zebrafish, the *kny* and *dvl* linear pathway of noncanonical Wnt signaling has a demonstrated role (see Chapter 2). Our previous experiments show that inhibiting *stbm* and *pk* separately or cooperatively does not result in secondary tail formation. To test whether *stbm* and *pk* suppress *dvl* as in the PCP pathway in the fly, we knocked down *stbm* or *pk* by morpholino to see whether this inhibits the secondary tail phenotype in *dvl2*/*3* morphants or *kny* mutants. Knocking down *stbm* consistently reduces the penetrance of secondary tail formation in *dvl2*/*3* morphants (Fig. A.1A) and *kny* embryos (Fig. A.1B). In the two homologues of *pk* we tested, knockdown of *pk1a* exhibited great efficacy in suppressing secondary tails in *kny* (Fig. A.1D) while *pk2b* has no obvious effect on secondary tail formation (Fig. A.1C,E). This is in line with the differential expression patterns of these two *pk* genes, suggesting a local requirement of these genes in the regulation of tail development. Our results fits the genetic interactions as deduced from the *Drosophila* PCP pathway, suggesting the noncanonical Wnt and PCP signaling are conserved in fish and fly. There seems to be no direct linkage between the severity of CE and occurrence of secondary tail, since knocking down *stbm* in *kny* show strong defect of CE movements causing extremely short embryos (data not shown) as knocking down *dvl2/3* in *kny,* but with much lower penetrance of secondary tail. Since we observed losing membrane localization of cadherin in the CNH is the key to cause secondary tail in *kny* (Fig. 2.5), it will be important to determine whether inhibiting *stbm* or *pk1a* is able to reestablish the membrane anchoring of cadherin in *kny* embryos. So far, we have not found any role for known noncanonical Wnt ligands in secondary

tail regulation, so identifying the roles of additional components in noncanonical Wnt signaling will be important to understand how noncanonical Wnt signaling functions to regulate tail morphogenesis. One good candidate is Diego/Diversion, an ankyrin repeat protein that functions to promote PCP signaling in *Drosophila* (Jenny et al., 2005) and acts downstream of *wnt5*/11 to regulate CE in zebrafish, and is capable of binding to Dsh (Moeller et al., 2006).

We have previously shown that inhibiting *dvl2*/3 together with *mfn* strongly enhances the secondary tail phenotype. To investigate whether other genes (*pk* and *stbm*) in the noncanonical Wnt pathway interact with BMP signaling in secondary tail formation, we performed serial knockdown experiments. Our results show that knocking down *stbm* greatly enhances the penetrance of secondary tails in *mfn* (Fig. A.2A,C). In contrast, *pk1a* knockdown suppresses the secondary tail in *mfn* (Fig. A.2B). *pk2b* knockdown does not result in any change in secondary tail formation in BMP-compromised embryos (Fig. A.2D). My future studies plan to better define these genetic interactions in secondary tail development in zebrafish.

Figures and Tables

Figure A.1

Percentage of secondary tail formation in embryos injected with indicated combination of morpholinos (1 mg/ml each, except for 'dvl2/dvl3 MO' condition, where a concentration of 3 mg/ml for each MO was injected). Embryos from at least three separate experiments were scored. Percentage of secondary tail of each separate experiment is calculated. Then the arithmetic mean of percentage of all replicates is calculated by dividing the sum of percentages with numbers of replicates. Then the variation from the mean is represented by calculated standard deviation. Error bars represent standard deviations of at least 3 replicates. Number of embryos scored for each column is shown in figures. Error bars represent the standard deviation of at least three replicates.

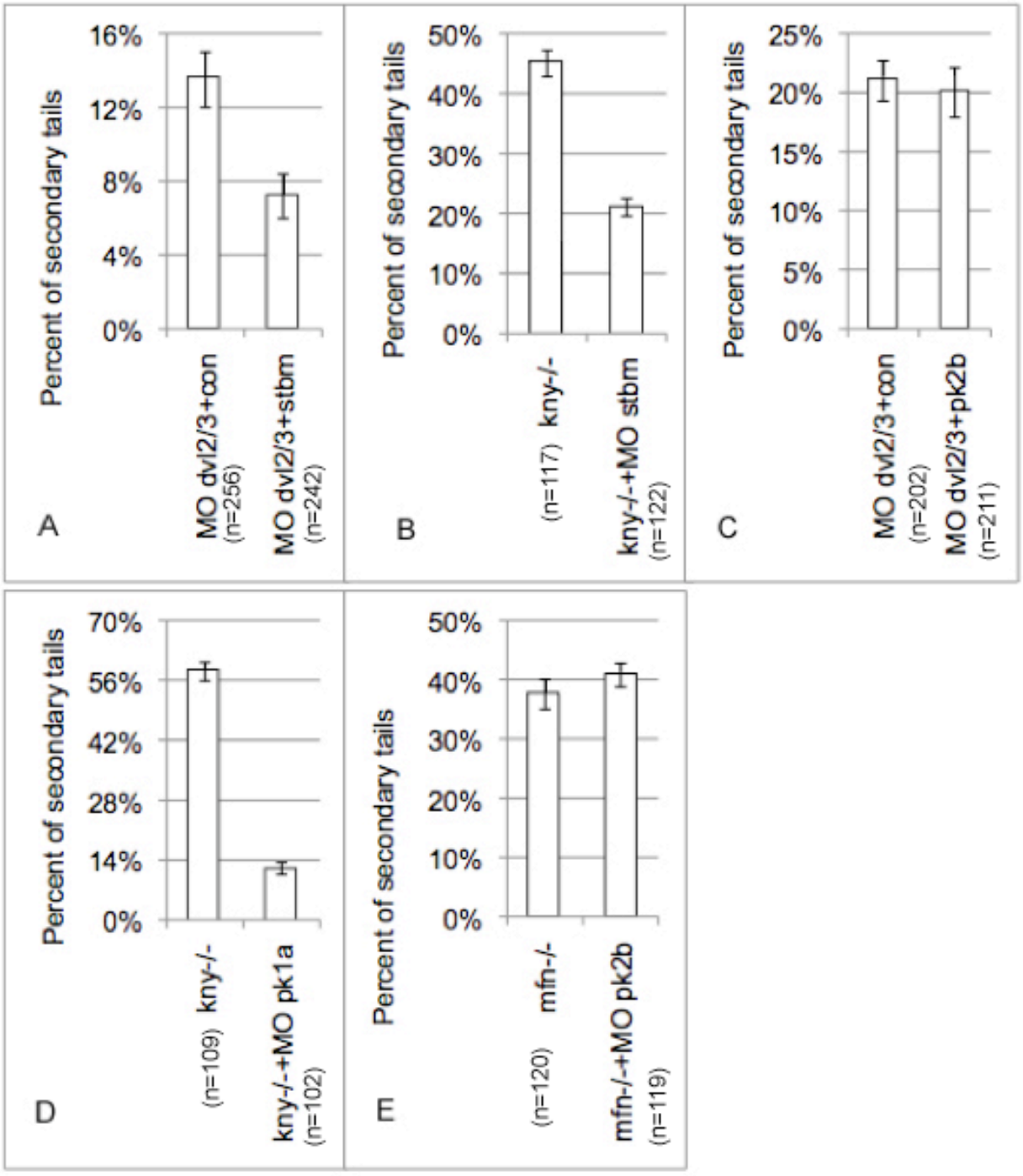
A
Percent of secondary tails
16%
12%
8%
4%
0%
MO dvl2/3+con
(n=256)
MO dvl2/3+stbm
(n=242)
B
Percent of secondary tails
50%
40%
30%
20%
10%
0%
(n=117) kny-/-
kny-/-+MO stbm
(n=122)
C
Percent of secondary tails
25%
20%
15%
10%
5%
0%
MO dvl2/3+con
(n=202)
MO dvl2/3+pk2b
(n=211)
D
Percent of secondary tails
70%
56%
42%
28%
14%
0%
(n=109) kny-/-
kny-/-+MO pk1a
(n=102)
E
Percent of secondary tails
50%
40%
30%
20%
10%
0%
(n=120) mfn-/-
mfn-/-+MO pk2b
(n=119)

Figure A.2

Percentage of secondary tail formation in embryos injected with indicated combination of morpholinos (1 mg/ml each, except for *mfn* MO, where a concentration of 2 mg/ml was injected). Embryos from at least three separate experiments were scored. Note the penetrance of secondary tails in *mfn* embryo is varied due to different wild-type background. Percentage of secondary tail of each separate experiment is calculated. Then the arithmetic mean of percentage of all replicates is calculated by dividing the sum of percentages with numbers of replicates. Then the variation from the mean is represented by calculated standard deviation. Error bars represent standard deviations of at least 3 replicates. Number of embryos scored for each column is shown in figures. Error bars represent the standard deviation of at least three replicates.

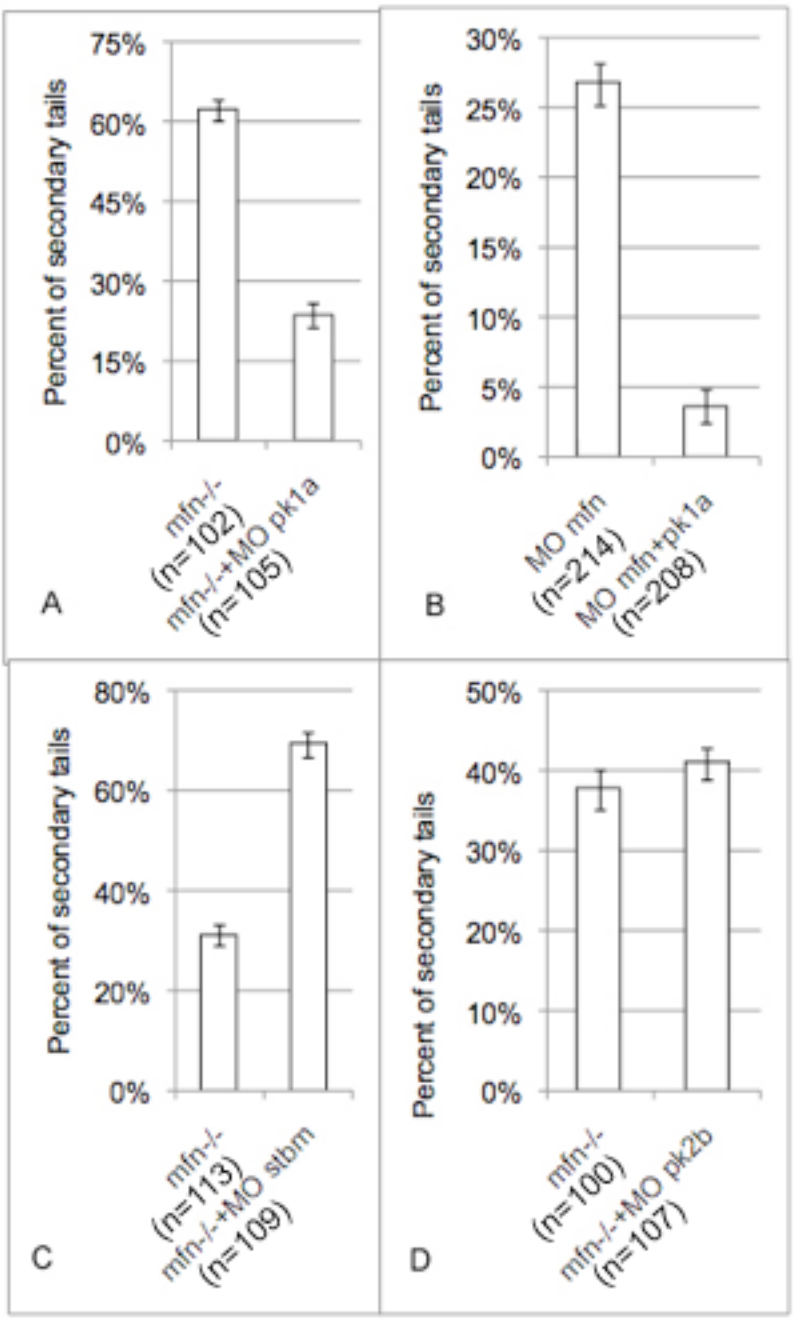
Percent of secondary tails
75%
60%
45%
30%
15%
0%
mfn-/- (n=102)
mfn-/-+MO pk1a (n=105)
A
Percent of secondary tails
30%
25%
20%
15%
10%
5%
0%
MO mfn (n=214)
MO mfn+pk1a (n=208)
B
Percent of secondary tails
80%
60%
40%
20%
0%
mfn-/- (n=113)
mfn-/-+MO stbm (n=109)
C
Percent of secondary tails
50%
40%
30%
20%
10%
0%
mfn-/- (n=100)
mfn-/-+MO pk2b (n=107)
D

References

Axelrod, J. D., Miller, J. R., Shulman, J. M., Moon, R. T. and Perrimon, N. (1998). Differential recruitment of Dishevelled provides signaling specificity in the planar cell polarity and Wingless signaling pathways. *Genes Dev* **12**, 2610-2622.

Jenny, A., Reynolds-Kenneally, J., Das, G., Burnett, M. and Mlodzik, M. (2005). Diego and Prickle regulate Frizzled planar cell polarity signalling by competing for Dishevelled binding. *Nat Cell Biol* **7**, 691-697.

Kanki, J. P. and Ho, R. K. (1997). The development of the posterior body in zebrafish. *Development* **124**, 881-893.

Kilian, B., Mansukoski, H., Barbosa, F. C., Ulrich, F., Tada, M. and Heisenberg, C. P. (2003). The role of Ppt/Wnt5 in regulating cell shape and movement during zebrafish gastrulation. *Mech Dev* **120**, 467-476.

Marlow, F., Gonzalez, E. M., Yin, C., Rojo, C. and Solnica-Krezel, L. (2004). No tail co-operates with non-canonical Wnt signaling to regulate posterior body morphogenesis in zebrafish. *Development* **131**, 203-216.

Moeller, H., Jenny, A., Schaeffer, H. J., Schwarz-Romond, T., Mlodzik, M., Hammerschmidt, M. and Birchmeier, W. (2006). Diversin regulates heart formation and gastrulation movements in development. *Proc Natl Acad Sci U S A* **103**, 15900-15905.

Topczewski, J., Sepich, D. S., Myers, D. C., Walker, C., Amores, A., Lele, Z., Hammerschmidt, M., Postlethwait, J. and Solnica-Krezel, L. (2001). The zebrafish glypican knypek controls cell polarity during gastrulation movements of convergent extension. *Dev Cell* **1**, 251-264.

Veeman, M. T., Axelrod, J. D. and Moon, R. T. (2003). A second canon. Functions and mechanisms of beta-catenin-independent Wnt signaling. *Dev Cell* **5**, 367-377.